# Study of the mechanisms of tRNA targeting into yeast and human mitochondria

Mariia Baleva

UNIVERSITÉ DE STRASBOURG

**Université de Strasbourg**

**Université de Moscou**

**2016**

**École doctorale des sciences de la vie et de la santé**

# THÈSE

**présentée pour l'obtention du grade de**

**DOCTEUR DE L'UNIVERSITÉ DE STRASBOURG**

**Discipline : Sciences du vivant**

**Domaine : Aspects moléculaires et cellulaires de la biologie**

**par**

**BALEVA MARIIA**

# ÉTUDE DES MÉCHANISMES D'ADRESSAGE D'ARN DE TRANSFERT DANS LES MITOCHONDRIES DE LEVURE ET HUMAINES

**Soutenue le 16 Decembre 2016 devant la commission d'examen:**

| | |
|---|---|
| **M.S. JOHANSEN** | **Rapporteur externe** |
| **M.M. PATRUSHEV** | **Rapporteur externe** |
| **M.M. BLAISE** | **Rapporteur externe** |
| **A-M. DUCHENE** | **Examinateur** |
| **M.I. TARASSOV** | **Examinateur** |
| **A.P. KAMENSKI** | **Co-directeur de thèse** |
| **M.B. MASQUIDA** | **Directeur de thèse** |

**UMR N°7156 UdS-CNRS**

**«Génétique Moléculaire, Génomique et Microbiologie»**

# TABLE OF CONTENTS

# ABBREVIATIONS

| | |
|---|---|
| aaRS | aminoacyl-tRNA synthetase |
| ADP | adenosine diphosphate |
| APS | ammonium persulfate |
| ATP | adenosine triphosphate |
| BSA | bovine serum albumin |
| DMEM | dulbecco modified Eagle's medium |
| DMSO | dimethyl sulfoxide |
| DNA | deoxyribonucleic acid |
| DTT | dithiothreitol |
| EDTA | ethylenediaminetetraacetic acid |
| EMSA | electrophoretic mobility shift assay |
| FRET | fluorescence resonance energy transfer |
| HEPES | 4-(2-hydroxyethyl)-1-piperazineethanesulfonic acid |
| HdV | hepatitis delta virus ribozyme |
| HMH | hammerhead ribozyme |
| IMS | intermembrane space |
| IPTG | isopropyl β-D-1-thiogalactopyranoside |
| ITC | isothermal titration microcalorimetry |
| $K_d$ | dissociation constant |
| kDa | kilo Dalton |
| KRS | cytosolic lysyl-tRNA synthetase |
| LB | lysogeny broth |
| mtDNA | mitochondrial DNA |
| MIA | mitochondrial intermembrane space import and assembly |
| MIM | machinery of the inner membrane |
| MISS | mitochondrial intermembrane space signal |
| MMP | mitochondrial processing peptidase |

| | |
|---|---|
| MIP | mitochondrial intermediate peptidase |
| MTS | mitochondrial targeting sequence |
| MW | molecular weight |
| NADH | nicotinamide adenine dinucleotide reduced |
| OD | optical density |
| PAM | presequence translocase associated motor |
| PBS | phosphate buffered saline |
| PIPES | piperazine-N,N'-bis(ethanesulfonic acid) |
| PNPase | polynucleotide phosphorylase |
| preMSK | precurcor of yeast mitochondral lysyl-tRNA synthetase |
| preKARS | precurcor of human mitochondral lysyl-tRNA synthetase |
| PAGE | polyacrylamide gel electrophoresis |
| RIC | RNA import complex |
| PCR | polymerase chain reaction |
| pI | isoelectric point |
| SAM | sorting and assembly machinery |
| SDS | sodium dodecylsulfate |
| siRNA | small interferring RNA |
| SSC | saline sodium citrate buffer |
| TAB | tubulin antisense-binding protein |
| TBE | tris-borate-EDTA buffer |
| TEMED | tetramethylethylenediamine |
| TOM | translocase of the outer membrane |
| Tris | (hydroxymethyl)aminomethane |
| tRNA | transfer RNA |
| UV | ultra violet |
| VDAC | voltage dependent anion channel |
| UPS | ubiquitin-proteasome system |
| $\Delta\psi$ | membrane potential |

# INTRODUCTON

## Origin and general structure of mitochondria

More than 1.5 billion years ago an α-proteobacteria–like ancestor gave the origin of mitochondria (Dyall et al, 2004; Gray, 2012). Moreover, mitochondria still have a set of features similar to modern prokaryotes. Thus, as well as plasma membrane of prokaryotes the mitochondrial membrane contains electron transport proteins, mitochondria also possess a circular genome and specific genetic code, mitochondrial transcription is coupled to translation (Shadel, 2004), organella division and replication occur independently of host cell division. In addition they are surrounded by a double-membrane.

The outer membrane contains diverse pore-forming proteins (porins) and translocases (Campo et al, 2016) that provide transport of different molecules ranging from ions and small uncharged molecules to proteins. The inner membrane is permeable only to oxygen, carbon dioxide, and water, while the other molecules reach the mitochondrial inner space by the means of specific membrane transport proteins. The inner mitochondrial membrane forms numerous invaginations called cristae, which greatly increase the total surface of the inner membrane. This increased surface confers to the inner membrane very effective transport capacities to the entire matrix volume. Cristae contain complexes of the electron transport chain and the ATP synthase. The inner membrane surrounds a mitochondrial matrix where the citric acid cycle and the other biosynthetic reactions take place. Membranes are separated by a thin gap (~20 nm) forming the intermembrane space. (Kühlbrandt, 2015)

## Protein Import Pathways into Mitochondria

Mitochondria possess their own genome, which reflects their bacterial origin as well as divergent evolution. Mitochondrial DNA shows a great deal of variation in size, physical form, coding capacity, modes of organization and expression (Gray, 2012).

The transition from autonomous endosymbionts to mitochondria results from genome reduction through the loss of the part of endosymbiotic genes or their transposition to the nucleus (Allen, 2003). To explain the retention of a set of genes as well as of mechanisms of

genome maintenance in mitochondria, several hypotheses were suggested. Thus, mitochondrial genome encodes eight highly hydrophobic membrane proteins, which are believed retained to avoid mistargeting. According to an alternative hypothesis, mtDNA keeps genes which expression can be regulated depending on the redox state of gene products (Allen, 2015). Furthermore, the non-canonical mitochondrial genetic code can make a barrier to expression of mitochondrial protein-coding genes in nucleus (Allen, 2003).

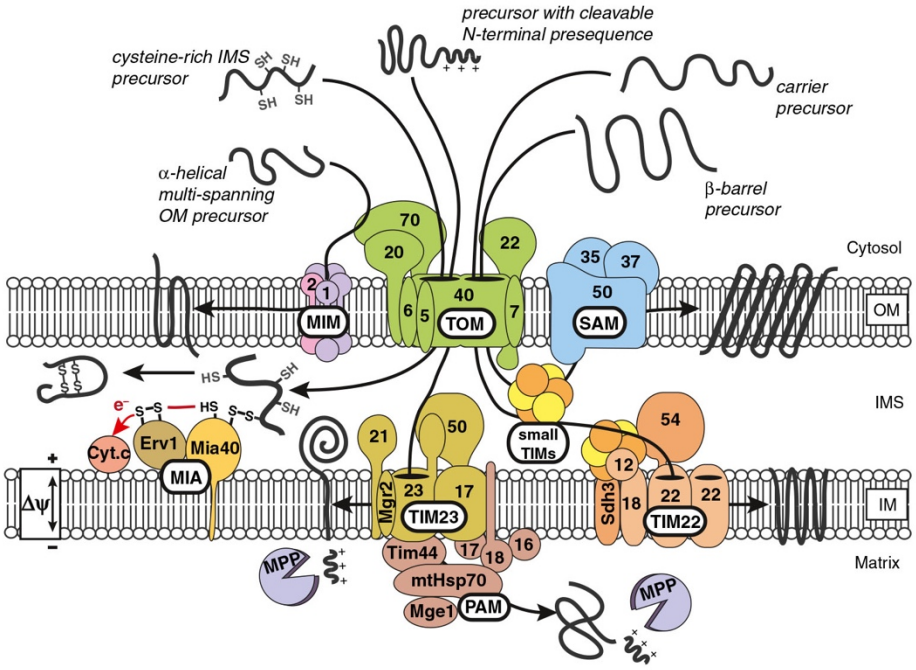


**Figure 1. Pathways sort mitochondrial precursor proteins into the mitochondrial subcompartments.** Precursors of multi-spanning outer membrane proteins are recognized by Tom70 and transferred to the MIM machinery, which mediates their integration and assembly into the membrane. The TOM complex forms the general entry gate for 90% of mitochondrial precursors Thereafter, sorting pathways branch off. With the help of small TIM chaperones, β-barrel precursors are directly transferred to the SAM complex, which mediates their integration into the outer membrane (OM). Precursors with a cleavable presequence are transferred to the TIM23 complex, which mediates either lateral release into the inner membrane (IM) or transport into the mitochondrial matrix. Precursor translocation via the TIM23 complex into the matrix additionally requires the ATP-consuming action of the PAM module. The presequence is removed upon import by the mitochondrial processing peptidase. The small TIM chaperones guide precursors of multi-spanning carrier proteins to the TIM22 complex, which facilitates their insertion into the inner membrane. The membrane potential across the inner membrane (Δψ) drives TIM23 and TIM22 dependent import. Mia40 sorts cysteine-rich precursors into the intermembrane space and mediates their oxidative folding. Erv1 shuttles the electrons from Mia40 to cytochrome c of the respiratory chain (adapted from (Böttinger et al, 2015). IMS – the intermembrane space.

Large-scale proteomic analysis and computational studies allow to identify ~1000 distinct proteins in fungi mitochondria and ~1500 - in animal mitochondria (Fukasawa et al, 2015). However the majority (~99%) of mitochondrial proteins have a nuclear origin

(Chacinska et al, 2009). They are synthesized in cytosol and imported to one of the four mitochondrial compartments by translocator complexes located in the mitochondrial membranes (Figure 1) (Bolender et al, 2008; Campo et al, 2016; Rao et al, 2012; Wenz et al, 2015).

## Targeting and sorting signals of mitochondrial precursor proteins

The precursors of mitochondrial proteins are firstly synthesized in the cytosol and then targeted to mitochondria. To reach the correct mitochondrial subcompartment, they possess cleavable or not-cleavable sequences, which mark the precise sorting pathway and determine the final location of imported proteins. While the nature of these signals is not uniform (Chacinska et al, 2009), they have rather common features (Figure 2).

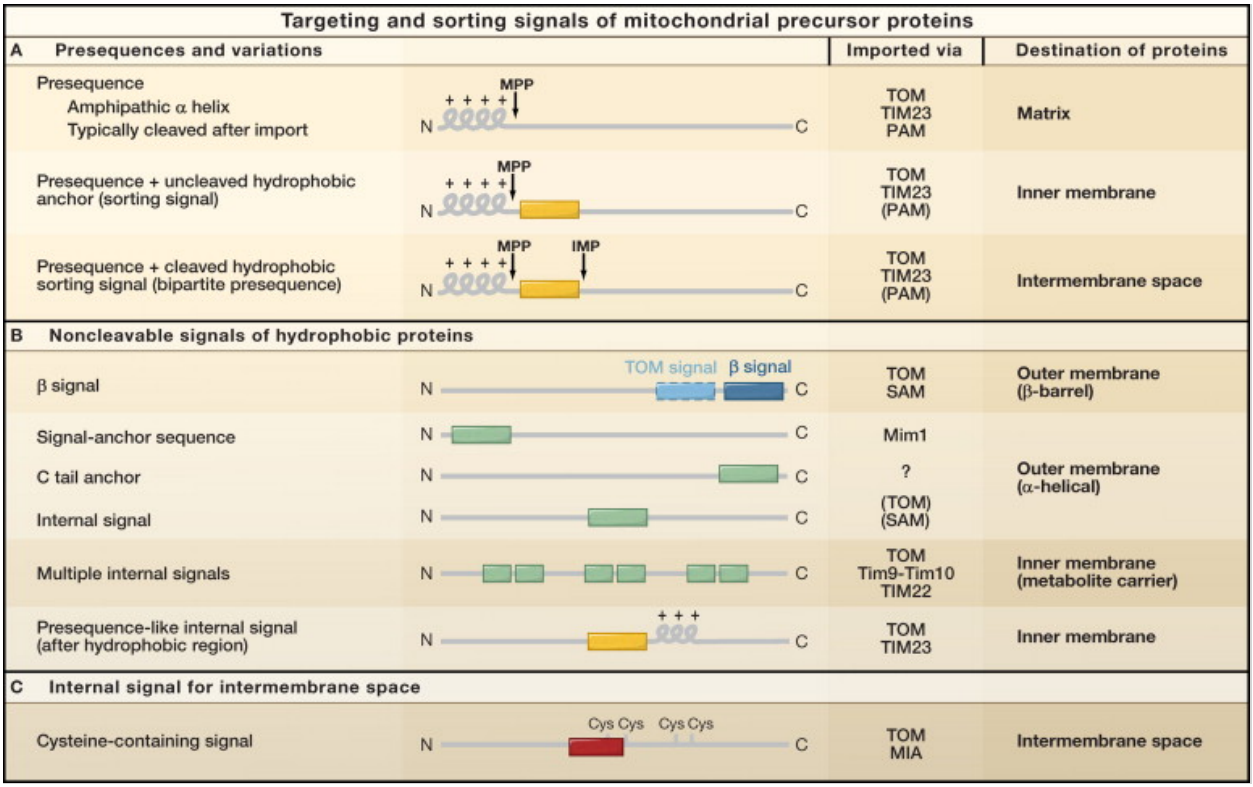


**Figure 2. Targeting and Sorting Signals of Mitochondrial Precursor Proteins.** Three groups of targeting signals can be identified (A) presequences located at the N-terminus, (B) multiple internal signals and (C) redox-regulated signals that provide transient covalent interaction with the corresponding import receptor (adapted from Chacinska et al., 2009).

Most matrix-targeting proteins contain a 10-50 amino acid cleavable pre-sequence located at the N-terminal extremity. Presequences are rich in positively charged, hydrophobic,

and hydroxylated amino acids, and tend to form amphiphilic α-helices. Both positive charges and amphipathic property of the presequence are important for its recognition by receptors of TOM-complex and following translocation (Abe et al, 2000). Upon translocation pre-sequences are usually cleaved by different peptidases such as the mitochondrial processing peptidase (MMP) (Taylor et al, 2001), mitochondrial intermediate peptidase (MIP) or others (Quiros et al, 2015). A few matrix proteins, as chaperonin 10, are synthesized with an amino-terminal presequence that remains a permanent part of the protein (Ryan et al, 1994). A hydrophobic stretch following the N-terminal presequence serves as additional sorting signal. It arrests the translocation of protein through the mitochondria inner membrane with following lateral release into the membrane (Glick et al, 1992).

A subset of mitochondrial proteins contains targeting signal at various positions within a mature protein, which are not cleaved upon translocation. Thus, the outer membrane β-barrel proteins bear the C-terminal targeting signal formed by the last β-strand which anchors the protein molecule in the membrane (Kutik et al, 2008). For the anchoring of Tom70 and Tom20 on the surface of mitochondria both N-terminal transmembrane domain and its positively charged C-flanking region are important (Kanaji et al, 2000). The outer membrane proteins of the α-helical type contain targeting sequences represented by the α-helical transmembrane segment often flanked by positively charged residues and located at the amino (signal anchor sequence) or at the carboxy terminus (tail anchor) as well as in the middle of the proteins (Chacinska et al, 2009).

Targeting signals of inner membrane proteins as metabolite carriers are more heterogeneous. Usually they consist of three to six domains, each of about 10 amino acid residues, scattered across the molecule. Cooperation of domains is required for recognition by import receptors and for efficient translocation of hydrophobic preproteins (Wiedemann et al, 2001).

Some mitochondrial inter-membrane space proteins contain non-cleaved signal (MISS) that include a conserved cysteine motif involved in transient disulfed-bonded intermediate formation with a receptor (Milenkovic et al, 2007; Milenkovic et al, 2009; Mordas and Tokatlidis, 2015).

## The TOM complex as the entry platform

TOM complex is the general entry gate for more than 90% of all mitochondrial proteins that transfers them to distinct translocators (Campo et al, 2016). In contrast to known membrane protein complexes, which structures have been defined, the TOM complex consists of both α-helical and β-barrel integral membrane proteins. Recently, the architecture of this complex was defined (Shiota et al, 2015). Tom20 is a general import receptor that cooperates with Tom22 to form a presequence receptor, *cis* site (Shiota et al, 2011; Yamano et al, 2008). While Tom20 interacts with the hydrophobic side of the presequence, Tom22 recognizes its hydrophylic region (Schulz et al, 2015). The proteins with internal targeting signals are preferably recognized by Tom70 (Brix et al, 1997; Endo and Kohda, 2002). Being recognized, precursor proteins cross the outer membrane through the β-barrel Tom40 channel (Gessmann et al, 2011), which possesses two different translocation pathways for different types of precursors. Cross-linking experiments revealed the acidic path within the Tom40 pore, while carrier proteins follow the path formed by hydrophobic residues (Gornicka et al, 2014; Shiota et al, 2015). Then the presequence is recognized by the so-called *trans* site of the TOM40 complex formed by the intermembrane space domain (IMS) regions of Tom40, Tom22, and Tom7 (Shiota et al., 2011). The increase in affinity toward the *trans* side provides the driving force for precursor translocation across the membrane (Schulz et al, 2015). It was demonstrated that the amino-terminal segment of Tom40 crosses the β-barrel from the cytosolic side to the intermembrane space possibly to block the pore or participate in translocation of the precursor proteins throughout the barrel (Shiota et al, 2015).

It was found that TOM complex presents two isoforms: the mature trimeric form dynamically exchanges with dimeric Tom22-less isoform providing the platform for reassembling and regulating protein transport (Shiota et al, 2015). TOM complex subunits could be phosphorylated: the phosphorylation of Tom40 precursor reduces import, whereas the phosphorylation of Tom6 precursor stimulates import and membrane integration (Rao et al, 2012; Schulz et al, 2015).

In addition, the small subunits Tom5, Tom6, and Tom7 are involved in the assembly and stability of the TOM complex (Sherman et al, 2005). The deletion of Tom6 destabilizes the

TOM complex, while the interaction of TOM subunits is stabilized in the absence of Tom7 (Becker et al, 2011b).

## Multifunctional inner membrane translocase TIM23

The TIM23 complex is one of the most complicated protein translocase in the cell presenting a highly dynamic structure. TIM23 contains the core proteins Tim23, Tim17, and Tim50, as well as Mgr2 and Tim21 as accessory subunits and the motor-associated proteins Pam 17, Tim16 (Pam16), Tim14 (Pam18), Tim44, mtHsp70, which are responsible for mediating the ATP-driven translocation across the inner membrane, and Mge1.

The TIM23 complex is a dynamic structure allowing translocation of proteins (Figure 3) with presequences into the mitochondrial matrix, as well as Mgr2/Tim17-dependent insertion of proteins bearing a stop transfer signal in the N-terminal region (Schulz et al, 2015).

Tim23 is the central subunit of the complex. The C-terminal and membrane bound domain of Tim23 form a channel while the unstructured IMS domain of Tim23 ($Tim23^{IMS}$) provides various interactions with different complex subunits, $Tom22^{IMS}$ and presequences (Alder et al, 2008; Waegemann et al, 2015). While Tim23 represents the minimal pore, the native translocase channel is built by Tim23/Tim17 oligomers. It was demonstrated that Tim17 is involved in substrate-induced voltage gating of the translocase channel, recruits with Pam17 and Pam18 of the PAM complex and participates in the lateral release of precursors into the inner membrane (Alder et al, 2008; Waegemann et al, 2015). The lateral release of precursors is also under control of Mgr2, the lateral gatekeeper (Ieva et al, 2014), which is, in addition, involved in Tim21 recruitment and cycling of Pam18 (Waegemann et al, 2015). Tim50 is the presequence receptor at the inner membrane (Schulz et al, 2011). Tim50 interacts with Tim23 via their IMS domains promoting the closed state of the channel in the absence of substrates, therefore maintaining the permeability barrier across the inner membrane (Meinecke, 2006).

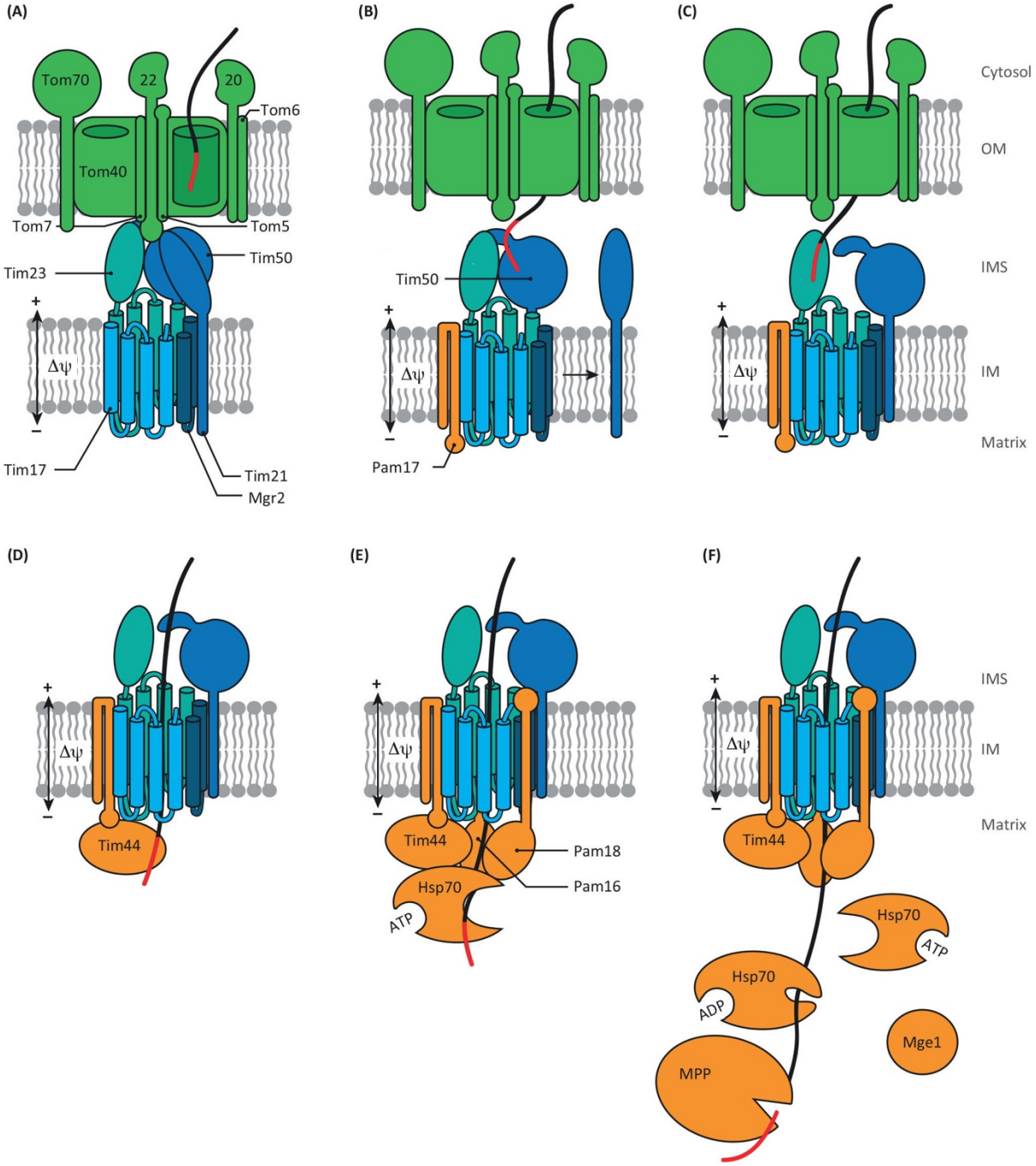


**Figure 3. The presequence pathway of mitochondrial protein import** (adapted from (Schulz et al, 2015). (A) TOM and TIM complexes are kept in close proximity by interactions of $Tom22^{IMS}$ with Tim50, Tim23 and Tim21. (B) Tim50 recognizes the presequence on the trans side of the TOM complex triggering Tim21 dissociation from the translocase and association of Pam17 with the complex. (C) Thereafter, presequence is passed to Tim23; (D) enters the channel and crosses the inner membrane driven by Δψ. On the matrix side, Tim44 binds the presequence. (E) Interaction of the presequence with Tim44, as well as assembling of the import motor, recruits Hsp70 in the ATP-bound state. (F) Pam18 stimulates Hsp70 to hydrolysis ATP and Hsp70 dissociation of Hsp70-ADP tightly bound to the substrate. Mge1 stimulates the precursor and Hsp70 dissociation by releasing of ADP. Thereafter, the pre-sequence can be removed by the mitochondrial processing peptidase and then processed by the intermediate cleaving peptidase 55 (Icp55) or the mitochondrial intermediate peptidase Oct1. OM – the outer membrane, IM – the inner membrane, IMS – inter-membrane space (Schulz et al, 2015).

The TIM23 complex cooperates with the TOM complex forming a path for effective translocation of ≈ 70% of proteins targeted into mitochondria (Waegemann et al, 2015). Complexes are kept in close proximity by interactions of $Tom22^{IMS}$ with Tim50 and Tim23 as well as Tim21 (Figure 3A), which also participates in the substrate-directed switching of the TIM23 complex between matrix translocation and inner membrane sorting modes (Mokranjac et al, 2005).

## TIM22 complex - a specialized translocase for metabolite carriers

A specialized TIM22 translocase is required for the biogenesis of a class of multispanning inner membrane proteins, including metabolite carriers or some translocase subunits like Tim17, Tim22, and Tim23. Upon translocation into the intermembrane space, this type of precursor is taken by small soluble Tim proteins arranged in subcomplexes, and is transferred to the TIM22 complex. The TIM22 translocase consists of four membrane subunits – Tim22, Tim18, Tim54, and Sdh3, and a peripheral Tim12 subunit (Campo et al, 2016). Large C-terminal domain of Tim54 exposed to the intermembrane space serves as a platform for docking of small Tim complexes bound with precursors. The protein-conducting channel of TIM22 consists of two pores formed by Tim22 (Rehling, 2003). The combined action of membrane potential and carrier precursor is responsible for the coordinated opening and closing of the TIM22 translocase (Peixoto et al, 2007). However, the mechanism of releasing of carrier precursors from the TIM22 complex into the inner membrane is still unknown.

## The MIA pathway: intermembrane space import and assembly

The biogenesis of IMS proteins with internal non-cleavable mitochondrial IMS-targeting/sorting signals (MISS) relies on Mia40, a redox-regulated IMS receptor that introduces disulfide bonds via several electron-transfer reactions (Chacinska et al, 2004). Another component of the MIA pathway is the thiol oxidase Erv1, which function is to recycle Mia40 by accepting electron from reduced Mia40 and transfering it to cytochrome c or molecular oxygen. A scheme of MIA pathway is represented on figure 4 (Mordas and Tokatlidis, 2015).

The import of IMS-targeted proteins does not require the inner membrane potential or matrix ATP hydrolysis. This is the only mitochondrial import pathway that results in a covalent modification of the imported precursors (Chacinska et al, 2004).

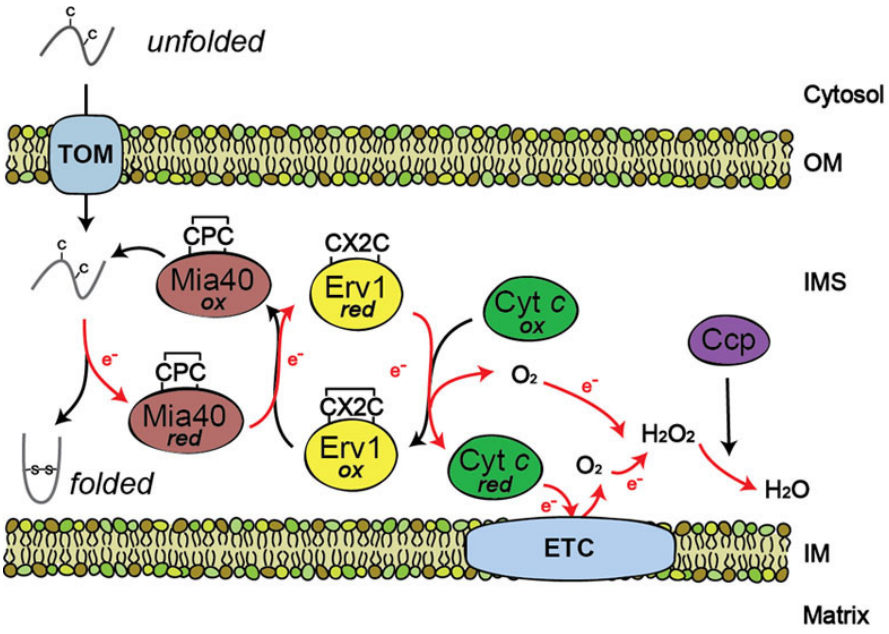


**Figure 4. The mechanism of the MIA pathway** (adapted from Mordas and Tokatlidis, 2015). The reduced and unfolded cytosolic precursor of IMS-protein containing MISS enters the mitochondria through the TOM complex following involvement into the MIA pathway. The reduced precursor donates the electron to the redox active cysteine-proline-cysteine (CPC) motif of Mia40. Erv1 reoxidizes Mia40 and transfere the electron to $O_2$ directly or through the cytochrome c (Cyt c) and cytochrome c oxidase. Ccp - cytochrome c peroxidase. ETC – the electron transport chain

## The SAM complex – a platform for β-barrel proteins biogenesis

β-barrel proteins of the outer membrane of mitochondria fulfill the protein and metabolite transport into mitochondria. Precursors of β-barrel proteins are imported via the TOM complex and directed by small Tim chaperons to the SAM (sorting and assembly machinery) complex, which mediates folding and integration of the precursors into the outer membrane (Wiedemann et al, 2003). The SAM complex consists of Sam50 (Tob55) (Kozjak et al, 2003), as central component of the complex, and two peripheral Sam35 and Sam37 subunits, which are largely exposed to the cytosol (Klein et al, 2012). Sam50 contains a soluble conserved polypeptide-transport associated domain (POTRA) and a transmembrane β-barrel channel (Stroud et al, 2011). The POTRA domain promotes a release of precursors from the SAM complex. Sam35 (Tob38) functions as a receptor that specifically recognizes the targeting

signal of β-barrel proteins (Waizenegger et al, 2004). Sam37 (Mas37) interacts with Tom22 on the cytosolic side of the mitochondrial outer membrane and thus contributes TOM–SAM supercomplex formation, as well as promotes SAM stability and precursor maturation (Wenz et al, 2015).

## The MIM machinery

The MIM (Machinery of the Inner Membrane) complex is crucial for the biogenesis of multispanning outer membrane proteins. Precursors of these proteins are recognized by the import receptor Tom70, but not its partner Tom20, and transfered to the MIM machinery, which mediates the insertion (Papić et al, 2011). The MIM complex is formed by multiple copies of Mim1 and Mim2 (Becker et al, 2011a; Dimmer et al, 2012). Mim1 associates with the SAM complex and is involved in the assembly pathway of β-barrel protein Tom40 (Becker et al, 2008). In addition, Mim1 stimulates the biogenesis of Tom20 and Tom70, which are anchored into the membrane via a single N-terminal α-helix (Becker et al, 2008). All these precursor proteins are delivered to the MIM machinery from the cytosolic side of the outer membrane. The insertion of precursors of other single-spanning outer membrane proteins from the cytosol involves TOM and SAM subunits or may occur independently.

An example of the MIM complex cooperation with protein import machineries of both membrane is demonstrated for Om45 . The precursor of Om45 is recognized by the receptors Tom20 and Tom22, translocated across the outer membrane by the means of the pre-sequence protein import machine but assembled into the outer membrane via the MIM machinery.

## RNA Import into Mitochondria

Apart from several protein genes, mitochondrial DNA contains a set of RNA genes including rRNAs and tRNAs. Except in the cases of land plants, a subset of green, red and brown algae, as well as protozoan *Reclinomonas*, most examined mitochondrial genomes lack a 5S rRNA gene (Adams and Palmer, 2003).

The number of mitochondria encoded tRNAs varies widely among eukaryotes from the absence of any tRNAs in apicoplexa or trypanosomatids (Pino et al, 2010; Tan et al, 2002) to self-sufficient in translation set of 22 to 27 tRNAs (Adams and Palmer, 2003). The absence of tRNA genes is rescued by mitochondrial import of nuclear-encoded tRNAs from cytosol. Sequence analysis of mitochondrial genomes suggests the existence of a mitochondrial tRNA import mechanism in a vast majority of species belonging to six eukaryotic supergroups (Figure 5). This analysis predicts the number of mitochondria tRNA genes and compares it with codons that are used by a corresponding mitochondrial translation systems. Hence, the import of cytosolic tRNA is suggested in case of absence of the relevant tRNAs genes in mtDNA. Nevertheless, yeast possess a complete set of tRNAs sufficient for mitochondrial translation but still require the import of nuclear-encoded $tRNA^{Lys}$ (Tarassov and Entelis, 1992). Such tRNAs candidates for «redundant» import cannot be identified by sequence analysis. Moreover, mitochondria encoded tRNAs can have non-canonical secondary structures, which depart significantly from canonical tRNA structures, that prevents their recognition using bioinformatic algorithms (Dörner et al, 2001).

There is no doubt that mitochondrial tRNA import appeared early in evolution (Lithgow and Schneider, 2010; Schneider and Maréchal-Drouard, 2000). There are lots of examples (especially in Opisthokonta) when one species possess a complete set of mitochondrial tRNAs while its close relative species lost all tRNAs. This argues in favour of the hypothesis of a polyphyletic origin of mitochondrial tRNA import: it was invented many times in different clades of the phylogenetic tree (Lithgow and Schneider, 2010; Schneider and Maréchal-Drouard, 2000).

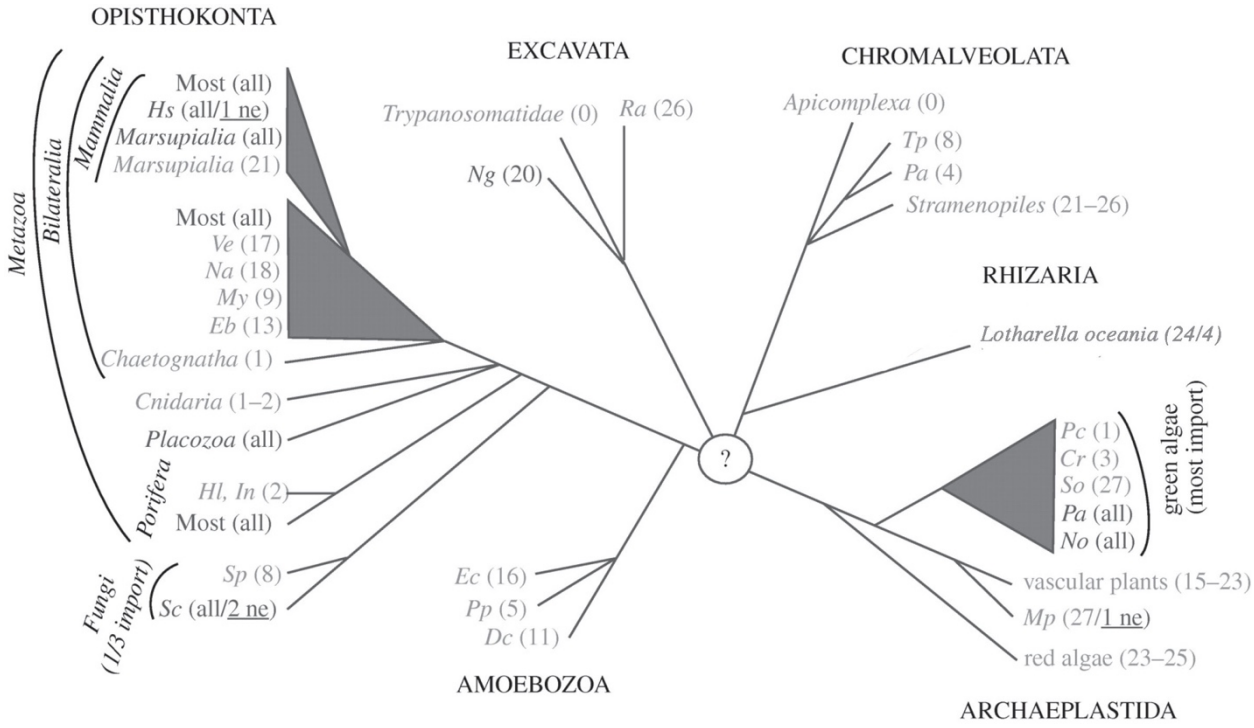


**Figure 5. Occurrence and distribution of mitochondrial tRNA import** (adapted from Lithgow and Schneider, 2010). Unrooted phylogenetic tree of the six eukaryotic supergroups (indicated in capitals). Branching order reflects the phylogenetic relationship of taxons but branch length is not to scale. Organisms having a complete set of mitochondrial tRNA genes are shown in dark grey. Organisms lack a variable number of apparently essential mitochondrial tRNA genes are shown in light grey. The numbers of tRNA genes encoded in the different mitochondrial genomes are indicated. «All» indicates that the mitochondrial-encoded tRNA gene set is complete and «0» indicates complete absence of mitochondrial tRNA genes. If organisms retain a single mitochondrial tRNA gene only it is always the $tRNA^{Met}$. The minimal number of tRNAs required for mitochondrial translation is, depending on the wobble rules and the genetic code variations, between 20–22. Even in organisms having more than 22 mitochondrial tRNA genes, the set of mitochondrial-encoded tRNA is often not complete and import of cytosolic tRNAs is required. In most of these cases, it is the $tRNA^{Thr}$ that is imported. In a few systems, import of a cytosolic tRNA that has the same decoding capacity as a still existing mitochondrial-encoded tRNA gene has been shown experimentally (shown underlined). Acronyms for species: *Hs, Homo sapiens*; *Ve, Vanhornia eucnemidarum*; *Na, Neomaskellia andropogonis*; *My, Mizuhopecten yessoensis*; *Eb, Epiperipatus biolleyi*; *Hl, Hypospongia lachne*; *In, Igornella notabilis*; *Sp, Spizellomyces punctatus*; *Sc, Saccharomyces cerevisiae*; *Ng, Naegleria gruberi*; *Ra, Reclinomonas americana*; *Tp, Tetrahymena pyriformis*; *Pa, Paramecium aurelia*; *Pc, Polytomella capuana*; *Cr, Chlamydomonas reinhardtii*; *Sc, Scenedesmus obliquus*; *Pa, Pseudendoclonium akinetum*; *No, Nephroselmis olivacea*; *Mp, Marchantia polymorpha*; *Ec, Entamoeba castelanii*; *Pp, Physarum polycephalum*; *Dc, Dictyostelium citrinum*. (Lithgow and Schneider, 2010).

The mitochondrial RNA import is a complex process which can be subdivided into two main stages – targeting a subpart of specific RNA pool to the surface of mitochondria followed by their translocation into organelles. Years of close scrutiny in a variety of organisms belonging to different phylogenetic branches suggest at least two distinct mechanisms of this process. The tRNA import in yeast, *T. brucei* and mammals seems to rely on protein factors while plants and *Leishmania* utilize factor-independent mechanism to deliver tRNAs into

organelles. The mitochondrial RNA import process is still largely not understood. The difficulty of studying mitochondrial RNA import stems from the lack of reliability of experimental *in vitro* system, which can satisfactorily reflect the in vivo situation. The better understood *in vitro* RNA import process of trypanosomatids does not rely on soluble factors to provide selectivity, which is crucial *in vivo* (Bouzaidi-Tiali et al, 2007; Tan et al, 2002). In *in vitro* import experiments with different cytosolic tRNAs into isolated *Solanum tuberosum* mitochondria, the *S. tuberosum* cytosol-specific $tRNA^{Gly}_{GCC}$ was imported into isolated mitochondria with the same efficiency as normally imported $tRNA^{Gly}_{UCC}$ (Delage et al, 2003a; Salinas et al, 2006), so this situation does not correspond to that *in vivo*.

## tRNA import into protozoan mitochondria

The mitochondrial genomes of trypanosomatids such as *T. brucei* and *Leishmania* spp. are devoid of tRNA genes (Schneider, 2011). So all mitochondrial tRNAs are imported from the cytosol, except $tRNA^{Met}_{i}$ and $tRNA^{Sec}$ that have exclusively cytosolic localization. The extent of mitochondrial localization of different nuclear-encoded tRNAs ranges from 1 to 7.5% (Tan et al, 2002). The mechanisms of regulation of those distributions have not been elucidated yet.

It is widely accepted that selectivity is based on the presence of tRNA import determinants, which favor the interaction with protein factors, and anti-determinants retaining non-importable tRNAs in the cytosol. Based on the discovery of import selectivity in different organisms, one can conclude that there is no universal import signaling. The signal for mitochondrial targeting can be represented as specific sequence or structural motifs spread over the tRNA molecules. In *Tetrahymena*, the anticodon of $tRNA^{Gln}$ apparently acts as an import determinant (Rusconi and Cech, 1996). Thus, *Tetrahymena* contains three $tRNA^{Gln}$ isoacceptors, two cytosol-specific ones, which decode codons UAA and UAG, while the third $tRNA^{Gln}_{UUG}$ is partly imported into mitochondria. Nucleotide substitutions in the UUG anticodon uniquely abolished import while substitution of a single anticodon nucleotide (UUA → UUG) confered import of a normally non-imported glutamine tRNA. All these facts demonstrate that the anticodon UUG is both necessary and sufficient for tRNA import (Rusconi and Cech, 1996).

The comparison of $tRNA^{Met}_i$ and the $tRNA^{Met}_e$ revealed that the pair U51:A63 in the T-stem is the main anti-determinant of mitochondria localization in *T. brucei*. It inhibits the import of $tRNA^{Met}_i$ and prevents its interaction with the cytosolic elongation factor eEF1a (Crausaz Esseiva et al, 2004). Such a mechanism is also inherent in $tRNA^{Sec}$ where the U8:U66 base pair also acts as anti-determinant and retains $tRNA^{Sec}$ in the cytosol by preventing binding with eEF1a (Bouzaidi-Tiali et al, 2007).

Chemical modifications may also affect the mitochondrial import process. The study of *Leishmania tarentolae* $tRNA^{Glu}_{UUC}$ and $tRNA^{Gln}_{UUG}$ demonstrated that cytosol-specific thiolation of tRNAs at wobble position of anticodon served as the anti-determinant for import of those RNAs (Kaneko et al, 2003). This mechanism is not general and does not seem to take place in *T. brucei*, a close relative of *Leishmania* (Bruske et al, 2009). The down regulation of TbNfs, the master desulfurase responsible for both Fe-S cluster formation and tRNA thiolation, led to reduction of the overall thiolation level but did not alter the distribution of *T. brucei* tRNAs (Paris et al, 2009).

In *Leishmania tropica* two types of import sequences were discernible depending on their localization: type I (D-arm motif YAGAGY of several imported tRNAs and D-arm motif shared by $tRNA^{Ile}$ and $tRNA^{Val}_{CAC}$ as well as anticodon arm of $tRNA^{Arg}_{ACG}$) and type II ($CUG_{3\text{-}4}U$ located in V-T region of $tRNA^{Ile}$ and other tRNAs) (Bhattacharyya et al, 2002). These types demonstrated different import abilities: type I RNAs are efficiently transferred through the inner membrane and are inhibited by type II whereas type II RNAs have poor inner membrane transfer efficiencies and are stimulated by type I (Bhattacharyya et al, 2002). Thus, regulation of tRNA pools inside mitochondria is provided by cooperative or antagonistical interaction of tRNAs with different receptors on the inner mitochondrial membrane in a so-called «ping-pong» import regulation model (Bhattacharyya et al, 2003).

Some tRNAs may have several determinants; for example, *L. tarentolae* $tRNA^{Ile}$ contains both the D domain and the V-T region motifs. D-arm exchange between the mainly cytosolic $tRNA^{Gln}$ and the efficiently imported $tRNA^{Ile}$ leads to increased localization of $tRNA^{Gln}$ in mitochondria, but does not prevent the mitochondrial localization of the chimeric $tRNA^{Ile}$ (Lima and Simpson, 1996).

It was observed that the determinants for tRNA cytosolic localization coincide with anti-determinants for eEF1a interaction (Bouzaidi-Tiali et al, 2007; Crausaz Esseiva et al, 2004). In addition, the depletion of eEF1a in *T. brucei* reduced import of newly synthesized tRNAs. All this indicates that eEF1a plays an important role in tRNA import process. eEF1a discriminates imported tRNAs, then hands them over toward the outer membrane where they interact with a specific receptor. The receptor is not able to discriminate between cytosol-specific tRNAs and imported tRNAs, which is consistent with the loss of specificity in *in vitro* tRNA import system lacking eEF1a (Bouzaidi-Tiali et al, 2007). To explain why a translation factor eEF1a helps a subpopulation of aminoacylated tRNAs to escape cytosolic translation and targets them to the mitochondria, the existence of two functionaly different eEF1a populations was suggested (Bouzaidi-Tiali et al, 2007).

A precise mechanism of the tRNA translocation across the mitochondrial double membrane in trypanosomatids is unknown but it depends on ATP hydrolysis. In *T. brucei* tRNA mitochondrial import shows a connection with the mitochondrial protein import like in *S. cerevisiae* and in plants but, unlike plants, does not require VDAC (Pusnik et al, 2009). *Tb*Tim17 and *Tb*mHsp70 are directly involved in tRNA import *in vivo* as deletion of these proteins leads to inhibition of tRNA import. However, possible reason for the tRNA import inhibition could be a lack of import of additional unknown tRNA import factor (Tschopp et al, 2011). It was suggested that *Tb*Tim17 and *Tb*mHsp70 are physically associated with other proteins including *Tb*11.01.4590 and *Tb*09.v1.0420 to form the tRNA translocon of *T. brucei* (Seidman et al, 2012).

In *L. tropica*, prior to translocation, tRNAs interact with the outer mitochondrial membrane receptors one of witch is TAB (tubulin antisense-binding protein) (Adhya et al, 1997; Bhattacharyya et al, 2002). The experiments with mutant forms of the D-arm of $tRNA^{Tyr}$ allowed suggesting the presence of distinct receptors in the outer and the inner membranes (Bhattacharyya et al, 2000). Northing is known about a pathway for tRNA translocation through the double-mitochondrial membrane. However, it was suggested that a unique channel found in *L. tropica* provides a transport of tRNAs through the inner mitochondrial membrane (Figure 6B).

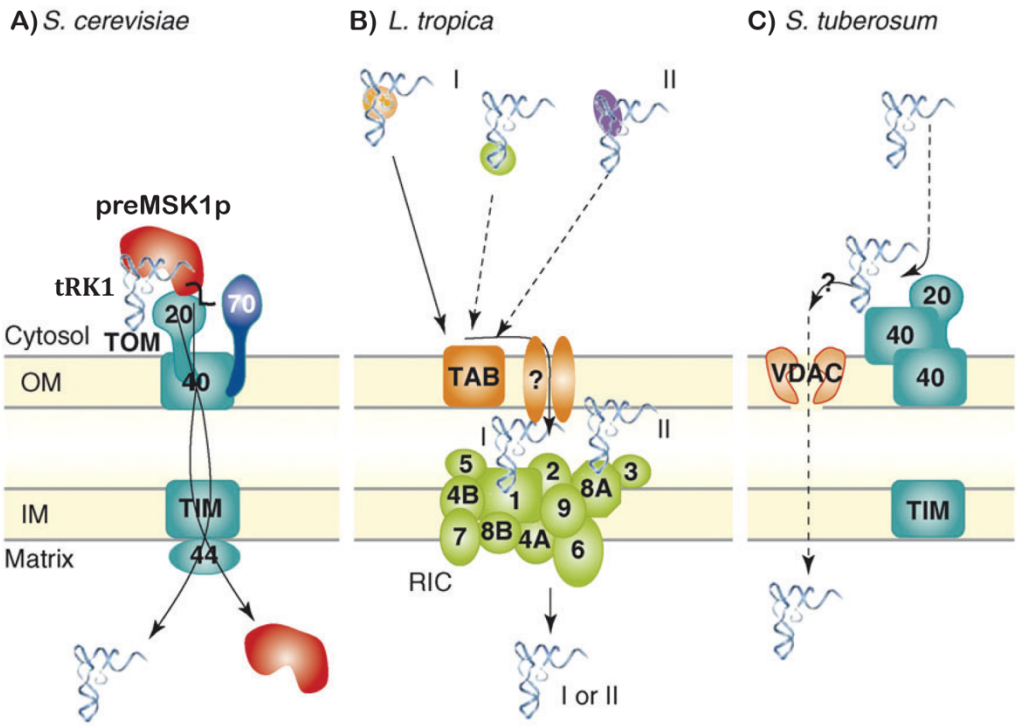


**Figure 6. Mitochondrial tRNA-import translocation pathways of *S. cerevisiae*, *L. tropica* and *S. tuberosum*** (adapted from Salinas et al., 2008). A) In *S. cerevisiae*, the import of the nuclear-encoded $tRNA^{Lys}_{CUU}$ (blue ribbon) relies on its non-canonical interaction with its carrier protein preMSK1p (red). The receptor Tom20 (turquoise) (but not Tom70; blue) of the TOM complex and Tim44 (turquoise) of the TIM complex are essential for tRNA import. B) In *Leishmania tropica*, tRNAs are first bound to outer mitochondrial membrane (OM) receptors one of which is TAB (orange). Next, tRNAs are translocated through the outer membrane via an unknown pathway. The translocation of tRNAs across the the inner membrane (IM) might occur through RIC complex. Two receptors, RIC1 and RIC8A, bind with tRNAs, which then are translocated through the pore constituted by RIC6 and RIC9. C) In *Solanum tuberosum*, tRNA import depend on two major components of the TOM complex, TOM20 (turquoise) and TOM40 (turquoise), which fix tRNAs at the mitochondrila surface. The voltage-dependent anion channel (VDAC; orange) creates a pore for tRNAs translocation through the outer mitochondrial membrane. A pathway of the inner membrane translocation remains unknown.

This is the 640 kDa tRNA import complex (RIC) located on the inner mitochondrial membrane. The system reconstructed with RIC in phospholipid vesicles demonstrated characteristic features of the *Leishmania* RNA import including the allosteric regulation between two different subsets of tRNAs (type I and type II) (Chatterjee et al, 2006). Native RIC contains 11 different subunits, 6 of which are essential and sufficient for import activity. The knockdown of these six subunits led both to inhibition of mitochondrial tRNA import and mitochondrial translation. RIC1 corresponds to the α subunit of the $F_1$-ATP synthase of the complex V and provides energy for import whereas RIC8A is the subunit 6b of complex III of the respiratory chain. As well as RIC1, RIC8A appeared as a receptor allosterically interacting with distinct tRNA subsets (Bhattacharyya et al, 2003; Mukherjee et al, 2007). Three other

components, RIC5, RIC6, and RIC9, are also parts of respiratory complexes. RIC9 transfers tRNA from receptors to the import pore. A voltage-gated minimal translocation pore of RIC is constituted by RIC6, RIC9, and RIC4A (Koley and Adhya, 2013). However, the published data raise several questions concerning the existence and functioning of RIC (Salinas et al, 2008). To date, the RIC complex has been identified only in *L. tropica* and it was demonstrated that mitochondrial tRNA import in *T. brucei* does not depend on Rieske protein, which is one component of RIC (Paris et al, 2009).

## tRNA import into plant mitochondria

In plants, the number and identitiy of imported tRNAs vary greatly even in closely related species. Nevertheless, the existence of exclusively cytosolic tRNAs and distinct extent of mitochondrial localization for different tRNAs point to a selection step in mitochondrial import. Different nucleotides or domains including the anticodon, the D-arm and T-domain in $tRNA^{Val}$ (Delage et al, 2003b; Laforest et al, 2005), position 70 in $tRNA^{Ala}$ (Dietrich et al, 1996) were revealed as import determinants. Absence of common import sequence signature led to a hypothesis that a conformation of the tRNA and not particular nucleotides may be specifically recognized during import (Laforest et al, 2005). Mutagenetic studies demonstrated a certain level of correlation between import and recognition by a cognate aminoacyl-tRNA synthetase indicating its involvement into mitochondrial RNA import in plants (Delage et al, 2003a). Although it is suggested that the aminoacyl-tRNA synthetase is implicated into tRNA mitochondrial import in plants but is not sufficient for that process. For example, in *S. tuberosum* two cytosolic $tRNA^{Gly}$ with UCC and CCC anticodons are selectively imported into mitochondria, and $tRNA^{Gly}_{GCC}$ is retained in cytosol while all isoacceptors can be recognized by the glycyl-tRNA synthetase (Delage et al, 2003a). As an explanation, it was suggested that the fate of a cytosolic tRNA depends on the interaction with either cytosolic aaRS, which addresses it to cytosolic translation, or precursor form of mitochondrial aaRS that directs it into mitochondria (Duchêne et al, 2011; Duchene et al, 2005).

tRNA import into plant mitochondria requires both a membrane potential and ATP. Whereas *in vitro* import of tRNAs can be achieved independently from additonal cytosolic factors, the selectivity of this system is limited (Salinas et al, 2006). Two components of the

plant TOM complex (Tom20 and Tom40) are required for ATP-dependent tRNA-binding at the mitochondrial surface *in vivo* (Salinas et al, 2006; Salinas et al, 2014). Thereafter, tRNAs are translocated across the membrane through a pore formed by VDAC (Figure 6C). An angagement of VDAC is confirmed by inhibition experiments of tRNA import into isolated mitochondria by VDAC antibodies and ruthenium red (Salinas et al, 2006).

## tRNA import into yeast mitochondria

The mitochondrial import of *Saccharomyces cerevisiae* $tRNA^{Lys}_{CUU}$ (tRK1) represents a highly selective system. A fraction lower than 5% of the cytosolic tRK1 was shown to associate with mitochondria, whereas the other isoacceptor $tRNA^{Lys}_{UUU}$ (tRK2) is restricted to cytosol (Tarassov and Entelis, 1992). Previously, it was suggested that the anticodon of tRK1 (especially the wobble position $C_{34}$ of the anticodon) and the acceptor stem contain determinants for its import selectivity (Entelis et al, 1998). Thereafter, it was assumed that a tRNA secondary structure rearrangement provides the major contribution to import selectivity (Figure 7). Only molecules comprising a folded TΨC hairpin, and which are able to adopt a particular F-hairpin immediately followed by the 3′-end (Figure 7B) proceed to the import pathway (Kolesnikova et al, 2010).

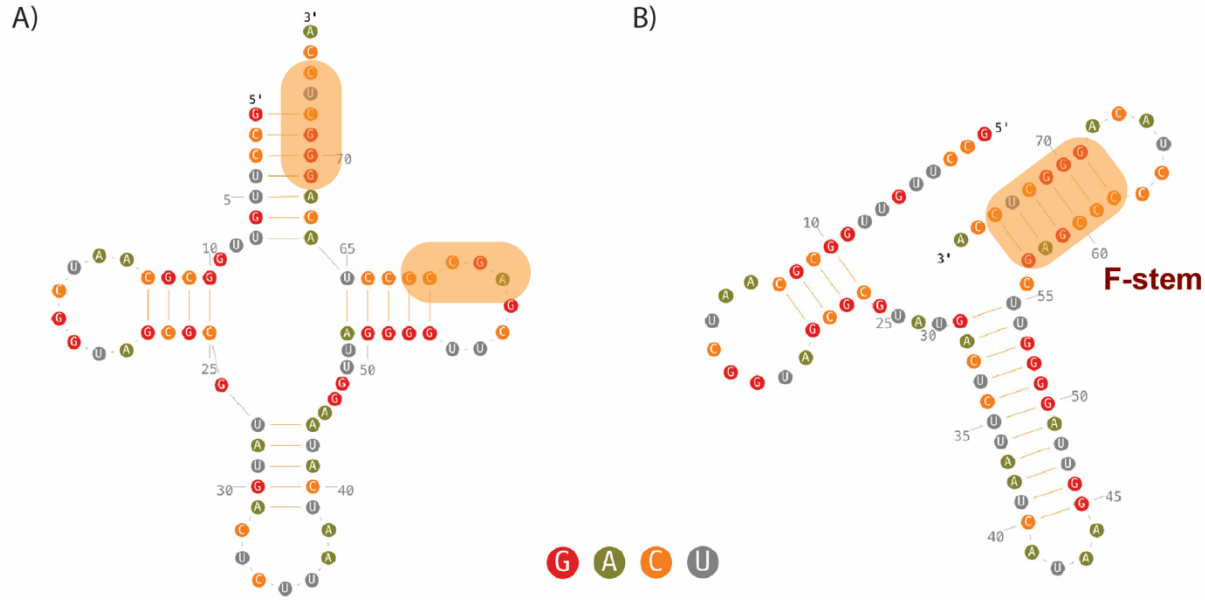


**Figure 7. Secondary structures of tRK1.** (A) classical clover-leaf structure and (B) F-form (Baleva et al, 2015). Regions of tRK1 involved in F-stem formation as well as F-stem are in color box.

Transfer RNAs are involved in cytosolic translation and recycled during protein synthesis. To be targeted into mitochondria nuclear-encoded tRNAs must escape the translation machinery cycle possibly due to interaction with protein factors (Figure 8A). In *S. cerevisiae*, the imported tRK1 is firstly charged by the cytosolic lysyl-tRNA synthetase (KRS) (Tarassov et al, 1995b), and then is specifically recognized by Eno2p - one of the two isoforms of the glycolytic enzyme enolase (Entelis et al, 2006). It was suggested that Eno2p induces conformational changes in the aminoacceptor stem of tRNA molecules and discriminates imported molecules. The tRNA-Eno2p-containing complex is then transfered toward the mitochondrial surface, where the tRNA is handed to the precursor of mitochondrial lysyl-tRNA synthetase (preMSK1p) (Tarassov et al, 1995b), which is synthesized mainly in the vicinity of mitochondria (Entelis et al, 2006). In complex with preMSK1p, tRK1 adopts an "intermediate" conformation, which thereafter facilitates re-folding of tRK1 into the classic L-shape structure (Kolesnikova et al, 2010). Enolase integrates into a glycolytic multiprotein complex that is associated with the mitochondrial outer membrane, whereas a tRK1-preMSK1p complex co-imports into mitochondria (Entelis et al, 2006).

In *S. cerevisiae*, tRK1 is co-imported with preMSK1p. While the translocation of preproteins through the mitochondrial membrane requires it to be unfolded, it is not clear how tRNA remains bound to the carrier protein. It is possible that while in complex with tRK1 during the import, preMSK1p adopts a conformation allowing interaction with tRNAs (Entelis et al, 1998). This agrees with the experimentally demonstrated targeting of branched polypeptides or chimeric proteins fused with single- or double stranded oligonucleotides into mitochondria (Brokx et al, 2002). In addition, the experiments with a nicked tRK1 transcript were in favor of import of folded tRK1 molecule as well as importance of the tRNA L-shape structure (Entelis et al, 1998).

The tRK1 translocation into mitochondria requires ATP and the membrane potential as well as the intact protein machinery. The investigation of tRK1 import in yeast strains carrying deletions of different receptors of TOM and TIM translocases revealed the importance of Tom20 and Tim44 (Figure 6A) (Tarassov et al, 1995a). The deletion of those proteins abolished tRK1 import while the absence of Tom70 did not show any effect (Tarassov et al, 1995a).

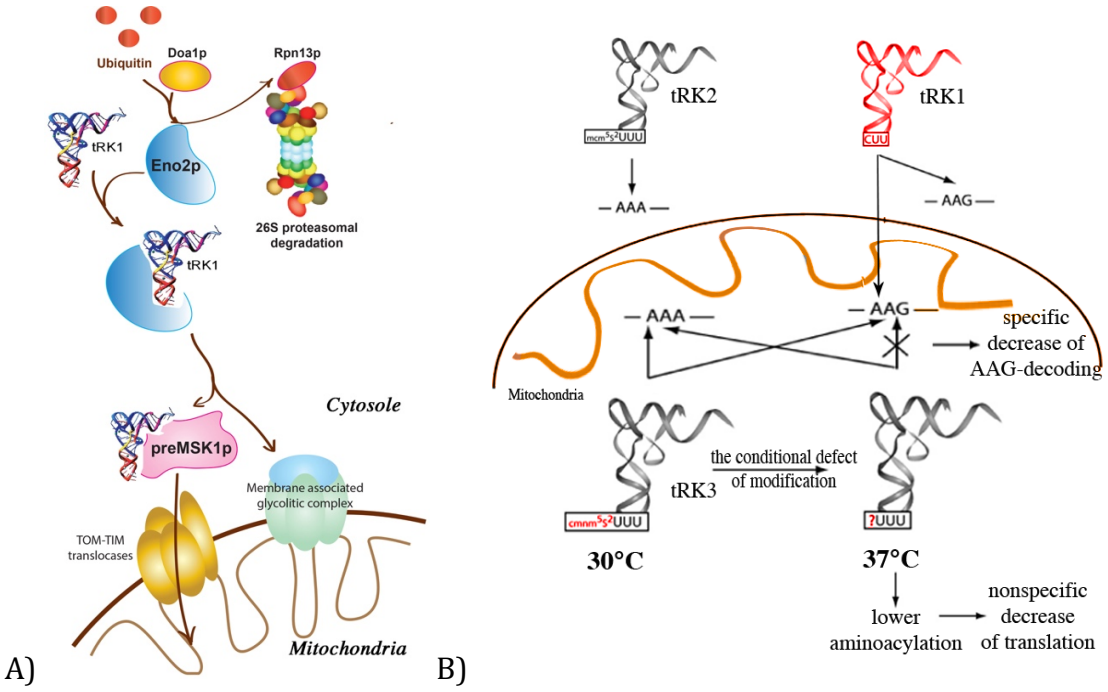


**Figure 8. Mitochondrial tRK1 import in *S. cerevisiae*, its possible regulation, and implication in the adaptation.** A) Aminoacylated tRK1 can be addressed either towards the cytosolic translation or towards the mitochondria. This choice can be determined by interaction of the RNA with either cytosolic retention factors or mitochondrial import factors and regulated by the ubiquitin-proteasome system (UPS). Two proteins were involved in this mechanism. Doa1p participates in specific ubiquitination of import factors as Eno2p or factors involved in tRK1 retention in cytosol while Rpn13p recognizes ubiquitinated proteins and degraded them by the proteasome (Brandina et al., 2007). Eno2p selects imported tRK1 molecules and deliver them to newly synthesised preMSK1p molecules at the mitochondrial surface. Eno2p participates to a large membrane associated glycolytic complex whereas tRK1 is delivered into mitochondrial matrix in complex with preMSK1p possibly via protein import translocases (Entelis et al., 2006) B) Adaptation mechanism involving tRK1 import (adapted from Kamenski et al., 2007). Mitochondrial tRK3 can decode both AAA and AAG codons in mitochondrial mRNAs at normal conditions (30°)C, while at non-permisive conditions (at 37°C) loose the ability for efficient decoding of AAG due to hypomodified U34 in the wobble position of tRK3. Thus, imported tRK1 can cure the deficiency by decoding the AAG codons.

In *S. cerevisiae*, cytosolic $tRNA^{Lys}_{CUU}$ (tRK1) is involved in organellar translation. Under normal conditions $tRNA^{Lys}_{CUU}$ import seems redundant since there is mitochondria-specific $tRNA^{Lys}_{UUU}$ (tRK3) that can decode AAA and AAG codons, both found in mitochondrial open reading frames. Yet, elevated temperature leads to modification defect of the 2-thio group of the $U_{34}$ from the tRK3 anticodon. The absence this modification may prevent translation of AAG codons, while the imported tRK1 cures this deficiency (Figure 8B) (Kamenski et al, 2007).

Since tRK1 role inside the mitochondria is conditional, tRK1 import can be also regulated conditionally. Thus, in *S. cerevisiae* two proteins, Rpn13p and Doa1p, which are the components of the ubiquitin-proteasome system (UPS), were identified as possible tRNA

mitochondrial import regulators (Brandina et al, 2007). Depletion either Rpn13p or Doa1p increased efficiency of tRK1 import. It was proposed that Doa1p participates in specific ubiquitination of import factors as Eno2p or others not yet identified, while Rpn13p recognizes them and proceeds to proteasome degradation (Figure 8A). Moreover, other proteins, which promote retention of the tRNA in the cytosol, can be substrates of UPS-degradation (Brandina et al, 2007) and regulation of their level can also influence tRK1 mitochondrial import efficiency.

It was published that nuclear-encoded $tRNA^{Gln}_{CUG}$ and $tRNA^{Gln}_{UUG}$ were imported into yeast mitochondria (Rinehart et al, 2005) as well as into rat and human mitochondria (Rubio et al, 2008). Unlike tRK1 import, the import of $tRNA^{Gln}_{CUG}$ and $tRNA^{Gln}_{UUG}$ *in vitro* does not require aminoacylation or any cytosolic factors. The $tRNA^{Gln}_{CUA}$ was able to suppress amber mutation of mitochondrial gene in yeast, which indicates its participation in mitochondrial translation (Rinehart et al, 2005). Nevertheless, the biological functions of *in vivo* import of those tRNAs are not clear. It was shown that mitochondria use the transamidation pathway to generate mitochondrial Gln-$tRNA^{Gln}$ that is used only by the mitochondrial translation apparatus to decode both CAG and CAA glutamine codons (Araiso et al, 2014; Frechin et al, 2009).

## Enolase in other life processes

Studies of RNA mitochondrial import have reported that the enzyme enolase could be a major player in this process (Entelis et al, 2006). That was confirmed by numerous tests (genetic and biochemical). Enolase is a very abundant protein in cell that somehow constraining cells to adapt many functions to its presence. Hence, with this idea in mind, it is interesting to describe in the present sub-part the numerous and very diverse functions in which enolase is involved, from bacterial infections to cancer response.

Enolase (or 2-phospho-D-glycerate hydrolase) is a highly conserved protein found in nearly all organisms both aerobic or anaerobic. Enolase is a metaloenzyme (Poyner et al, 2001) that is responsible for the reversible catalysis of the conversion of 2-phosphoglycerate to phosphoenolpyruvate (Figure 9) in glycolysis and gluconeogenesis.

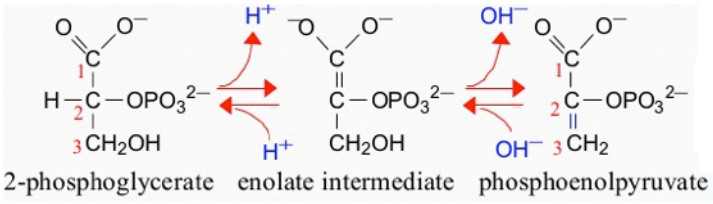


Figure 9. The scheme of the reaction catalyzed by enolase showing the removed hydroxyl group on carbon 3 and the resulting formation of the enol moiety.

Many organisms have different enolase isoforms, the expression of which vary according to the pathophysiological conditions of cells, metabolic demands, or developmental stage of the organism (McAlister and Holland, 1982; Tanaka et al, 1985; Barbieri et al, 1990). In mammals, like in all vertebrates, enolase occurs as three isoenzymes: α-enolase is found in a variety of tissues including liver, β-enolase is muscle specific and γ-enolase is found in neuron and neuroendocrine tissues (Royds et al, 1982). Expression of different enolase isoforms changes during embryonic development for example β-enolase is expressed in differentiated skeletal muscles, while in the embryonic primary fibers and myotubes enolase is presented mainly by -isoform (Barbieri et al, 1990).

Yeast have two isoforms of enolase. The expression of yeast enolase isozymes is dependent on the carbon source, glucose, or a nonglycolytic substrate, while their kinetic properties are very similar (McAlister and Holland, 1982).

Recent studies have reported a lot of other functions for enolase in addition to its innate glycolytic function (Pancholi, 2001; Diaz-Ramos et al, 2012). Thus, enolase was identified as τ-crystallin in fish, reptiles, birds and lamprey eye lens. In lens, enolase is present as monomer and shows significantly low enzymatic activity (Wistow et al, 1988).

The alternative translation of the α-enolase mRNA results in a 37 kDa protein which lacks the first 96 amino acid residues - c-myc promoter-binding protein 1 (MBP-1). Unlike enolase, which has cytosolic localization, MBP-1 is found in the nucleus. MBP-1 binds the c-myc P2 promoter and down-regulates expression of the c-myc proto-oncogen, which plays an important role in the regulation of cell growth and differentiation (Subramanian and Miller, 2000).

In *Saccharomyces cerevesiae*, enolase was identified as a heat-shock protein (HSP48) involved in thermal tolerance and growth control (Iida and Yahara, 1985).

Enolase was found as a strong plasminogen-binding receptor on the surface of different cells such as hematopoetic cells, epithelial cells, neuronal cells, carcinoma cells and also on Gram-positive cocci, *Candida* and parasites. α-enolase interacts with plasminogen and induces activation of plasminogen by plasminogen activation system (PAs) and protects plasmin from inhibition by α2-antiplasmin (Figure 10). (Diaz-Ramos et al, 2012)

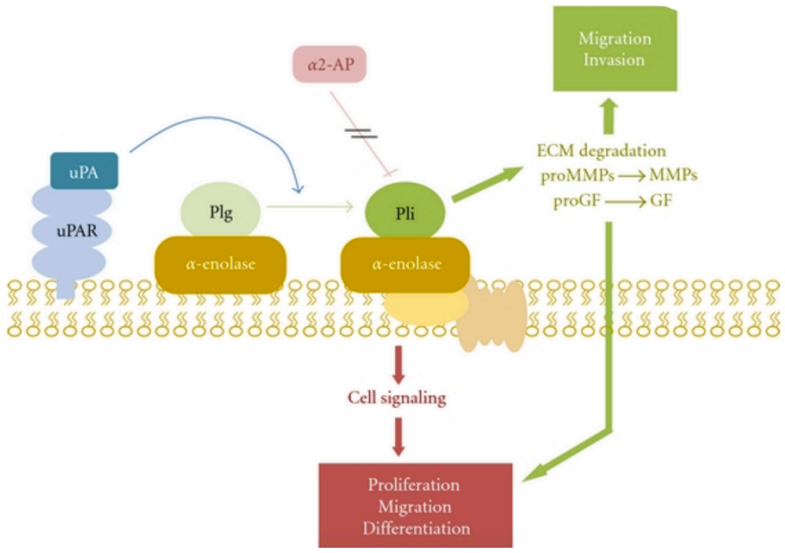


Figure 10. Scheme of α-enolase/plasminogen interaction on the cell surface. α-Enolase enhances plasminogen activation on the cell surface, concentrates plasmin proteolytic activity on the pericellular area and protects plasmin from its inhibitor α2-antiplasmin. Once activated, plasmin can degrade most of the components of the extracellular matrix, directly or indirectly by activating metalloproteases. It is also capable to activate prohormones of progrowing factors. Abbreviations: Plg, plasminogen; Pli, plasmin, α2-AP, α2-antiplasmin; uPA, urokinase-type plasminogen activator, uPAR, urokinase-type plasminogen activator; ECM, extracellular matrix; MMPs, metalloproteases; GF, growing factors. (Diaz-Ramos et al, 2012)

Plasminogen binding ability of cell surface expressed enolases results in the involvement of enolase in initiating some disease processes, tumor invasion and metastasis through activation of a serine-protease involved in extracellular matrix degradation. Yet, enolase participates in remodelling of actin cytoskeleton by induction of actin polymerisation and distribution and regulation of the PhoA cyclin-dependent kinase (Hafner et al, 2012). In addition, enolase interacts with actin and tubulin and could contribute to myogenesis (Keller et al, 2007). Similarly, interaction of enolase with the cytoskeleton may be closely related to the invasiveness of cancer cells (Trojanowicz et al, 2009). Another major contribution of

enolase to tumor progression is its requirement for maintaining the Warburg effect (aerobic glycolysis) in cancer cells. Enolase knockdown rescues oxidative phosphorylation and impairs the tumor growth (Capello et al, 2016). Enolase also acts as pro-survival factor supporting cancer cells adaptation to different stresses including hypoxia, chemo- and radiotherapy (Yan et al, 2011).

Taken together, these finding strongly suggest that enolase could be used as a promising therapeutic target for cancer diagnosis and anti-cancer therapy (Jung et al, 2013; Benjamin et al, 2016)

## Mitochondrial RNA import in mammals

Mammalian mitochondria encode 13 proteins, 2 rRNAs and a set of 22 tRNAs required for reading all codons (Florentz et al, 2003). Since mammalian mitochondria possess a full minimum set of tRNAs for efficient translation, there is no reason to suggest the existence of mitochondrial tRNA import. Nevertheless, the analysis of human mitochondrial transcriptome demonstrated more diverse population of mitochondrial RNAs than previously suggested (Mercer et al, 2011), together with the enrichment of several nuclear RNAs including several tRNAs. In addition, it is not known yet whether nuclear-encoded mammalian $tRNA^{Lys}$ can be imported into mitochondria while $tRNA^{Lys}$ is absent in the marsupial mitochondrial genome (Dörner et al, 2001). Moreover, the sequence analysis of the only nuclear-encoded tRNA which is associated with highly pure mitochondria, shows the enrichment of $tRNA^{Lys}$ (Dörner et al, 2001).

Demonstration of yeast tRK1-targeting into isolated human mitochondria in the presence of yeast import factors has unraveled the existence of a cryptic mechanism for tRNA import (Kolesnikova et al, 2004). This mechanism presents similarities with that of yeast (Gowher et al, 2013). Thus, preKARS2, the precursor of human mitochondrial lysyl-tRNA synthetase, is implicated both *in vitro* and *in vivo* in tRNA import in human mitochondria (Gowher et al, 2013). Moreover, yeast or rabbit enolase facilitated tRNA-preKARS2 interaction *in vitro* and further import of this complex into isolated human mitochondria. Artificial RNA minimal import substrates bearing two hairpins characteristic of the tRK1 F-

form were also efficiently imported into human mitochondria *in vivo* and *in vitro* (Gowher et al, 2013).

Import of RNA components of RNase MRP and RNase P was also suggested. RNase MRP is a site-specific endoribonuclease that is suggested to be involved in the processing of mitochondrial RNAs and also in mitochondrial DNA replication (Stohl and Clayton, 1992).

Mammalian RNase P participates in the processing and removal of tRNAs separating the regions coding for oxydative phosphorylation (OXPHOS) protein subunits (Doersen et al, 1985; Klemm et al, 2016). The mitochondrial genome of *S. cerevisiae* encodes the RNase P RNA but lots of species do not possess a certain gene in their mtDNA. The first evidence for import of both RNaseP RNA and RNase MRP RNA came when their processing activity was recovered from isolated human mitochondria pretreated with micrococcal nuclease (Doersen et al, 1985). Thereafter, two RNAs were identified to be identical in sequence to nuclear H1 RNA and MRP RNA by Nothern blot hybridization (Puranam and Attardi, 2001).

Nothing is known about the mechanisms that address these RNAs to mitochondria. However, a highly conserved 3′→5′ exoribonuclease, PNPASE, seems to be implicated in the import of RNase P and MRP RNA components (Wang et al, 2010). It was suggested that a 20 ribonucleotide stem-loop of both RNAs interact with PNPASE in a manner that triggers only import rather than processing. Moreover, a fusion of this structure with non-imported RNA allowed import of these constructions (Wang et al, 2010; Wang et al, 2012). However, the mitochondrial import of RNA component of RNase P was questioned after reporting that human mitochondrial RNase P is proteinaceous and consists of three MRPP subunits (for PROtein-only RNase P or PROteinaceous RNase P) (Holzmann et al, 2008; Klemm et al, 2016). PROPR was also found in plant mitochondria and chloroplasts. PROPR proteins were able to functionally replace RNA-containing RNase P in complementation experiments in *Escherichia coli* (Gobert et al, 2010) and *Saccharomyces cerevisiae* (Weber et al, 2014). Nevertheless, at present, it is assumed a possibility for a co-existence of both types of RNase P within mitochondria (Wang et al, 2010).

5S rRNA is an integral part of the large ribosomal subunit of all cytosolic ribosomes, but mitochondria of only land plants, algaes and few protists encode its gene (Adams and Palmer,

2003). It was demonstrated that cytosolic 5S is imported into mitochondria representing an example of a highly selective targeting system. 5S RNA is rather short (120 nt) with highly conserved secondary and tertiary structures (Smirnov et al, 2008b).

It adopts a three-domain Y-shaped organisation (Figure 11). The α-domain is formed by helix I, domains β and γ have a heterogenous structure that includes both helical and loop regions. Two regions of 5S rRNA, the proximal part of helix I containing the conserved G7-U112 pair and the site associated with the loop E-helix IV region of domain γ, were discribed as determinants of mitochondrial localization. Destruction or destabilisation of these parts significantly decreased the import efficiency, whereas disruption of both sites led to loss of import (Smirnov et al, 2008a).

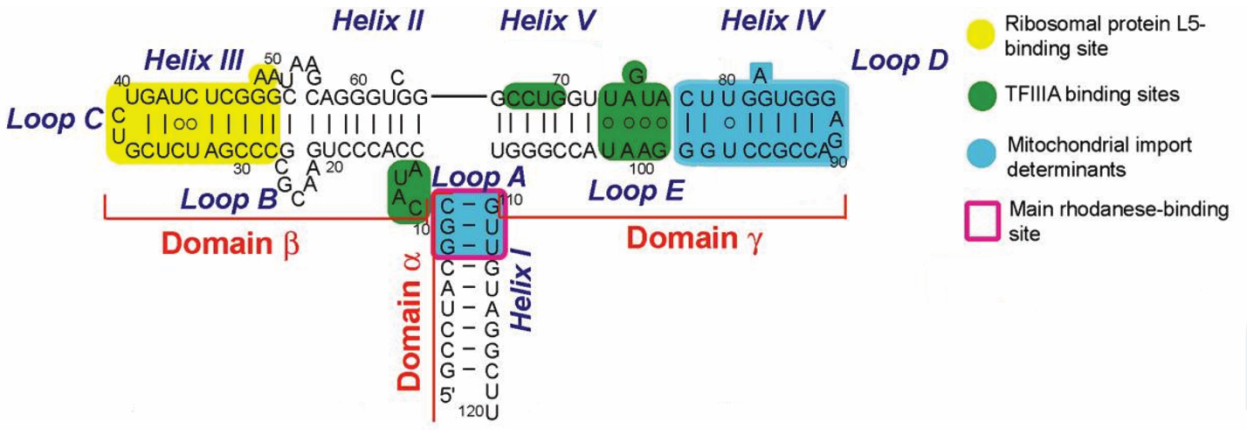


**Figure 11. The secondary structure of human 5S rRNA** (adapted from Smirnov et al., 2011). TFIIIA is involved in the export of newly synthesized 5SrRNA from the nucleus. The following fate of 5S rRNA then depends on interaction with protein factors. Ribosomal protein L5 reimports 5S rRNA molecules into nucleus while the mitochondrial ribosomal protein L18 (preMRP-L18) and rhodanese target them to mitochondria.

Two proteins were identified as targeting factors delivering 5S rRNA. 5S rRNA escapes from the "back to the nucleus" pathway due to interaction with a precursor of mitochondrial ribosomal protein L18 (preMRP-L18), which changes the RNA conformation making it unrecognizable by ribosomal protein L5. Then, 5S rRNA is handed to rhodanese, a mitochondrial thiosulfate sulfurtransferase, and transported to the mitochondrial surface. The translocation of 5S rRNA across the mitochondrial membrane requires ATP, an electrochemical membrane potential, and an intact protein import apparatus (Smirnov et al, 2010; Smirnov et al, 2008a) suggested by the observation that blocking protein import also inhibits 5S rRNA mitochondrial import.

In summary, RNA mitochondrial import does not reveale a unique universal mechanism but some features seem to be common. They are a requirement of ATP, protein factors providing the selectivity, and involvement of protein import machinery at least it receptor part. Mechanisms governing tRNA targeting into mitochondria remain poorly understood as well as protein factors involved in this process either have not identified or their functioning is not clear enough.

# THESIS PROJECT AND OBJECTIVES

The main objective of the present work was to decrypt the mechanisms of transfer RNA targeting into yeast and human mitochondria. This work focused mainly on the initial targeting step of tRK1 import into mitochondria both in human cells and yeast as well as on the role of glycolytic enzyme Eno2p in this process.

Functional studies of the mitochondrial import in yeast have suggested that a second isoform of the glycolytic enzyme enolase is an essential part of the tRK1 mitochondrial targeting process (Entelis et al., 2006). Together with another protein factor, preMSK1p, this enzyme represents a minimum system sufficient to provide the mitochondrial import of tRK1 *in vitro*. There are data indicating the interaction between Eno2p and tRK1 as well as a chaperone activity of Eno2p in the complex with tRK1 (Entelis et al., 2006; Kolesnikova et al., 2010). Nevertheless, the nature of this interaction is still unkown. We also hypothesized that human cells use a similar mechanism for induced tRK1 import implicating human enolase as well. This hypothesis was based on previous studies indicating the engagement of orthologous proteins for the tRNA mitochondrial import in human cells.

In order to reach the stated objective, we:

- ✓ Study whether human enolases are involved in tRK1 import into human mitochondria *in vitro* and *in vivo*;
- ✓ Study differences of conformational features of tRK1 and tRK2 in solution;
- ✓ Study the process of targeting of tRK1 into yeast mitochondria;
- ✓ Study the structures of tRK1-protein complexes involved in tRK1 import into yeast mitochondria.

# RESULTS

## A moonlighting human protein is involved in mitochondrial import of tRNA

It was previously demonstrated in our laboratory that yeast $tRNA^{Lys}_{CUU}$ as well as some of its synthetic transcripts can be targeted into human mitochondria indicating the existence of a cryptic mechanism for tRNA mitochondrial import (Entelis et al, 2001; Gowher et al, 2013). Moreover, this mechanism presents a certain level of similarity with the mitochondrial targeting of tRK1 in yeast. *In vitro* studies revealed that the human precursor of mitochondrial lysyl-tRNA synthetase (preKARS2) and also rabbit muscle enolase are both necessary and sufficient to direct import of tRK1 into mitochondria (Gowher et al, 2013). It could then be hypothesized that the human enolase was implicated in the tRNA mitochondrial import pathway in human cells by playing a role similar to that of Eno2p in this process in yeast.

In human, as in all vertebrates, enolase is represented by three isoenzymes: α-enolase (Enolase 1) is found in a variety of tissues, while two others are tissue specific. β-enolase (Enolase 3) is mainly found in muscles and γ-enolase (Enolase 2) is only present in neurons and neuroendocrine tissues. All isoforms are very conserved and show similar kinetic properties (Díaz-Ramos et al, 2012).

We studied the capacity of human enolases to participate in the tRK1 mitochondrial import process by applying various *in vitro* approaches. These results and their discussion are presented in publication 1 (See below). Each of three isoforms of human enolase was overexpressed and $His_6$-tag-purified in *E. coli*. We studied the capacity of human enolases to participate in tRK1 import process by means of electrophoretic mobility shift assay (EMSA) and *in vitro* import approach. All isoforms revealed comparable abilities to direct import of synthetic tRK1 into isolated human mitochondria in the presence of recombinant preKARS2. EMSA is commonly used method in the characterization of protein-nucleic acid interactions based on the differential migration of complexes and free nucleic acid during native gel electrophoresis. According to results of EMSA, recombinant human enolases possess affinities to labeled synthetic transcript of yeast tRK1. The apparent $K_d$ for this interaction is 2.0 ± 0.5

μM, which is close to 2.5 ± 0.2 μM apparent $K_d$ of tRK1 and yeast Eno2p interaction (Entelis et al, 2006). Human enolases as well as yeast Eno2p showed lower affinity to tRK1 transcript than preKARS2 (or preMSK1p in yeast), so in the presence of preKARS2, all tRK1 was shifted to forming the complex tRK1-preKARS2.

In addition, human enolases facilitated the tRK1-preKARS2 complex formation resulting in decreasing the apparent $K_d$ by 10 fold from 300 nM to less than 20 nM. The same trend was observed for the yeast recombinant Eno2p. Yeast Eno2p decreases the apparent $K_d$ of tRK1-preMSK1p from 180 nM to 40 ± 10 nM.

Summing up the results of these experiments, we suggested that human enolases seemed to participate in tRNA mitochondrial import in human cells fulfilling the same targeting functions as Eno2p in yeast cells. The data also support the idea that human cells possess a cryptic tRNA import mechanism that can be activated under specific conditions.

.

## PUBLICATION I

# A Moonlighting Human Protein Is Involved in Mitochondrial Import of tRNA

*Int. J. Mol. Sci.* **2015**, *16*, 9354-9367; doi:10.3390/ijms16059354

OPEN ACCESS
International Journal of
**Molecular Sciences**
**ISSN 1422-0067**
www.mdpi.com/journal/ijms

*Article*

# A Moonlighting Human Protein Is Involved in Mitochondrial Import of tRNA

**Maria Baleva [1,2,†], Ali Gowher [1,†,‡], Piotr Kamenski [2], Ivan Tarassov [1], Nina Entelis [1] and Benoît Masquida [1,*]**

[1] Department of Molecular and Cellular Genetics, UMR 7156 Génétique Moléculaire, Génomique, Microbiologie (GMGM), CNRS—Université de Strasbourg, 67084 Strasbourg, France; E-Mails: mary-bw@mail.ru (M.B.); qureishi83@gmail.com (A.G.); i.tarassov@unistra.fr (I.T.); n.entelis@unistra.fr (N.E.)

[2] Department of Molecular Biology, Biology Faculty of Moscow State University, 119992 Moscow, Russia; E-Mail: piotr.kamenski@gmail.com

† These authors contributed equally to this work.

‡ Present address: Genome Institute of Singapore, #02-01 Genome, Singapore 138672.

* Author to whom correspondence should be addressed; E-Mail: b.masquida@unistra.fr; Fax: +33-3-6885-1365.

Academic Editor: Michael Ibba

*Received: 28 January 2015 / Accepted: 15 April 2015 / Published: 24 April 2015*

---

**Abstract:** In yeast *Saccharomyces cerevisiae*, ~3% of the lysine transfer RNA acceptor 1 (tRK1) pool is imported into mitochondria while the second isoacceptor, tRK2, fully remains in the cytosol. The mitochondrial function of tRK1 is suggested to boost mitochondrial translation under stress conditions. Strikingly, yeast tRK1 can also be imported into human mitochondria *in vivo*, and can thus be potentially used as a vector to address RNAs with therapeutic anti-replicative capacity into mitochondria of sick cells. Better understanding of the targeting mechanism in yeast and human is thus critical. Mitochondrial import of tRK1 in yeast proceeds first through a drastic conformational rearrangement of tRK1 induced by enolase 2, which carries this freight to the mitochondrial pre-lysyl-tRNA synthetase (preMSK). The latter may cross the mitochondrial membranes to reach the matrix where imported tRK1 could be used by the mitochondrial translation apparatus. This work focuses on the characterization of the complex that tRK1 forms with

human enolases and their role on the interaction between tRK1 and human pre-lysyl-tRNA synthetase (preKARS2).

**Keywords:** human mitochondria; tRNA targeting; enolase

## 1. Introduction

Mitochondria are the centres of critical cellular processes, such as oxidative phosphorylation, apoptosis, fatty acids, amino acids and Fe–S cluster metabolisms. Despite this central role, mitochondria present genomes only encoding a fistful of proteins and RNAs dedicated to oxidative phosphorylation or mitochondrial translation. The regulation of mitochondrial activities thus relies on nuclear-encoded factors, which need to be imported in a concerted way in order to tune mitochondrial activity with cytosolic conditions [1,2]. The process of mitochondrial import of cytosolic proteins is far better understood than the process of RNA import, although mitochondrial RNA import has been described in fungi, protozoa, plants and mammals [3].

Regarding tRNAs, the existence of mitochondrial genomes encoding few or no tRNAs in certain organisms such as cniderians or protozoa, respectively, certainly indicates that tRNAs import is necessary for translation [4,5]. However, tRNAs can also be imported in mitochondria of organisms with a full set of mitochondrial DNA-encoded tRNAs. In the yeast *Saccharomyces cerevisiae*, $tRNA^{Lys}$ acceptor 1 (tRK1) is imported despite the presence of a mitochondrial encoded $tRNA^{Lys}$ (tRK3) [6]. In this case, a ~3% fraction of the tRK1 cytosolic pool is constitutively routed towards mitochondria. The import of tRK1 does not confer any obvious advantage to the cell *per se*, except when position 34 of tRK3 becomes hypomodified at non-permissive temperature (37 °C), which creates a dependence of mitochondrial translation upon tRK1 import [7].

Yeast tRK1 can also be imported in human mitochondria *in vitro* [8] and *in vivo* [9], despite that $tRNA^{Lys}$ mitochondrial import has not been demonstrated so far in mammals. At present, the reasons for maintaining this cryptic mechanism in human cells are unknown. The capacity of human cells to import tRK1 into mitochondria points to the possibility to use tRK1 as a vector to target foreign RNA into the mitochondrial matrix. This strategy has been demonstrated experimentally by achieving replacement of the non-functional $tRNA^{Lys}$ in the case of the MERRF syndrome [9], or by the inhibition of the replication of mitochondrial genomic copies harbouring deletions or mutations [10–12]. These studies suggest that RNA import mechanisms in yeast and human mitochondria should be related, and the factors involved in tRK1 import in human mitochondria are expected to share the functional characteristics necessary for RNA import in yeast mitochondria [13]. Better understanding of the targeting mechanism in yeast and human cells is critical for optimisation of potential therapeutic approaches.

During the last decade, significant efforts have resulted in identifying the factors responsible for tRK1 mitochondrial targeting in yeast [14–16]. According to this mechanism, tRK1 is handled by the glycolytic enzyme enolase in the first place, and further targeted to the mitochondrial membrane where it forms a complex with the precursor of the mitochondrial lysyl-tRNA synthetase (preMSK) (Figure 1A). The RNA determinants, which confer tRK1 import selectivity *versus* tRK2 have been analyzed [17,18] and show that the CUU anticodon and nucleotides from the acceptor arm are critical.

These determinants apparently promote the formation of an alternative structure (named the F-form) induced by enolase, composed of three hairpins (Figure 1B,C) [18]. Among those, the D stem-loop is structurally conserved while the two other ones result from reshuffling of the AA- and T-strands of tRK1, which consequently build F form-specific hairpins. Strikingly, from the two enolase isoforms in yeast, only Eno2p allows for tRK1 conformational rearrangement and targeting to preMSK, albeit their sequences are 97% identical.

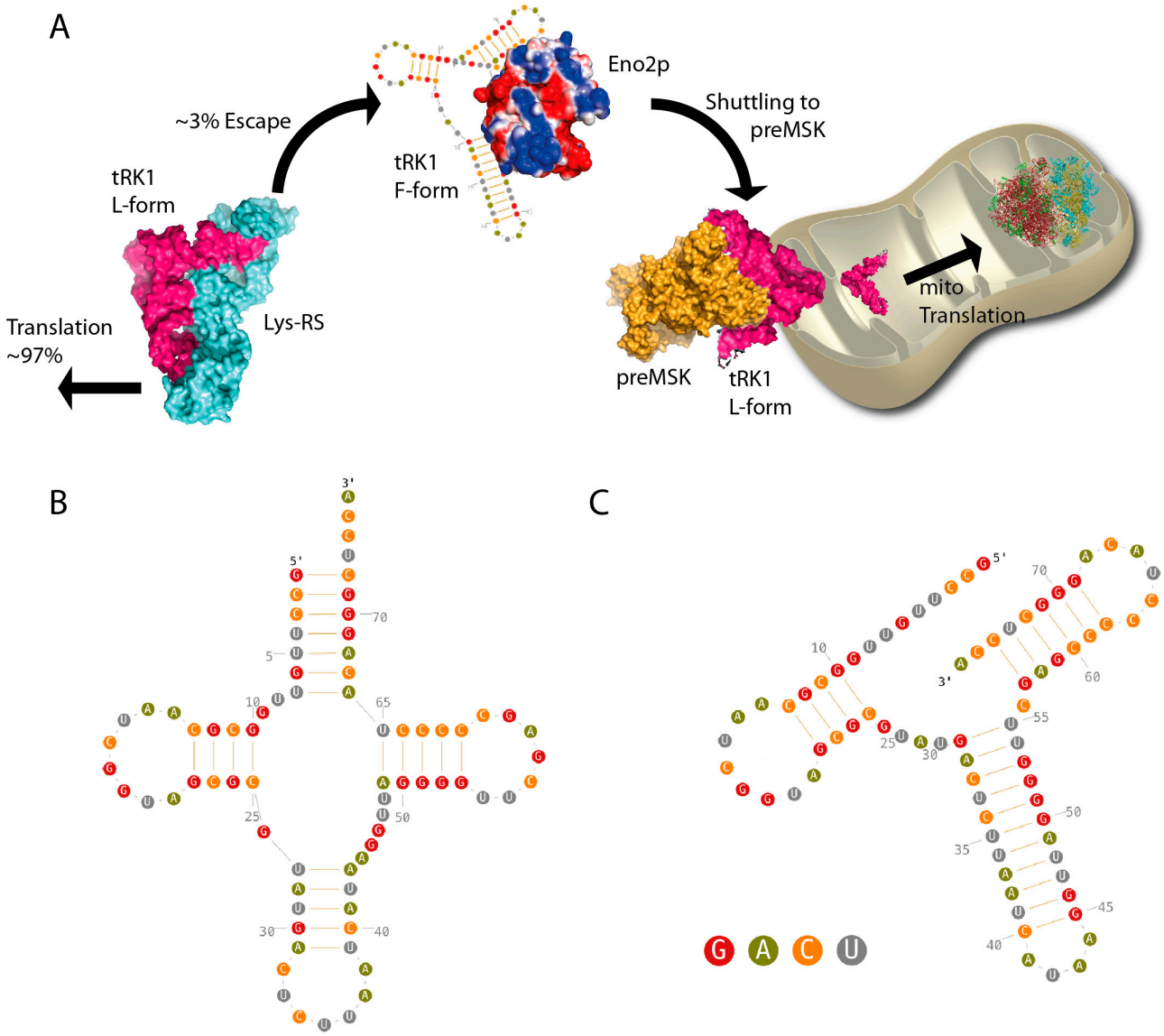


**Figure 1.** (**A**) Mitochondrial targeting of tRK1 in yeast is achieved by the successive actions of enolase 2 and the precursor of the mitochondrial lysyl-tRNA synthetase (preMSK). At the mitochondrial outer membrane, preMSK takes over enolase to start the import process properly; A fraction of the canonical tRNA L-form (**B**) tRK1 pool is deviated from the cytosolic translation process by the enolase 2, which favors the tRNA conformational change leading to the formation of the F-form (**C**). The D stem-loop is the only domain of the tRNA, which is not scrambled during this process. The nucleotide color code is indicated in panel (**C**).

This mechanism seems to be very close to a potential mechanism in human mitochondria since tRK1 import can be directed *in vitro* using human pre-lysyl-tRNA synthetase (preKARS2) and rabbit enolase [13]. The existence of a cryptic mitochondrial import mechanism of tRNA in human cells and its *in vitro* reconstitution points to human enolases as putative factors in this process.

In the present study, we address the capacity of human enolases to participate in the tRK1 import process by *in vitro* import assay, electrophoretic mobility shift assay (EMSA), and by determining the influence of α, β and γ human enolases on the affinity of preKARS2 for tRK1. Our results show that human enolases promote tRK1 import into mitochondria isolated from HepG2 cells. We also show that enolase is capable of binding to tRK1 and that pre-incubating tRK1 with enolase improves the preKARS2 binding efficiency by decreasing the dissociation constant by one order of magnitude. These results indicate that human enolases participate in the mitochondrial import pathway of tRK1 in human cells together with preKARS2, demonstrating the high similarity between the mechanisms occurring in yeast and human cells.

## 2. Results

The three human forms of enolase (α, β, γ) are also very conserved and present average identities of 62% with respect to the yeast enolase 2 (Figure 2) [19]. To compare the import-directing capacities of human enolase isoforms, we overexpressed and tag-purified each of the three isozymes of human enolase in *E. coli*. The *in vitro* import test was performed by incubating proteins and labelled RNA with purified mitochondria from HepG2 cells, as described previously [13]. Upon addition of recombinant preKARS2, a small proportion of the tRK1 pool was protected from nuclease degradation (Figure 3), indicating its import into mitochondria. The amount of imported RNA was determined by comparison of the band densities of the protected full-sized RNA isolated from the mitoplasts after the import assay *versus* an aliquot of the input (labelled RNA). tRK1 was very poorly imported with preKARS2 alone. However, its import was significantly increased upon addition of any of the human enolases. Each of the three isozymes demonstrated comparable import-directing capacities (Figure 3). A mock-import test without mitochondria excludes artifactual protection of the RNA by the recombinant proteins. This experiment shows that human counterparts of yeast RNA import factors, the glycolytic enzyme enolase and the cytosolic precursor of mitochondrial lysyl-tRNA synthetase, are sufficient to direct tRK1 import into human mitochondria.

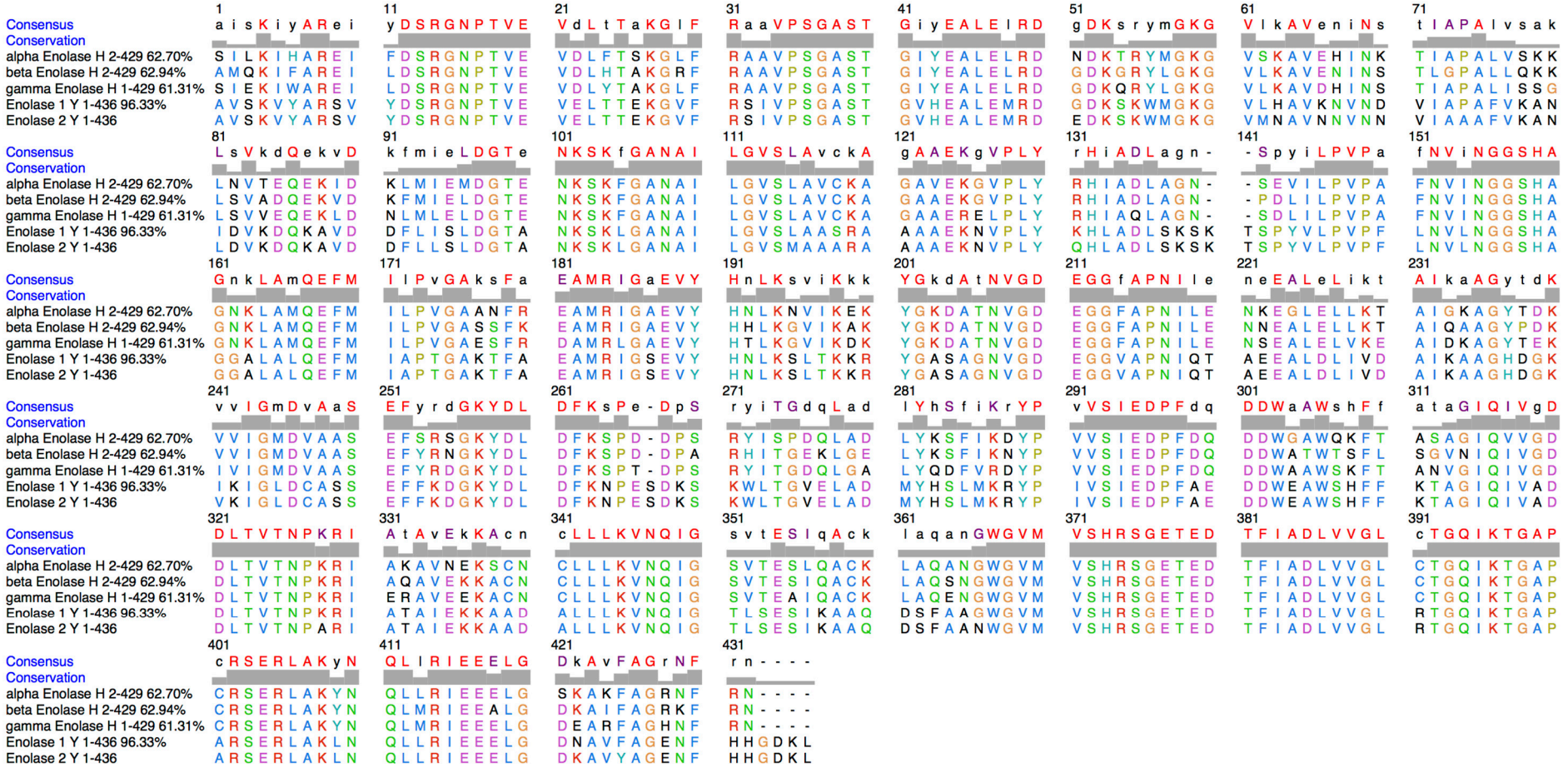


**Figure 2.** Sequence alignment of the three human enolases and of the two yeast enolases. Genebank Identification of sequences are as follows: α-Enolase 693933; β-Enolase 16878083; γ-Enolase 55669906; Enolase-1 628257676; Enolase 2 6321968.

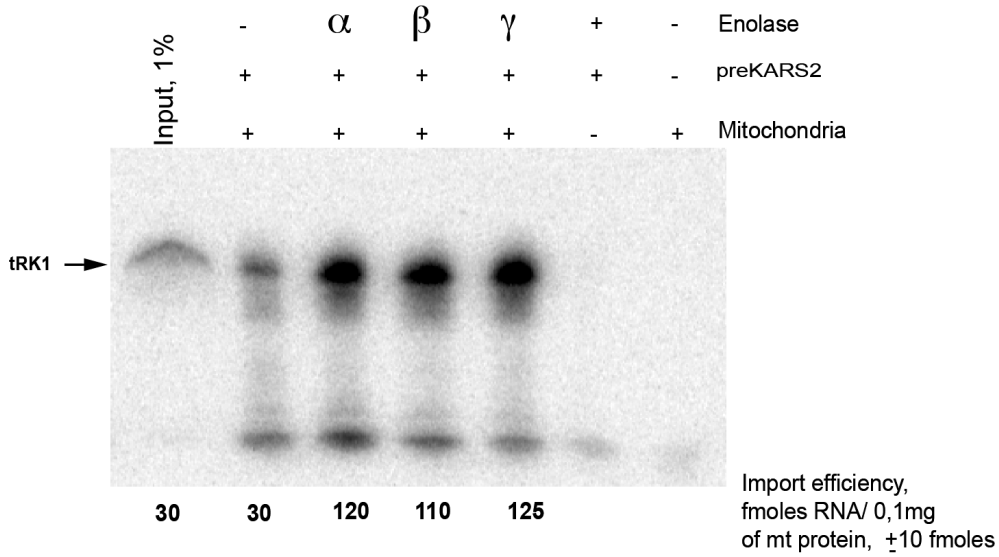


**Figure 3.** Import of tRK1 into isolated HepG2 mitochondria. An example of the *in vitro* import test, autoradiograph of RNA isolated from purified mitochondria and separated in denaturing 12% polyacrylamide gel (PAAG) is presented. The full-size RNA is indicated by an arrow at the left. Input, 1% of RNA used for each assay (as indicated above the lane), corresponding to 30 fmoles of labeled RNA. Mitochondria (+) correspond to the import assay, Mitochondria (−) to the mock import assay without mitochondria, used as a control for non-specific protein-RNA aggregation. The RNA import efficiency was calculated by comparing the signal with the input and indicated below each lane. One example from three independent experiments is presented, ±SD indicated.

The interaction of purified human enolase isoforms with labeled tRK1 was tested by electrophoretic mobility shift assay (EMSA). We found that all three isoforms of human enolase can form a complex with labelled tRK1 (Figure 4A), with an apparent dissociation constant ($K_d$) of 2.0 ± 0.5 μM (data not shown). Therefore, human enolase isozymes are capable of interacting with yeast $tRNA^{Lys}$ with the same affinity as yeast enolase Eno2p [15]. When preKARS2 and human γ enolase were present in the mixture, no ternary complex tRK1-preKARS2-enolase was detected. Instead, in the presence of low preKARS2 concentrations, tRK1 was shifted from binding to the enolase to forming a complex with preKARS2 (Figure 4B). Such a pattern is characteristic for consecutive reactions, indicating that the first protein (enolase) binds to the substrate (tRK1) and then transfers it to the second protein (preKARS2). Moreover, the presence of enolase significantly increased the efficiency of tRK1-preKARS2 complex formation (apparent $K_d$ decreased from 300 nM to less than 20 nM).

To compare and quantify the effect of the three human enolase isoforms on tRK1-preKARS2 complex formation, we used EMSA followed by Scatchard plot analysis. For this, increasing concentrations of labeled tRK1 (1–50 nM) and fixed concentration of proteins (0.5 μM of preKARS2 and 1 μM of enolase) were used. The results demonstrate that in the absence of enolase, preKARS2 binds tRK1 with a dissociation constant of 300 nM (Figure 4A,B). Addition of enolase isoforms significantly improves the efficiency of tRK1-preKARS2 complex formation resulting in more than 10-fold $K_d$ decrease (from 300 to 12–25 nM) (Figure 5B). These data show that human enolases indeed facilitate the interaction between tRK1 and preKARS2.

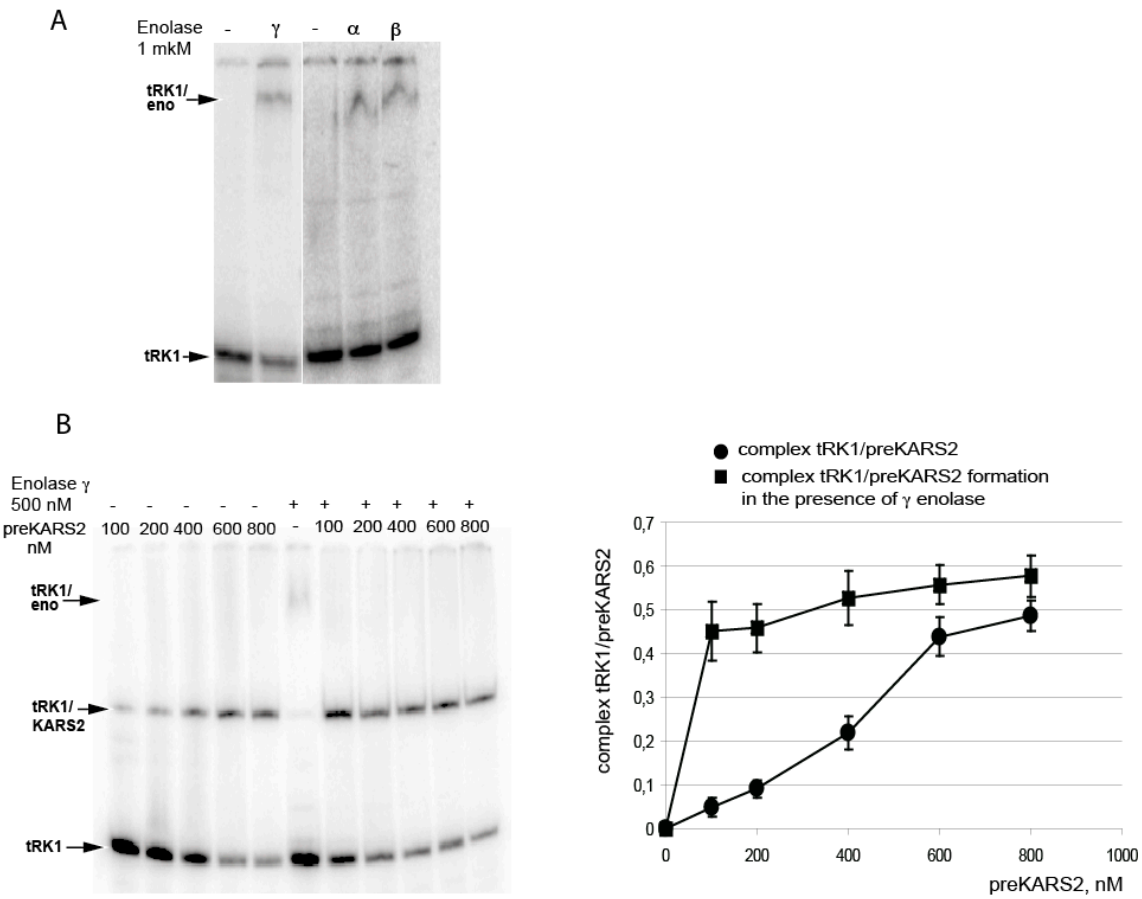


**Figure 4.** Analysis of RNA-protein interactions by electrophoretic mobility shift assay. (**A**) Autoradiographs of native PAGE-separations of labeled tRK1 in the presence of purified human enolase isoforms; (**B**) The effect of γ enolase on tRK1–KARS2 complex formation. Autoradiograph of the native gel is shown at the **left**, quantification of tRK1–KARS2 complex formation—at the **right**. TRK1, the band corresponding to the free tRK1; RNA-protein complexes are shown with arrows. One example from three independent experiments is presented.

## 3. Discussion

*In vitro* assays of tRK1 import in yeast mitochondria have enabled identification of a set of proteins involved in the process. In *Saccharomyces cerevisiae*, enolase 2 (Eno2p) hijacks ~3% of the tRK1 cytosolic pool, which undertakes conformational changes resulting in the formation of a deeply remodeled secondary structure (F-form [18]), which can be transferred to preMSK to be ultimately imported into mitochondria [15]. Strikingly, such a mechanism exists in human cells but remained unsuspected until recently [8,20]. Further investigations have resulted in a better understanding of the tRNA structural requirements [18], as well as in identifying the precursor of human mitochondrial lysyl-tRNA synthetase (preKARS2) as a factor critical for the mitochondrial import of tRNA in human cells and to hypothesize that mammalian enolases could be involved in the process [13]. These studies show a striking similarity between the tRK1 import pathways occurring in yeast and human cells. It is thus reasonable to anticipate that, among the three forms of human enolases, at least one may participate in the import mechanism.

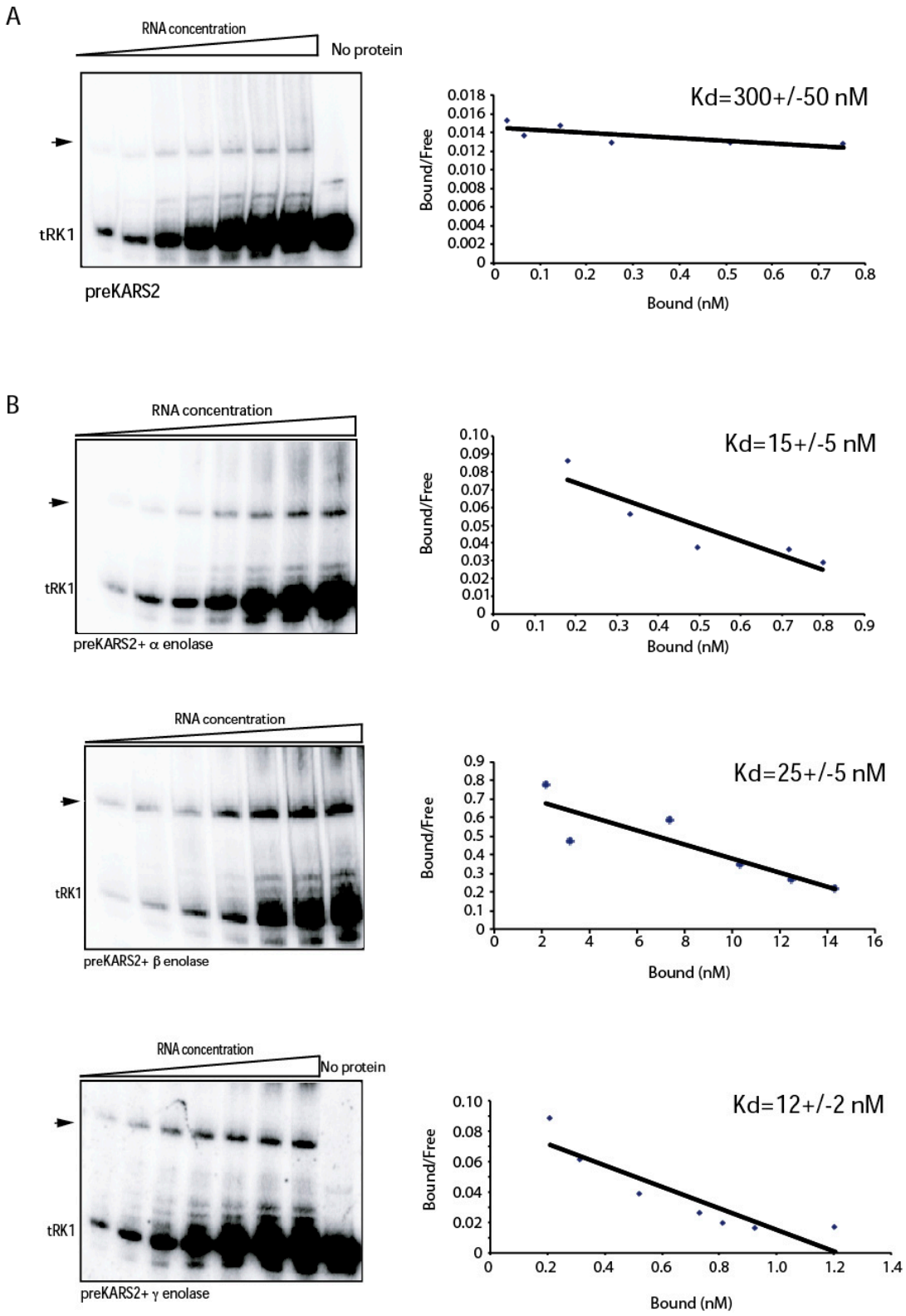


**Figure 5.** Interaction between labeled tRK1 and preKARS2 in the absence or presence of human enolases. Scatchard plot determination of dissociation constants for preKARS2–tRK1 complex in the absence of enolase (**A**); or in the presence of various isoforms of human enolases, as indicated below the panels (**B**). The bottom band corresponds to the free tRK1; preKARS2–tRK1 complex is shown with an arrow. One example from three independent experiments is presented, $K_d$ ± SD is indicated at the right.

In the present study, we indeed show that the three isoforms α, β and γ of human enolase are able to promote mitochondrial import *in vitro*, interact physically with tRK1 (Figures 3 and 4), and potentialize the affinity of preKARS2 for tRK1 (Figure 5). The human α enolase is expressed ubiquitously, while β and γ are muscle and neuron specific, respectively [21]. The human enolases are very similar to yeast Eno2p with average identities of 62% (Figure 2). Their theoretical isoelectric pH (pI) indicate that all are negatively charged at physiological pH, a situation opposite to RNA binding proteins in general, and raises concern about the ability of this protein family to interact with nucleic acids. In order to identify potential binding sites for tRK1 on members of this protein family, electrostatic potential isosurfaces were calculated. Among the five enolase forms studied, the most acidic pI and electrostatic surface potential are observed in the case of γ enolase, which presents scarce positive charges on the solvant interface, despite its ability to bind tRK1 and to promote *in vitro* mitochondrial targeting, as demonstrated in the present work. Strikingly, the largest positively charged patches are concentrated at the dimerization interface (Figure 6). The interaction of enolase with tRK1 may thus interfere with its dimerization, and, therefore, with enzymatic activity, since only enolase dimers are active during glycolysis [19].

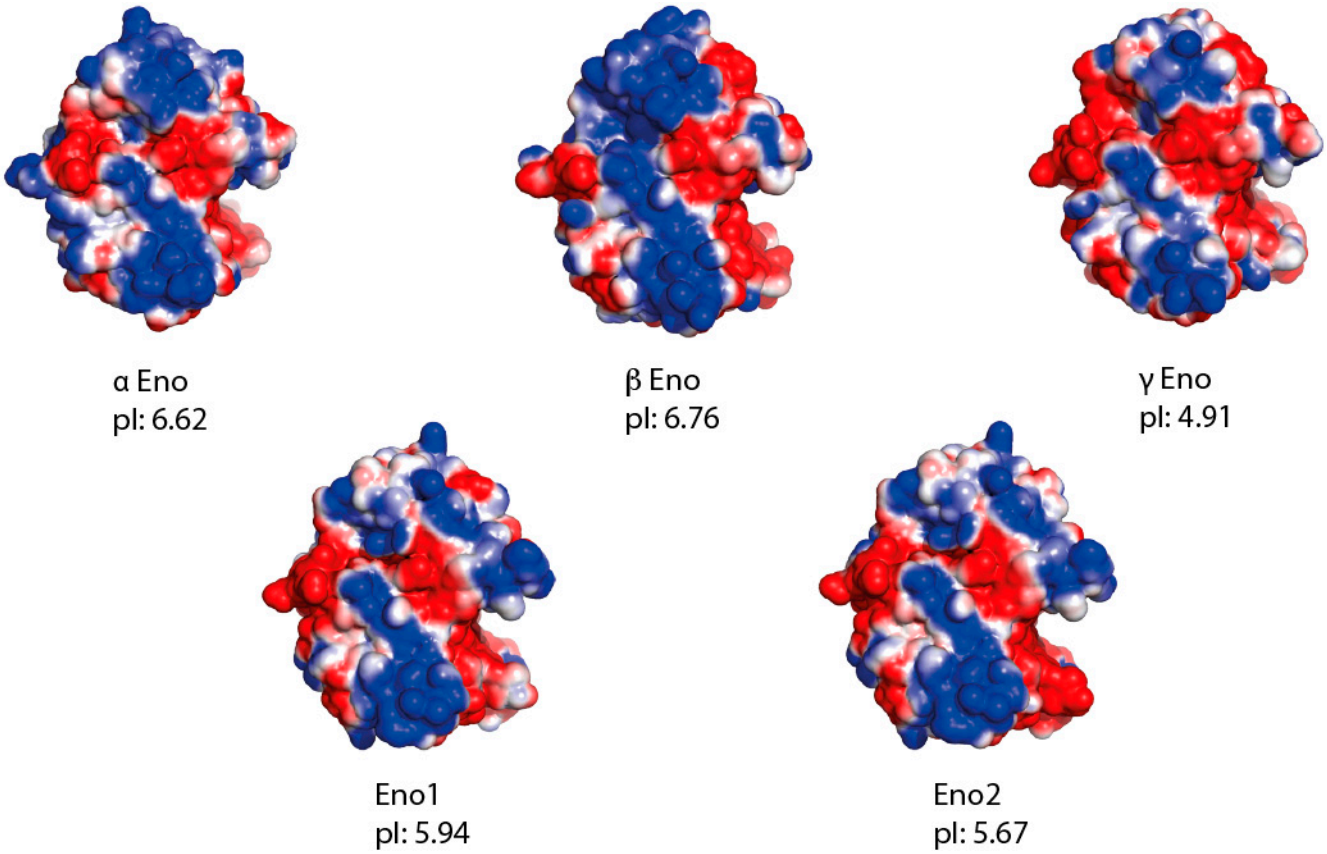


**Figure 6.** Electrostatic surface potentials visualized from the dimerization interface, corresponding to the region showing the highest density of positively charged residues, which may be responsible for tRK1 binding. Theoretical isoelectric points (pI) are also indicated.

However, it was previously demonstrated that the glycolytic activity of enolase 2 is not correlated to its mitochondrial import activity [15]. Enolase is such an abundant protein that biological processes interfering with its enzymatic activity would be negligible for the cell. This assumption is supported by

several observations that human enolase is a multifunctional protein. It is active in plasminogen recognition [22], and a form lacking the first 93 *N*-terminal residues encode a DNA binding protein, MBP, which binds the *c-myc* promoter [23]. In some vertebrates, a processed form of enolase also serves as a structural component of the eye lens (τ crystallin) and retains enzymatic activity, albeit reduced [24].

Therefore, our study strongly suggests that the tissue-specific enolase isoforms may perform the moonlighting function in RNA mitochondrial import in human cells, similarly to yeast Eno2p. The latter seems to act as an RNA chaperone, which redirects part of the tRK1 to the mitochondrial import pathway by favoring the structural rearrangement of tRK1, adding to the list of already known moonlighting functions of this protein. The present data support the idea that human cells possess a cryptic tRNA import mechanism that can be activated in the presence of importable RNAs.

## 4. Experimental Section

### *4.1. Expression and Purification of Recombinant Proteins*

Purification of recombinant preKARS2 protein was done as described previously [13]. Plasmids containing human cDNAs encoding enolase isoforms ENO1 (α), ENO2 (γ, neuronal) and ENO3 (β, muscle) were purchased from OriGene (Rockville, MD, USA). Coding regions with a *C*-terminal His-tag were inserted into pET30a expression vector. The resulting full-length tagged proteins were expressed in *Escherichia coli* strain BL21 codon plus (DE3)-RIL cells (Stratagene, Agilent technology, Santa Clara, CA, USA). The transformed cells were grown in LB broth to a cell density $A_{600}$ = 0.6, the protein expression was induced by 0.5 mM Isopropyl β-D-1-thiogalactopyranoside. After incubation for 3 h at 30 °C, cells were harvested, treated with 1 mg/mL of lysozyme on ice for 30 min and sonicated 10 × 20 s in 50 mM sodium phosphate buffer (pH 8.0), 300 mM NaCl and 10 mM imidazole. The clarified lysate was applied to Ni-NTA beads (Qiagen, Hilden, Germany) for 2 h at 4 °C. After washing three times with the same buffer containing 20 mM imidazole, enolases were eluted from the beads with 200 mM imidazole, dialyzed against 50 mM Tris-HCl (pH 8.0), 300 mM NaCl and 40% glycerol and stored at −20 °C. The purity of the proteins was checked by SDS-PAGE with Coomassie blue staining.

### *4.2. Electrophoretic Mobility Shift Assay (EMSA)*

TRK1 T7 transcripts were obtained *in vitro* using the Ribomax kit (Promega, Fitchburg, WI, USA). Following transcription, the DNA template was removed by digestion with RQ1 RNase-Free DNase (Promega), and RNA was purified by 8 M urea −12% PAGE. After elution and ethanol precipitation, RNA was dephosphorylated with alkaline phosphatase (Boehringer Mannheim, Mannheim, Germany) and labeled at the 5'-end with γ-$^{32}$P-ATP using T4 polynucleotide kinase (Promega). For the RNA binding assay, labeled RNA was denatured at 100 °C and then allowed to slowly cool down to room temperature. The appropriate amounts of protein and labeled RNA were mixed in 20 μL of a buffer containing 20 mM Tris-HCl pH 7.5, 150 mM NaCl, 10 mM $MgCl_2$, 5 mM DTT, 10% glycerol, 0.1 mg/mL BSA and incubated at 30 °C for 15 min. The mixture was fractionated by native 8% PAGE in 0.5× Tris-borate buffer (pH 8.3) and 5% glycerol [25], followed by Typhoon-Trio (GE Healthcare,

Fairfield, CT, USA) scanning and quantification as described previously [26]. For Scatchard plot analysis, several standard EMSA reactions were performed in which the concentrations of proteins (0.5 mM for preKARS2 and 1 mM for human enolase isoforms) were kept constant, and the concentration of labeled tRK1 varied from 1 to 100 nM. Calculation of the dissociation constant $K_d$ from the linear regression of experimental data was done as described in [27].

### *4.3. In Vitro Import Assay*

The *in vitro* import assay was performed as in [8]. For this, purified HepG2 mitochondria were incubated with $^{32}$P 5' labeled RNA and purified proteins in import buffer: 0.6 M Sorbitol, 20 mM HEPES-KOH (pH 7), 10 mM KCl, 2.5 mM $MgCl_2$, 5 mM DDT and 2 mM ATP. For a standard *in vitro* assay, 3 pmoles of labelled RNA were added to 100 µL of reaction mixture containing 0.1 mg of mitochondria (measured by the amount of mitochondrial protein). This corresponds to 100% RNA input. After incubation for 15 min at 34 °C, 50 µg/mL of RNase A (Sigma Aldrich, Saint Louis, MO, USA) was added and the reaction further incubated for 15 min to digest all the RNA that was not imported. Mitochondria were washed three times with buffer containing 0.6 M sorbitol, 10 mM HEPES–KOH (pH 6.7) and 4 mM EDTA, then resuspended in 100 µL of the same buffer and treated with an equal volume of 0.2% digitonin (Sigma) solution to disrupt the mitochondrial outer membrane, followed by purification of mitoplasts. The mitoplast pellet was resuspended in a solution containing 100 mM $CH_3COONa$, 10 mM $MgCl_2$, 1% SDS and 0.05% Diethylpyrocarbonate (DEPC) and heated at 100 °C for 1 min. RNA was extracted at 50 °C using water saturated acidic phenol. RNA was precipitated with ethanol and fractionated by 12% PAGE containing 8 M urea, followed by quantification by a Typhoon-Trio scanner using Image Quant-Tools software (GE Healthcare). The amount of imported RNA was determined by comparison of the band density of protected full-sized RNA isolated from the mitoplasts after the import assay with an aliquot (2%–5%) of the RNA input.

### *4.4. Protein Alignment, Molecular Modelling and Electrostatic Surface Calculation*

Sequences were obtained using blastp [28], aligned by clustalw [29] and visualized using chimera [30]. The three-dimensional molecular model of Eno2p was obtained by automatic homology modeling using the SWISS-MODEL pipeline [31]. The best template was 2al1 [32] from the protein databank. Electrostatic potential surfaces were represented in PyMOL [33] using PDB2PAQR [34] and APBS [35] plugins. Theoretical pI were determined using ExPASy tools [36].

## Acknowledgments

MB was supported by a PhD fellowship from the SUPRACHEM network. This work has been published under the framework of the LABEX ANR-11-LABX-0057_MITOCROSS. This work was supported by the Russian Ministry for Education and Science (Agreement 14.604.21.0113/ RFMEFI60414X0008 for Moscow State University).

## Author Contributions

Nina Entelis, Ivan Tarassov, Piotr Kamenski and Benoît Masquida designed research; Ali Gowher, Maria Baleva, Nina Entelis and Benoît Masquida performed research; Ali Gowher, Maria Baleva, Nina Entelis, Ivan Tarassov, Piotr Kamenski and Benoît Masquida analyzed data; Nina Entelis and Benoît Masquida wrote the paper.

## Conflicts of Interest

The authors declare no conflict of interest.

## References

1. Frechin, M.; Enkler, L.; Tetaud, E.; Laporte, D.; Senger, B.; Blancard, C.; Hammann, P.; Bader, G.; Clauder-Münster, S.; Steinmetz, L.M.; *et al.* Expression of nuclear and mitochondrial genes encoding atp synthase is synchronized by disassembly of a multisynthetase complex. *Mol. Cell* **2014**, *56*, 763–776.
2. Entelis, N.S.; Kolesnikova, O.A.; Martin, R.P.; Tarassov, I.A. RNA delivery into mitochondria. *Adv. Drug Deliv. Rev.* **2001**, *49*, 199–215.
3. Sieber, F.; Duchêne, A.-M.; Maréchal-Drouard, L. Chapter four—Mitochondrial RNA import: From diversity of natural mechanisms to potential applications. In *International Review of Cell and Molecular Biology*; Kwang, W.J., Ed.; Academic Press: New York, NY, USA, 2011; Volume 287, pp. 145–190.
4. Emblem, A.; Karlsen, B.O.; Evertsen, J.; Johansen, S.D. Mitogenome rearrangement in the cold-water scleractinian coral lophelia pertusa (cnidaria, anthozoa) involves a long-term evolving group I intron. *Mol. Phylogenet. Evol.* **2011**, *61*, 495–503.
5. Jackson, K.E.; Habib, S.; Frugier, M.; Hoen, R.; Khan, S.; Pham, J.S.; Pouplana, L.R.D.; Royo, M.; Santos, M.A.S.; Sharma, A.; *et al.* Protein translation in plasmodium parasites. *Trends Parasitol.* **2011**, *27*, 467–476.
6. Martin, R.P.; Schneller, J.M.; Stahl, A.J.; Dirheimer, G. Import of nuclear deoxyribonucleic acid coded lysine-accepting transfer ribonucleic acid (anticodon CUU) into yeast mitochondria. *Biochemistry* **1979**, *18*, 4600–4605.
7. Kamenski, P.; Kolesnikova, O.; Jubenot, V.; Entelis, N.; Krasheninnikov, I.A.; Martin, R.P.; Tarassov, I. Evidence for an adaptation mechanism of mitochondrial translation via tRNA import from the cytosol. *Mol. Cell* **2007**, *26*, 625–637.
8. Entelis, N.S.; Kolesnikova, O.A.; Dogan, S.; Martin, R.P.; Tarassov, I.A. 5 S rRNA and tRNA import into human mitochondria. Comparison of *in vitro* requirements. *J. Biol. Chem.* **2001**, *276*, 45642–45653.
9. Kolesnikova, O.A.; Entelis, N.S.; Jacquin-Becker, C.; Goltzene, F.; Chrzanowska-Lightowlers, Z.M.; Lightowlers, R.N.; Martin, R.P.; Tarassov, I. Nuclear DNA-encoded tRNAs targeted into mitochondria can rescue a mitochondrial DNA mutation associated with the MERRF syndrome in cultured human cells. *Hum. Mol. Genet.* **2004**, *13*, 2519–2534.

10. Comte, C.; Tonin, Y.; Heckel-Mager, A.M.; Boucheham, A.; Smirnov, A.; Aure, K.; Lombes, A.; Martin, R.P.; Entelis, N.; Tarassov, I. Mitochondrial targeting of recombinant RNAs modulates the level of a heteroplasmic mutation in human mitochondrial DNA associated with kearns sayre syndrome. *Nucleic Acids Res.* **2013**, *41*, 418–433.
11. Tonin, Y.; Heckel, A.M.; Dovydenko, I.; Meschaninova, M.; Comte, C.; Venyaminova, A.; Pyshnyi, D.; Tarassov, I.; Entelis, N. Characterization of chemically modified oligonucleotides targeting a pathogenic mutation in human mitochondrial DNA. *Biochimie* **2014**, *100*, 192–199.
12. Tonin, Y.; Heckel, A.M.; Vysokikh, M.; Dovydenko, I.; Meschaninova, M.; Rotig, A.; Munnich, A.; Venyaminova, A.; Tarassov, I.; Entelis, N. Modeling of antigenomic therapy of mitochondrial diseases by mitochondrially addressed RNA targeting a pathogenic point mutation in mitochondrial DNA. *J. Biol. Chem.* **2014**, *289*, 13323–13334.
13. Gowher, A.; Smirnov, A.; Tarassov, I.; Entelis, N. Induced tRNA import into human mitochondria: Implication of a host aminoacyl-tRNA-synthetase. *PLoS ONE* **2013**, *8*, e66228.
14. Brandina, I.; Graham, J.; Lemaitre-Guillier, C.; Entelis, N.; Krasheninnikov, I.; Sweetlove, L.; Tarassov, I.; Martin, R.P. Enolase takes part in a macromolecular complex associated to mitochondria in yeast. *Biochim. Biophys. Acta* **2006**, *1757*, 1217–1228.
15. Entelis, N.; Brandina, I.; Kamenski, P.; Krasheninnikov, I.A.; Martin, R.P.; Tarassov, I. A glycolytic enzyme, enolase, is recruited as a cofactor of tRNA targeting toward mitochondria in *Saccharomyces cerevisiae*. *Genes Dev.* **2006**, *20*, 1609–1620.
16. Kamenski, P.; Smirnova, E.; Kolesnikova, O.; Krasheninnikov, I.A.; Martin, R.P.; Entelis, N.; Tarassov, I. tRNA mitochondrial import in yeast: Mapping of the import determinants in the carrier protein, the precursor of mitochondrial lysyl-tRNA synthetase. *Mitochondrion* **2010**, *10*, 284–293.
17. Entelis, N.S.; Kieffer, S.; Kolesnikova, O.A.; Martin, R.P.; Tarassov, I.A. Structural requirements of $tRNA^{Lys}$ for its import into yeast mitochondria. *Proc. Natl. Acad. Sci. USA* **1998**, *95*, 2838–2843.
18. Kolesnikova, O.; Kazakova, H.; Comte, C.; Steinberg, S.; Kamenski, P.; Martin, R.P.; Tarassov, I.; Entelis, N. Selection of RNA aptamers imported into yeast and human mitochondria. *RNA* **2010**, *16*, 926–941.
19. Pancholi, V. Multifunctional α-enolase: Its role in diseases. *Cell. Mol. Life Sci.* **2001**, *58*, 902–920.
20. Kolesnikova, O.; Entelis, N.; Kazakova, H.; Brandina, I.; Martin, R.P.; Tarassov, I. Targeting of tRNA into yeast and human mitochondria: The role of anticodon nucleotides. *Mitochondrion* **2002**, *2*, 95–107.
21. Qin, J.; Chai, G.; Brewer, J.M.; Lovelace, L.L.; Lebioda, L. Structures of asymmetric complexes of human neuron specific enolase with resolved substrate and product and an analogous complex with two inhibitors indicate subunit interaction and inhibitor cooperativity. *J. Inorg. Biochem.* **2012**, *111*, 187–194.
22. Diaz-Ramos, A.; Roig-Borrellas, A.; Garcia-Melero, A.; Lopez-Alemany, R. Enolase, a multifunctional protein: Its role on pathophysiological situations. *J. Biomed. Biotechnol.* **2012**, *2012*, 12.
23. Sedoris, K.C.; Thomas, S.D.; Miller, D.M. c-Myc promoter binding protein regulates the cellular response to an altered glucose concentration. *Biochemistry* **2007**, *46*, 8659–8668.

24. Wistow, G.J.; Lietman, T.; Williams, L.A.; Stapel, S.O.; de Jong, W.W.; Horwitz, J.; Piatigorsky, J. Tau-crystallin/α-enolase: One gene encodes both an enzyme and a lens structural protein. *J. Cell Biol.* **1988**, *107*, 2729–2736.
25. Kaminska, M.; Deniziak, M.; Kerjan, P.; Barciszewski, J.; Mirande, M. A recurrent general RNA binding domain appended to plant methionyl-tRNA synthetase acts as a *cis*-acting cofactor for aminoacylation. *EMBO J.* **2000**, *19*, 6908–6917.
26. Smirnov, A.; Entelis, N.; Martin, R.P.; Tarassov, I. Biological significance of 5 S rRNA import into human mitochondria: Role of ribosomal protein MRP-L18. *Genes Dev.* **2011**, *25*, 1289–1305.
27. Henis, Y.I.; Levitzki, A. An analysis on the slope of scatchard plots. *Eur. J. Biochem.* **1976**, *71*, 529–532.
28. Altschul, S.F.; Madden, T.L.; Schäffer, A.A.; Zhang, J.; Zhang, Z.; Miller, W.; Lipman, D.J. Gapped blast and psi-blast: A new generation of protein database search programs. *Nucleic Acids Res.* **1997**, *25*, 3389–3402.
29. Larkin, M.A.; Blackshields, G.; Brown, N.P.; Chenna, R.; McGettigan, P.A.; McWilliam, H.; Valentin, F.; Wallace, I.M.; Wilm, A.; Lopez, R.; *et al.* Clustal W and clustal X version 2.0. *Bioinformatics* **2007**, *23*, 2947–2948.
30. Pettersen, E.F.; Goddard, T.D.; Huang, C.C.; Couch, G.S.; Greenblatt, D.M.; Meng, E.C.; Ferrin, T.E. UCSF chimera—A visualization system for exploratory research and analysis. *J. Comput. Chem.* **2004**, *25*, 1605–1612.
31. Biasini, M.; Bienert, S.; Waterhouse, A.; Arnold, K.; Studer, G.; Schmidt, T.; Kiefer, F.; Cassarino, T.G.; Bertoni, M.; Bordoli, L.; *et al.* Swiss-model: Modelling protein tertiary and quaternary structure using evolutionary information. *Nucleic Acids Res.* **2014**, *42*, W252–W258.
32. Sims, P.A.; Menefee, A.L.; Larsen, T.M.; Mansoorabadi, S.O.; Reed, G.H. Structure and catalytic properties of an engineered heterodimer of enolase composed of one active and one inactive subunit. *J. Mol. Biol.* **2006**, *355*, 422–431.
33. *The Pymol Molecular Graphics System*, version 1.3r1; Schrodinger, LLC: New York, NY, USA, 2010.
34. Dolinsky, T.J.; Czodrowski, P.; Li, H.; Nielsen, J.E.; Jensen, J.H.; Klebe, G.; Baker, N.A. PDB2PQR: Expanding and upgrading automated preparation of biomolecular structures for molecular simulations. *Nucleic Acids Res.* **2007**, *35*, W522–W525.
35. Baker, N.A.; Sept, D.; Joseph, S.; Holst, M.J.; McCammon, J.A. Electrostatics of nanosystems: Application to microtubules and the ribosome. *Proc. Natl. Acad. Sci. USA* **2001**, *98*, 10037–10041.
36. Gasteiger, E.; Gattiker, A.; Hoogland, C.; Ivanyi, I.; Appel, R.D.; Bairoch, A. Expasy: The proteomics server for in-depth protein knowledge and analysis. *Nucleic Acids Res.* **2003**, *31*, 3784–3788.

## Human enolase overexpression or down-regulation does not affect tRK1 mitochondrial import *in vivo.*

We revealed that human enolases possess the ability to bind tRK1 transcript. Moreover, they increase the efficiency of tRK1-preKARS2 complex formation and direct tRK1 import into isolated mitochondria in the presence of recombinant preKARS2. To verify a role of human enolases in *in vivo* mitochondrial import, we tested the effect of enolase down-regulation or overexpression on the efficiency of tRK1 mitochondrial import in human cells.

The expression of enolases was repressed by transient transfection of cultured human HepG2 cells of a mixture of siRNAs specifically designed against all human enolases. After 48 h a more than 70% decrease of enolase level was observed by Western blot (Figure 12A). The control cells were transfected control siRNAs. Thereafter, cells were transfected with the T7 transcript of tRK1. Total RNAs and mitochondrial RNAs isolated from control and down-regulated cells were analysed by northern blot (Figure 12B). In parallel, we tested tRK1 import in the same cell line overexpressing α-enolase. Cells were transiently transfected with the plasmid expressing this isoform. After 48h a 2-fold increase of enolase amount was detected by western blot (Figure 12C) and cells were transfected with the T7 transcript of tRK1. The RNAs of cells overexpressing α-enolase were analysed as discribed above (Figure 12D) compared to a control cells transfected without enolase-expression plasmids.

In addition, we tested the effect of overexpression of different isoforms of human enolase on tRK1 mitochondrial import in Hek293T cells (Figure 12E, F).

The results showed a slight decrease of tRK1 mitochondrial import in cells where enolase was down-regulated, while the overexpression of human enolases did not showed any effect on import efficiency of tRK1, suggesting a potential regulation of the import mechanisms.

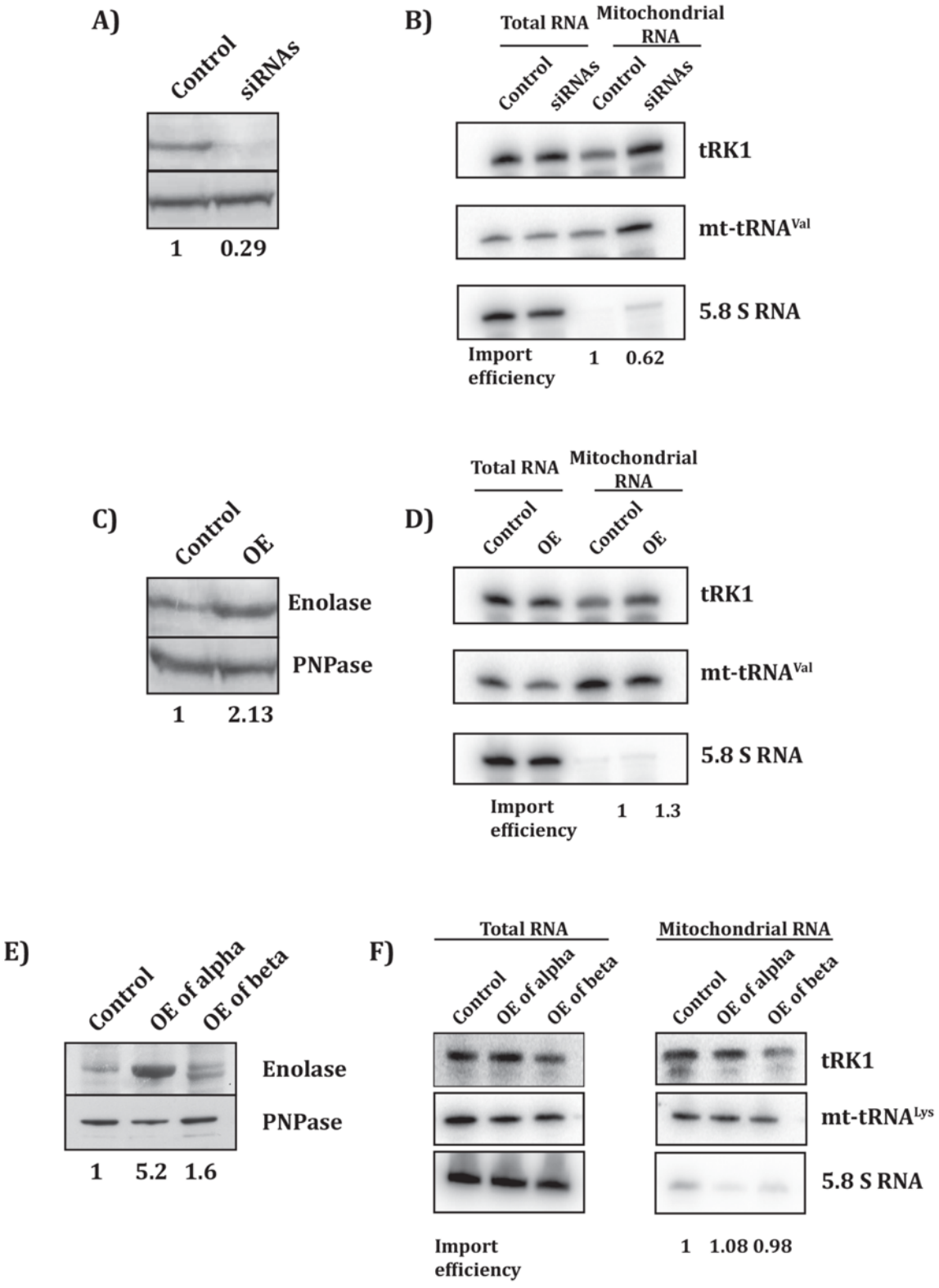


**Figure 12. The effect of down-regulation and overexpression of human enolases on tRK1 mitochondrial import *in vivo* in human cells.** (A) Western blot analysis of enolase down-regulation in HepG2 cells transiently transfected with siRNAs; (B) Northern blot hybridization of total and mitochondrial RNAs isolated from control cells and cells down-regulating the enolase. (C) Western

blot analysis of α-enolase overexpression in HepG2 cells transiently transfected with plasmid expressing this protein; (D) Northern blot hybridization of total and mitochiondrial RNAs isolated from control cells and cells overexpressing α-enolase. (E) Western blot analysis of Hek293T cells overexpressing (OE) α-enolase or β-enolase; (F) Northern blot hybridization of total and mitochiondrial RNAs isolated from control cells and cells overexpressing (OE) either α-enolase or β-enolase. Antibodies used for immunodetection are indicated at the right of each panel with western blot analysis. The hybridization probes are indicated at the right of each panel with Northern blot hybridization. The absolute import efficiency taken as 1 for control cells is shown below the panels. Mitochondrial (mt) $tRNA^{Val}$ or $tRNA^{Lys}$ probes were used as loading control. The cytosolic 5.8S rRNA probe was used to check the level of cytosolic RNA contamination.

## Probing tRK1 and tRK2 conformations

It was suggested that the tRK1 mitochondrial import could be realized through the formation of alternative structures distinct from a classical L-form tRNA model (Kolesnikova et al, 2010). In particular, in a complex with Eno2p, tRK1 adopts a specific F-hairpin conformation in which the 3'-end and C56 are close to each other. *In-gel* FRET analysis confirmed that the estimated distance between certain positions of tRK1 in the presence of Eno2p favored the predicted F-hairpin structure. Nevertheless, such rearrangement appears as a consequence rather than as a cause for the interaction. We hypothesized that the conformational differences and dynamics between tRK1 and tRK2 may account for the possibility for tRK1 to interact with Eno2p.

We studied the structural differences of tRK1 and tRK2 T7 transcripts in solution by in-line probing and RNases T1 and V1 probing techniques. RNase T1 cuts after unpaired G residues and RNase V1 cuts in double-stranded sequences or higher-order structures, such as stacked regions. The in-line probing technique is based on the natural tendency for RNA to self-cleave in regions characterized by more flexibility. The tRNA structures were probed after labeling at their 5'-end. Two types of ladder were used for identifying the cleavage positions including T1 ladder obtained by RNase T1 digestion of tRNA under denaturing conditions and an alkaline ladder prepared by hydroxyl cleavage at pH ≥ 9.

For refolding of T7 tRNA the following procedure was used. A low ionic strength solution of [$^{32}$P]-labeled T7 tRNA was heated at 92°C for 1 minute, mixed with the buffer containing 50 mM MES-KOH pH 6.5, 4 mM $MgCl_2$ and 100 mM KCl, heated 1 extra minute at 92°C and placed on ice.

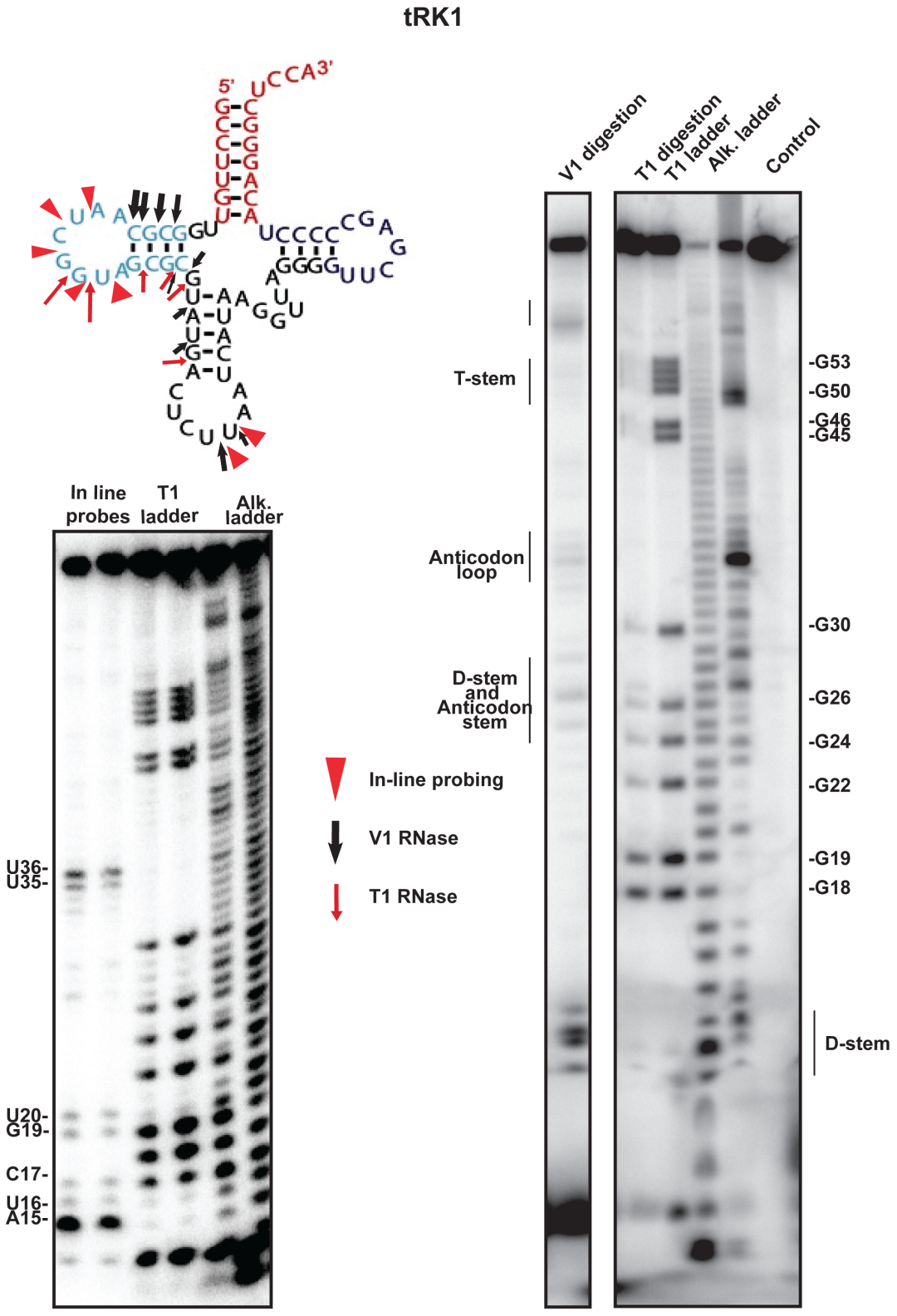


**Figure 13. Probing of tRK1**. RNase V1 (V1 digestion), T1 (T1 digestion) and in-line probing (In-line probes) of T7 tRK1. Two ladders were used – T1 ladder and alkaline ladder (Alk. ladder). Control is the tRNA before any manipulations. Sites of cleavage are mapped on the scheme of cloverleaf structure of tRK1.

Enzymatic probing as well as in-line probing of tRK1 (Figure 13) and tRK2 (Figure 14) revealed a certain level of differences between their conformational states. In the case of tRK1, RNase V1 exhibited a clear signal for D-stem and also for T-stem. RNase V1 cut in anticodon stem-loop. The sites for RNase T1 were mainly found in D-arm and anticodon stem. D-loop as well as anticodon loop underwent spontaneous cleavage in in-line probing assays.

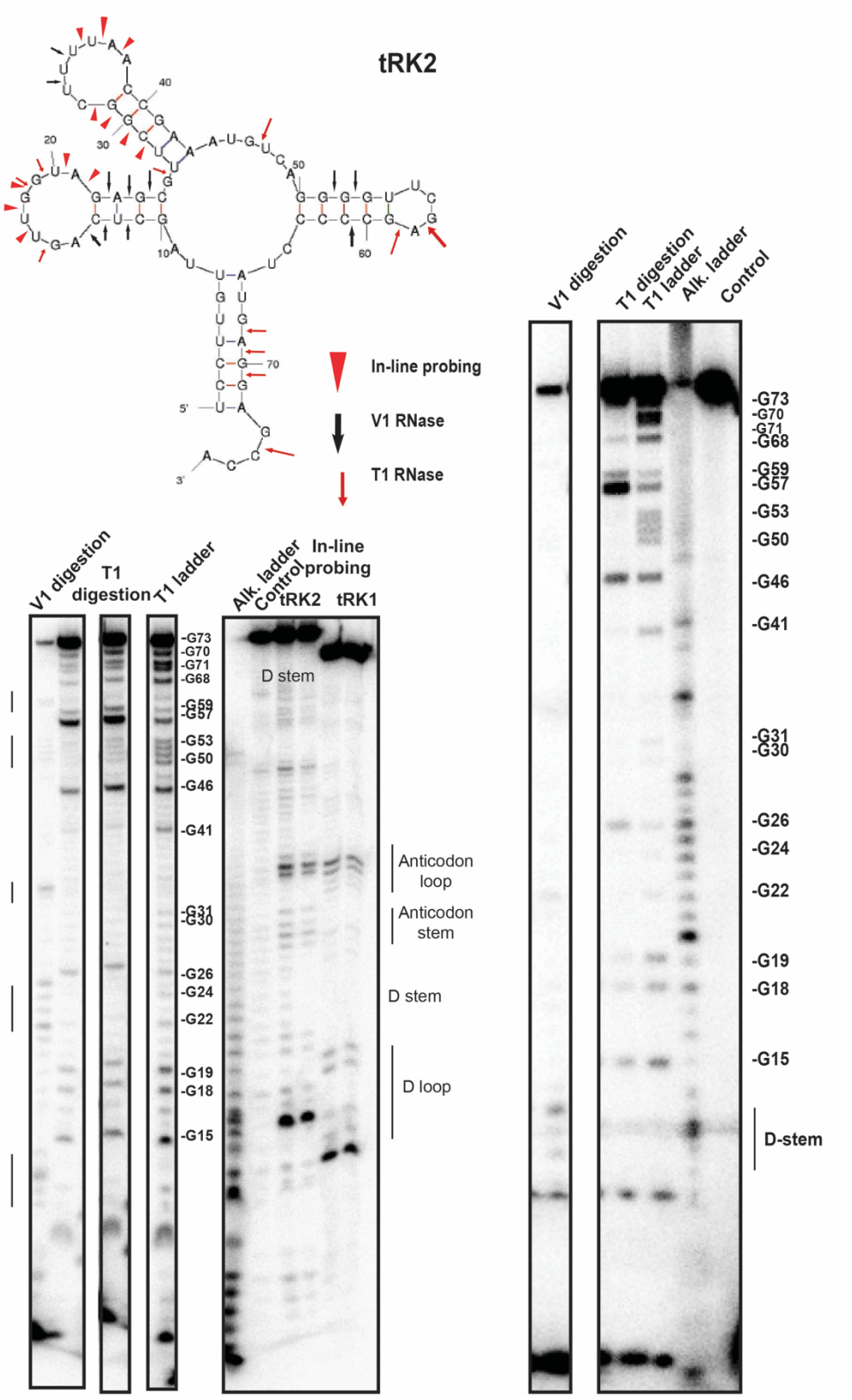


**Figure 14. Probing of tRK2**. RNase V1 (V1 digestion) and T1 (T1 digestion) and in-line probing (In-line probes) of T7 tRK2. Two ladders were used – T1 ladder and alkaline ladder (Alk. ladder). Control is the tRNA before any manipulations. Sites of cleavage are mapped on the scheme of structure of tRK2.

Enzymatic probing of the structure of tRK2 transcripts revealed differences in a cleavage pattern as compared to tRK1. The most obvious one was the sensitivity of aminoacceptor stem to RNase T1 digestion. RNase V1 cut in D-stem, T-stem as well as in anticodon loop of tRK2 similarly to tRK1. In-line probing revealed more flexibility for tRK2 than for tRK1.

We mapped the cutting sites on the possible alternative structures of tRK1 predicted by Mfold (RNA folding form ver. 2.3 energies) (folding temperature 0°C) (Figure 15).

The cleavage pattern that was obtained in probing experiments reflected the existence of different conformers for tRNA in solution. While it was not possible to conclude which folding forms predicted for tRK1 existed, specific signatures of some conformers could be observed, like for the form IV.

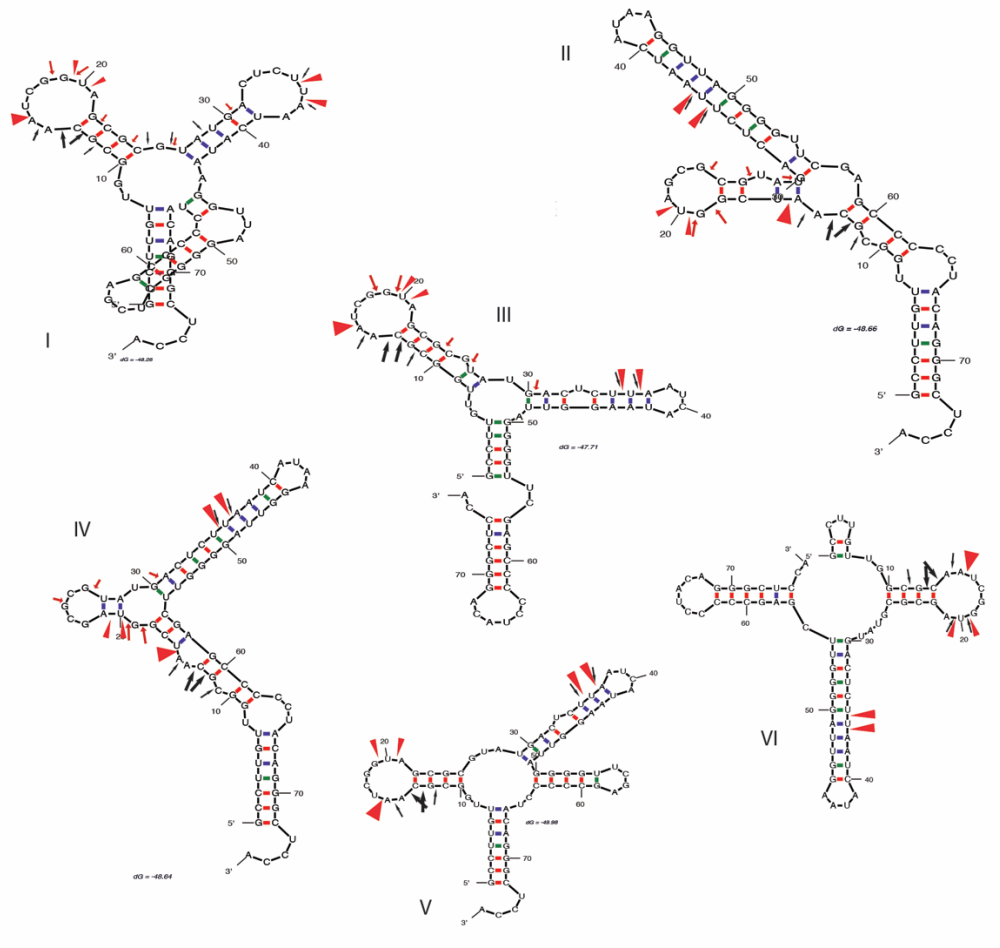


**Figure 15. Cleavage sites of tRK1**: cleavage sites of Rnase T1 (red arrow), Rnase V1 (black arrow), and in-line (red triangular) mapped on secondary ctructures of tRK1 predicted by Mfold (folding temperature is 0°C)

We also mapped the cutting sites on the possible alternative structures of tRK2 predicted with Mfold (RNA folding form ver. 2.3 energies) (folding temperature is 0°C) (Figure 16). G46 site of RNase T1 cleavage represented conformations II and IV, G26, G15 site of RNase T1 cleavage was found in all conformations, but weak signal indicated that they should by protected possibly due to high-order interaction. This seemed to be true for G18 and G19 sites found in I and IV eigher those conformers were not aboundant.

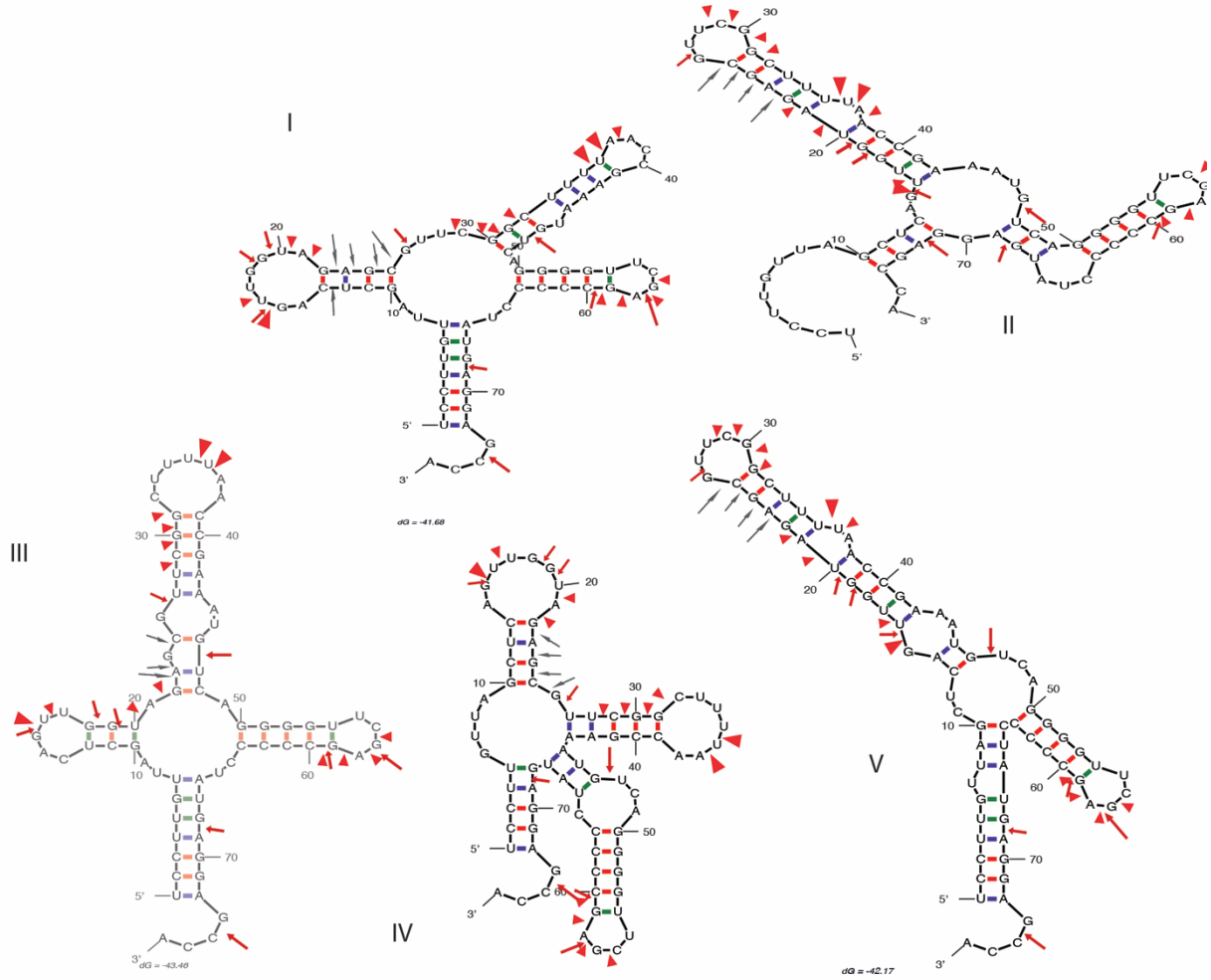


**Figure 16. Cleavage sites of tRK2**: cleavage sites of Rnase T1 (red arrow), Rnase V1 (black arrow) and in-line (red triangular) mapped on secondary ctructures of tRK2 predicted by Mfold (folding temperature is 0°C)

In-line probing revealed sensitivity of D-loop and anticodon-loop in both molecules. In addition, tRK2 exhibited additional site of in line cleavage including anticodon stem or D-stem possibly due to contribution of such conformers as I, II and V.

## Factors beyond enolase 2 and mitochondrial lysyl-tRNA synthetase precursor are required for tRNA import in yeast mitochondria

To investigate the structural aspects of complex forming between yeast Eno2p and tRK1, we needed to optimize the purification protocol of $His_6$-tagged recombinant enolase. To achieve this goal, additional chromatographic step was performed after Ni-NTA purification. While the purity of recombinant Eno2p containing sample increased, its ability to retardate tRK1 in EMSA decreased significantly. The absence of interaction between tRK1 and Eno2p was also confirmed by ITC.

We hypothesized that the purification procedure eliminated contamination as well as a factor that might be required for the interaction between tRK1 and recombinant Eno2p. The contribution of *E. coli* contamination to EMSA results also could not be ruled out. To check this, we extracted *E. coli* proteins presenting affinity to Ni-NTA resin and so might copurify with recombinant Eno2p. We observed that *E. coli* proteins could also bind tRK1 in EMSA yielding a complex of the same size as with Eno2p-containing samples.

To avoid false-positive results due to *E. coli* contamination as well as to confirm the role of Eno2p in promoting tRK1 mitochondrial import, Eno2p-enriched protein samples were obtained directly from yeast extracts. The ability of these samples to direct the tRK1 mitochondrial import was evaluated by *in vitro* import assay in the presence of preMSK1p. The results confirmed that Eno2p significantly increases import efficiency unlike a fraction of *E. coli* proteins that had demonstrated the affinity to tRK1.

To check the hypothesis that additional factors may be required to mediate Eno2p interaction with tRK1, we studied how a relative protein composition of Eno2p-enriched fractions could affect RNA mitochondrial import *in vitro*. Two strategies were exploited. The first one based on serial fractionation of yeast extracts using increasing ammonium sulfate concentrations and the second strategy consisted in performing affinity chromatography on heparin matrix. Only fractions containing Eno2p retardated T7 tRK1 in EMSA as well as presented import directing activity. In addition, endogenous yeast Eno2p-enriched fractions did not show the same selectivity towards tRK1 and tRK2 transcripts.

The study demonstrated that Eno2p does not interact with tRK1 transcripts *in vitro*. Moreover, interactions between some Eno2p-deprived protein fractions and tRK1 could be observed in EMSA. Nevertheless, the presence of Eno2p is required for import of tRK into mitochondria. Since Eno2p alone does not capable to direct *in vitro* import of tRK1, cellular unknown factors adding to Eno2p are thus necessary to direct import.

# Factors beyond enolase 2 and mitochondrial lysyl-tRNA synthetase precursor are required for tRNA import in yeast mitochondria

Mariia Baleva[1,2], Mélanie Meyer[3], Nina Entelis[1], Ivan Tarassov[1], Piotr Kamenski[2,4] & Benoît Masquida[1*]

[1]GMGM, CNRS – University of Strasbourg, UMR 7156, 4 allée Konrad Roentgen, 67081, Strasbourg, France

[2]Molecular Biology Department, Faculty of Biology, M.V. Lomonosov Moscow State University, 1/12 Leninskie Gory, 119991 Moscow, Russia

[3]Present Address: IGBMC, CNRS – University of Strasbourg, UMR 7104, 1 rue Laurent Fries, 67404 Illkirch, France

[4]Institute of Chemistry and Biology, Immanuil Kant Baltic Federal University, 14 Alexandra Nevskogo, 236038 Kaliningrad, Russia

*To whom correspondance should be addressed : b.masquida@unistra.fr

Received May 27, 16
After revision July 21, 16

## Abstract

In yeast, the import of $tRNA^{Lys}$ with CUU anticodon (tRK1) relies on a complex mechanism where interaction with enolase2 (Eno2p) dictates a deep conformational change of the tRNA. This event is believed to mask the tRNA from the cytosolic translational machinery in order to re-direct it towards the mitochondria. Once in the vicinity of the mitochondrial outer membrane, the precursor of the mitochondrial lysyl-tRNA synthetase (preMSK1p) takes over enolase to carry the tRNA within the mitochondrial matrix where it is supposed to participate in translation following correct refolding. Biochemical data presented in this manuscript focus on the role of enolase. They show that despite the inability of Eno2p alone to form a complex with tRK1, mitochondrial import can be recapitulated in vitro using fractions of yeast extracts sharing either recombinant or endogenous yeast Eno2p as one of the main components. Taken together, our data suggest the existence of a protein complex containing Eno2p, which involved in RNA mitochondrial import.


Keywords: RNA mitochondrial import; RNA chaperone; tRNA-enolase interaction; enolase; moonlighting protein

## Introduction

Occurrences of mitochondrial RNA import have been characterized throughout the eukaryotic tree of life. Genetic analysis of the mitochondrial DNA organization of highly divergent eukaryotes point to tRNAs as potentially representing the largest RNA family imported into mitochondria. In plasmodia, the mitochondrial DNA encodes no tRNA nor rRNA, but three proteins necessary to the oxidative phosphorylation [1]. In trypanosomatids, the mitochondrial DNA also does not encode any tRNA [2] and tRNAs are massively imported. Moreover, in some species of cnidarians like the *Lophelia pertusa* coral, the mitochondrial DNA encodes only two tRNA genes, and seven proteins [3, 4]. Massive tRNA import is thus expected to support mitochondrial translation in these organisms, although their RNA import mechanism has been less studied than in plants [5].

Our laboratory has demonstrated that tRNA mitochondrial import occurs naturally in yeast [6, 7] and that yeast cytosolic tRNA derivatives can be imported in mitochondria of cultured human cells [8], even though their mitochondrial DNA encodes complete sets of tRNA. In addition, the human 5S ribosomal RNA is also imported into human mitochondria [9, 10] although its function once imported remains elusive. In yeast, the import of tRK1 ($tRNA^{Lys}$ with anticodon CUU) rescues mitochondrial translation at non-permissive temperature when the mitochondrial $tRNA^{Lys}$ (tRK3) is hypo-modified and becomes inefficient at decoding rare AAG codons [11]. Moreover, yeast tRNA derivatives can fortuitously suppress mutations leading to MELAS [12] or MERRF [13] syndromes, functionally replacing host mitochondrial $tRNA^{Leu}$ or $tRNA^{Lys}$, respectively. These studies suggest participation of imported cytosolic type molecules in the mitochondrial translation process.

The mechanisms of RNA mitochondrial import appear to rely importantly on RNA refolding by means of proteins acting as molecular chaperones. Mitochondrial import of either tRK1 or of 5S rRNA casts very much alike mechanisms. A first step of RNA hijacking by a cytosolic protein triggers RNA refolding and further escape from cytosolic pathways of a small fraction of the RNA pool (~5%). The first protein carries its RNA freight to the mitochondrial surface where it is transferred to a second carrier facilitating the translocation to the mitochondrial matrix. Although this late stage is believed to rely on the VDAC and/or TOM/TIM channels [14], no undisputed molecular mechanism was proposed for yeast or human mitochondria. The glycolytic enzyme enolase is first involved as a carrier of tRK1, and the precursor of the lysyl-tRNA synthetase (preMSK1p) takes it in charge during the second step (**Figure 1**). In the case of the 5S rRNA, the

precursor of the mitochondrial ribosomal protein L18 (MRPL18) firstly hijacks the 5S RNA, then followed by rhodanese, an enzyme apparently involved in cyanide detoxication.

Our recent studies have shown that the three human enolases (α, β, γ) promote mitochondrial import of tRK1 as does enolase 2 in yeast [15]. However, in our efforts to characterize the complex between tRK1 and enolase 2 in order to conduct structural studies, we have realized that additional factors seem to be required. The present study summarizes original, nevertheless preliminary, biochemical evidence, which show that enolase alone is not competent to interact with tRK1, and present experimental conditions under which it was possible to produce a tRK1-enolase molecular complex, competent in mitochondrial in vitro import. Yet, this complex is built up from additional proteins that need to be further identified.

## Material and Methods

### In vitro transcription of tRNAs

Plasmid DNA templates were typically obtained from XL1blue cells using the QIAGEN Plasmid Maxi Kit, and linearized with MvaI (BstNI) (Fermentas, Thermo Fisher Scientific). The construct of tRK1 and tRK2 are preceded by a hammerhead ribozyme preserving the loop-loop tertiary interaction between stems I and II in order to produce transcripts with wild type 5' and 3' sequences following design principles reported in [16]. Transcription reactions of BstN1-linearized hammerhead ribozyme-tRNA constructs (tRK1: 5'-TAATACGACTCACTATAGGGCGCCACCAAGGCCTGACGAGTCTCTGAGATGAGACGAAACTCTTCGCAAGAAGAGTCgCCTTGTTGGCGCAATCGGTAGCGCGTATGACTCTTAATCATAAGGTTAGGGGTTCGAGCCCCCTACAGGGCTCCA-3', tRK2: TAATACGACTCACTATAGGGTGAGCATACCAAGGACTGACGAGTCTCTGAGATGAGACGAAACTCTTCGCAAGAAGAGTCtCCTTGTTAGCTCAGTTGGTAGAGCGTTCGGCTTTTAACCGAAATGTCAGGGGTTCGAGCCCCCTATGAGGAGCCA, where the 5' nucleotide of each tRNA is in small case) were incubated during 4 h at 37°C in 40 mM Tris-HCl (pH 8.0), 5 mM DTT, 0.01% Triton X-100, 1 mM spermidine, 5 mM ATP, 5 mM CTP, 5 mM UTP, 5 mM GTP, 22 mM $MgCl_2$, 60 µg/mL purified recombinant T7 RNAP (homemade), 1 units/mL *E. coli* inorganic pyrophosphatase, and 50 µg/mL linearized plasmid DNA template. The hammerhead ribozyme was

optimized for cleavage tRK1 as in (15). RNA transcripts were purified by 8-10% denaturing PAGE [17].

**Recombinant enolase 2 expression and purification**

Native wild-type yeast enolase 2 (Eno2p) with a C-terminal $His_6$-tag was expressed from a plasmid pET3a derivative transformed in *Escherichia coli* strain BL21. The bacteria were grown at 37°C in LB media containing 0.1 mg/mL ampicilline until the $OD_{600}$ reached 0.6. Protein expression was induced by 0.5 mM IPTG for 2-3 h at 30°C. Cells were harvested by centrifugation and re-suspended in NP buffer (50 mM $NaH_2PO_4$, 300 mM NaCl pH 8.0) supplemented with Complete EDTA-free protease inhibitor tablets (Roche). Cells were incubated in the presence of lysozyme (1 mg/mL), 30 min on ice and lysed by sonication. Cell debris were collected by centrifugation at 20,000 *g* for 1 h at 4°C. The supernatant was incubated overnight at 4°C in the presence of 1 mL of Ni-NTA slurry (Qiagen) per 4 mL of cleared lysate supernatant and 10 mM imidazole. The resin was then washed with NP-buffer containing 10, 20 or 30 mM imidazole. The bound Eno2p was eluted from the resin with NPI-buffer containing imidazole concentrations increasing from 100 mM to 200 mM. The protein sample was then dialyzed at 4°C against a buffer containing 50 mM HEPES-KOH pH 7.5, 100 mM KCl, 1 mM $MgCl_2$. The concentration of protein was determined by measuring absorbance at 280 nm (E1% = 8.95). The purity of the protein was estimated from Coomassie-stained SDS-PAGE. Molecular weights of proteins were estimated using PageRuler Prestained Protein Ladder (Fermentas).

**Purification of yeast enolase 2**

Yeast Eno2p was purified under native conditions from Δ*ENO1* yeast cells at the end of the exponential phase (*ENO1* gene was deleted in W303 yeast strain by *KanMX4* cassette replacement). Yeast cells were grown in liquid YPD medium (1% yeast extract, 2% peptone, 2% glucose/dextrose) supplemented with 0.2 mg/mL of G418 at 30°C in a shaking incubator (Infors HT Multitron, 250 rpm) for 18 h. The cells were harvested by centrifugation and washed with pre-chilled milliQ water.

Disruption of cells was performed using a FastPrep-24™ Homogenizer (MP Biomedical) after addition of glass beads to the breakage buffer (0.6 M Sorbitol, 10 mM Tris-HCl, pH 7.5, 1 mM EDTA and protease inhibitor cocktail) used to resuspend the pellet. Cell debris were collected by

centrifugation at 40 000 *g* for 30 min at 4 °C. The supernatant was transferred to a fresh tube and then 67% saturated with ammonium sulfate by addition of solid ammonium sulfate. After centrifugation at 40 000 *g* at 4°C for 30 min, the supernatant was then 100% saturated and centrifuged again at 40 000 *g* at 4°C for 30 min. The supernatant was discarded and the pellet re-suspended in 20 mM Tris–HCl buffer, pH 8.3, containing 5 mM $MgSO_4$, 1 mM EDTA; dialyzed overnight against the same buffer and applied to a mono-Q column (HiTrap Q XL, GE Healthcare) equilibrated with 10 mM Tris–HCl buffer, pH 8.3, containing 5 mM $MgSO_4$, 1 mM EDTA. Proteins were fractionated with a linear NaCl gradient (0-1 M). Eno2p-enriched fractions were applied to a Superdex-200 Increase 10/300 GL column (GE Healthcare) equilibrated with 50 mM HEPES-KOH, pH 7.5, 150 mM KCl, 5 mM $MgSO_4$ and 1 mM EDTA. A final step of hydroxyapatite chromatography (CHT5-1 BioRad) was used to eliminate nucleases. At each purification step, protein-containing fractions were probed by dot-blot analysis using an anti-enolase antibody.

**Isothermal titration microcalorimetry (ITC)**

ITC experiments were conducted on a MicroCal ITC200 (GE Healthcare). Prior to the experiment, the protein and RNA samples were dialyzed against the same buffer (25 mM HEPES-KOH (pH 7.5), 100 mM KCl, 1 mM $MgCl_2$, 0.1 mM EDTA). Data treatment was performed with the software Origin 7.0. Typical experiments according to the manufacturer guidelines were conducted using 300 µL of a solution of Eno2p at 30 µM in the main adiabatic cell, while the syringe was loaded with a solution containing 300 µM RNA refolded under the same conditions as for EMSA experiments. Injections of 1.5 µL of tRK1 solution were performed until complete titration was achieved.

**Electrophoretic Mobility Shift Assay (EMSA)**

T7 transcripts of tRK1 were 5’ end-labeled with γ-$^{32}$P-ATP using T4 polynucleotide kinase (Promega). The labeled RNA was denatured at 92°C and then slowly cooled down to room temperature in the presence of 4 mM EDTA. EMSA was conducted as described in (24). Appropriate amounts of proteins and labeled tRK1 transcripts were mixed in 10 µL of a buffer containing 25 mM HEPES-KOH (pH 7.5); 100 mM KCl; 1 mM $MgCl_2$, 0.1 mM EDTA and incubated for 20 min at 30°C. RNA-protein complexes were separated from free RNA by native 8% PAGE containing 5% glycerol in 0.5x TBE buffer (pH 8.3).

### In vitro mitochondrial import assay

Mitochondria were purified from yeast YPH499 as described earlier [18]. A standard 100 $\mu$L in vitro mitochondrial import reaction contained 50,000 cpm of 5'-$^{32}$P-labeled tRK1, 60 nM recombinant preMSK1p, 0.1 mg of mitochondria and 10 $\mu$g of the assayed protein fractions as determined by Bradford assay. The import assays were carried out at 30°C during 15 min in import buffer (0.6 M sorbitol, 20 mM HEPES-KOH (pH 6.8), 20 mM KCl, 2.5 mM $MgCl_2$, 1 mM ATP, 5 mM DTT, 0.5 mM phosphoenol pyruvate and 4 units of pyruvate kinase). Thereafter, 50 $\mu$g/mL of RNase A (Sigma) was added in order to degrade non-imported RNAs and the samples were further incubated for 10 min on ice. After washing three times the samples with a buffer containing 0.6 M sorbitol, 10 mM HEPES-KOH (pH 6.7) and 4 mM EDTA, mitochondria were pelleted by centrifugation. RNAs were extracted using 100 $\mu$l of TRIzol reagent (Thermo Fisher Scientific), precipitated with ethanol and further separated by 8% denaturing PAGE (8 M urea). Bands of RNA were quantitated using a Typhoon-Trio scanner and the Image Quant-Tools software (GE Healthcare). The amount of imported RNA was determined by comparing the band density of the protected full-size RNA isolated from the mitochondria after the import assay with an aliquot representing 2-6% of the RNA input.

### Western blot

For immunoblotting, proteins were separated on SDS-PAGE and transferred to a nitrocellulose membrane. Goat antibodies directed against enolase were used (Molecular Probes, C-19: sc-7455, Santa Cruz Biotechnology). Western-blots were conducted as described earlier [19].

### S100 protein extract and its fractionation by heparin chromatography

The initial protein sample represents an extract of wild-type cells. An overnight 1 L culture of yeast W303 was centrifuged, washed twice with ice cold water, re-suspended in 10 mM HEPES-KOH (pH 6.8), 50 mM KCl, 1 mM EDTA, 5 mM DTT, 10% glycerol, Complete protease inhibitor cocktail (Roche). Cells were lyzed by shaking in the presence of glass beads (FastPrep-24™ Homogenizer, MP Biomedicals). Cell debris were pelleted by low (2000 g) speed centrifugation. The supernatant was centrifuged at 100,000 *g* for 30 min at 4°C. The S100 fraction was dialyzed against 20 mM HEPES-KOH (pH 6.8), 10 mM NaCl; 0.5 mM PMSF, 1 mM DTT and 10% glycerol, and applied to a heparin-sepharose column (Hi Trap Heparin HP 1 mL, GE Healthcare) equilibrated with the same buffer. Proteins were eluted by a step gradient of sodium chloride (0.1, 0.2, 0.5 and 1 M). Fractions containing high level of Eno2p as deduced by western blot analysis

were pooled and further dialyzed against 20 mM HEPES, pH 6.8, 1 mM DTT, 10 mM KCl and 50% glycerol including protease inhibitor cocktail, and stored at -20°C.

## Results

### Improving the purity of recombinant enolase 2 reduces interaction with tRK1 transcripts

The His-tagged recombinant enolases (wild-type, H373F) used in our biochemical assays were purified by affinity chromatography using Ni-NTA resin. Resulting samples contained fairly pure Eno2p, although some contaminants were still detected by SDS-PAGE (**Figure 2A).** Ni-NTA samples proved to be active in electrophoretic mobility shift assays (EMSA) (**Figure 2B**), suggesting that tRK1 could form a complex with recombinant Eno2p. Since our original goal was to solve the crystal structure of the cytosolic import complex of tRK1, we decided to purify further the recombinant Eno2p, since the presence of protein contaminants is known to generally preclude successful crystallization. We decided to further improve purification by addition of chromatographic steps (**Figure 2C, D).**

Hydroxyapatite chromatography under native conditions of the overexpressed recombinant Eno2p indeed led to a highly pure protein sample. Yet, the propensity of the pure recombinant protein to interact with and to retard tRK1 was significantly reduced (**Figure 2B**). The results of these experiments suggest that some contaminants may be required to promote the interaction between tRK1 and Eno2p. Since enolases from yeast and *E. coli* present ~42% of identity [20] and are both very abundant in both organisms, it is also likely that some proteins from *E. coli* may be efficient in binding the recombinant Eno2p, and furthermore tRK1. This possibility is strengthened by the fact that very tiny amounts of RNA are used in EMSA, thus requiring small amounts of putative interacting proteins. Moreover, EMSA performed on larger amounts of unlabeled RNA failed to detect a visible mobility shift of tRK1. Nevertheless, we could observe that proteins from *E. coli* (BL21 with empty pET-3 plasmid) prepared under the same conditions as for the His-tagged Eno2p (**Figure 3A**) could also bind tRK1 in EMSA yielding a complex of same size as with Eno2p samples. This observation indicates that proteins from *E. coli* capable of interacting with tRK1 may form a complex mimicking the complex formed between tRK1 and the recombinant Eno2p (**Figure 3B**). Yet, we did not investigate whether *E. coli* enolase could replace Eno2p on this occasion.

We turned towards isothermal titration microcalorimetry (ITC) to determine whether pure recombinant Eno2p could interact with tRK1 transcripts. ITC is a very sensitive and suitable method to determine whether molecules interact in solution in an unbiased experimental setup and do not require labeled molecules. Since ITC requires much larger amounts of material than EMSA, the contribution of contaminanting proteins to the signal can be neglected as opposed to EMSA. In a classical ITC experiment, a concentrated sample containing the ligand is added step by step to a large volume of a solution containing the receptor. At each step, the solution under continuous stirring is incubated untill the mix reaches equilibrium as monitored by the stabilization of the heat transfer. In our case, a concentrated solution of tRK1 was added step by step to a concentrated solution of Eno2p. Strikingly, no release or absorption of heat could be measured indicating that tRK1 transcripts and Eno2p do not interact (data not shown). These results confirmed abolition of complex formation with a pure recombinant Eno2p sample, corroborating results obtained by EMSA (**Figure 2**).

**Samples enriched with either recombinant or endogenous yeast Eno2p direct in vitro import and form a detectable RNA-protein complex**

The inability of recombinant Eno2p to interact even transiently with tRK1 transcripts in vitro suggested that additional factors might favor tRNA mitochondrial import. In order to investigate this hypothesis and to confirm the role of Eno2p, the ability to promote tRK1 mitochondrial import of Eno2p-enriched protein samples obtained from yeast extracts was evaluated. Wild-type Eno2p-enriched samples were obtained by purification from yeast strain *ΔENO1* to avoid interference of Eno1p with tRK1. Enolases 1 and 2 abundance in yeast represents 3.6% and 6.2% of the total protein mass, respectively [21]. SDS-PAGE patterns of individual fractions were assayed by western blot to assess the presence and amounts of Eno2p (**Figure 4**). Results of in vitro import experiments of tRK1 into isolated yeast mitochondria confirmed that Eno2p significantly increases import efficiency as compared to the very low level observed with preMSK1p alone (**Figure 5**). The fraction of *E. coli* proteins yielded background level signal comparable to preMSK1p, indicating that the unspecific interactions detected in EMSA between *E. coli* proteins and tRK1 do not promote in vitro mitochondrial import.

Furthermore, we wanted to check whether changing the relative protein composition of Eno2p-enriched fractions could affect RNA mitochondrial import. Two strategies were undertaken

to fractionate yeast cell extracts. The first one consisted in serial fractionation of yeast extracts using increasing ammonium sulfate concentrations [22] (Figure 6A) and the second one consisted in performing affinity chromatography on heparin matrix (Figure 7). Relative amounts of Eno2p in ammonium sulfate fractionated samples were determined by western blot (**Figure 6B**) and further assayed for their ability to direct mitochondrial import in vitro. Only fractions containing Eno2p showed import directing capabilities (**Figure 6C**). These findings were confirmed by tests on samples obtained by heparin chromatography. The flow-through fraction (HP-0), which contains the majority of the Eno2p pool (**Figure 7**) was mainly active in both EMSA and mitochondrial in vitro import assays (**Figure 8**). As for the recombinant Eno2p sample, we noted that yeast endogenous Eno2p-enriched samples underwent gradual loss of import directing capabilities after hydroxyapatite chromatography (**Figure 5**).

The Eno2p-enriched fractions obtained directly from yeast are supposed to discriminate better between tRK1 and tRK2 (the second cytosolic lysine tRNA isoacceptor with UUU anticodon) transcripts than recombinant Eno2p accompanied by bacterial contaminants. In order to check if this was the case in our experiments, the capabilities of the Eno2p-enriched fractions to import tRK2 transcripts were evaluated (**Figure 6D**). These data show that the hydroxyapatite fractionation step also affects tRK2 mitochondrial import capability of samples processed as indicated in figure 4A. These results indicate that protein partners of enolase likely to be critical to the import process are partly removed by this treatment. The results from the mitochondrial import assays also show that transcripts of tRK1 are slightly better imported than those of tRK2 **(Figure 6E)** indicating a slight but significant discrimination between the two transcripts. These results are in agreement with those on recombinant Eno2p, hence supporting the conclusion that the mitochondrial import process requires the participation of factors other than enolase.

## Discussion

The motivation of the present study was to characterize the interaction between Eno2p and tRK1 transcripts in order to conduct crystallographic studies of the complex supposedly formed between these two molecules. Eno2p has been identified as a necessary factor for the initial step of tRK1 mitochondrial import in yeast [22]. Recombinant Eno2p samples obtained through nickel affinity chromatography successfully retardated tRK1 transcripts in electrophoretic mobility shift assays (EMSA). Nevertheless, an additional purification step using hydroxyapatite chromatography

significantly reduced tRK1 retardation. Further thermodynamic studies performed by isothermal titration microcalorimetry led to the conclusion that, indeed recombinant Eno2p was not capable of interacting with tRK1 transcript without the help of other cellular factors, which remain to be identified. This observation is supported by the fact that Eno2p, with a fairly low isoelectric point of ~5.7, is not adapted to interact with heavily negatively charged molecules such as RNAs at physiological pH. Most RNA binding proteins present large positively charged electrostatic surfaces and isoelectric point usually beyond 8.0. Eno2p thus appears as a necessary, but not as a sufficient factor to promote tRK1 mitochondrial import. It could be argued that the absence of chemical modifications of tRK1 in vitro transcripts may prevent the two molecules to interact, although the observation that the transcripts can be sucessfully imported into mitochondria by Eno2p-enriched fractions contradicts this hypothesis. Nevertheless, the absence of chemical modifications could in principle affect import specificity, since tRK2 transcripts can also be imported in vitro, albeit not in vivo [23].

Our study indicates that fractions enriched either with recombinant or yeast-purified Eno2p are able to direct mitochondrial import in agreement with previously published results [22]. In all cases, it appears that contaminants favor this phenomenon, whether they originate from *E. coli* or yeast proteins. Enolases from these organisms share a high level of identity (42%) [20], which may partially rationalize why recombinant Eno2p may benefit from *E. coli* factor(s) to carry out mitochondrial import. Since Eno2p is a very abundant cytosolic protein and that only ~5% of the tRK1 pool follows the mitochondrial import route in vivo, proteins that are not stoichiometric with enolase or in other words much less abundant may be involved in this mechanism. Consequently, it is possible to hypothesize that the amount of tRK1 import complex could be controlled by a limiting protein cofactor, which may also serve to regulate the process under stress conditions. It results from this assumption that *E. coli* contaminants participating in the process should be fairly rare molecules, hence difficult to characterize. These arguments explain why an interaction between a picomolar amount of labeled tRK1 can be detected by EMSA, while ITC, which requires micromolar amounts is less perturbed by the presence of contaminants. In spite of these evidence, we cannot completely rule out that tRK1 transcripts may be retardated by other *E. coli* proteins. A recent example describes an interaction artefact between bacterial non-coding RNAs and Hfq, which was enriched by Ni-NTA purification due to the presence of several histidine residues in the Hfq hexamere, further leading to spurious mobility shift of the target non-coding RNAs [24]. Nevertheless, *E. coli* proteins obtained following the recombinant Eno2p purification protocol were

able to retardate tRK1 transcripts (EMSA), but did not show significant ability to promote mitochondrial import in vitro in the presence of preMSK1p.

The present study demonstrates that Eno2p alone is not capable of interacting with tRK1 transcripts in vitro, or to direct in vitro mitochondrial import. The data are not in contradiction with previously published ones since fractions not containing Eno2p could not direct import, and vice-versa. Nonetheless, interactions between some Eno2p-deprived protein fractions and tRK1 could be detected by EMSA. Cellular unknown factors adding to Eno2p are thus necessary to direct import. The involved unidentified bacterial factors may also share high sequence identities with the yeast proteins that are necessary to the action of yeast Eno2p. Their identification will rely on further studies based on mass-spectrometry and sequence homology analysis between the *E. coli* and yeast proteins.

## Acknowledgements

The authors thank Eric Ennifar and Cyrielle Silva Da Veiga for help with ITC measurements and data interpretation. This research is supported by the Centre National de la Recherche Scientifique (LABEX ANR-11-LABX-0057_MITOCROSS), the University of Strasbourg, the Government of the Russian Federation (State Assignment AAAA-A16-116021660073-5) and 5-100 program of Ministry of Education and Science of Russia to Baltic Federal University. MB is supported by the Russian Foundation for Basic Research (Grant 16-34-00978) and French Ambassy in Moscow (Russian Federation) and Collège Doctoral Européen from the University of Strasbourg.

## References

1. Sharma A, Sharma A (2015) Plasmodium falciparum mitochondria import tRNAs along with an active phenylalanyl-tRNA synthetase. *The Biochemical journal*, **465**(3),459-469.

2. Tschopp F, Charriere F, Schneider A (2011) In vivo study in Trypanosoma brucei links mitochondrial transfer RNA import to mitochondrial protein import. *EMBO reports*, **12**(8),825-832.

3. Emblem A, Karlsen BO, Evertsen J, Miller DJ, Moum T, Johansen SD (2012) Mitogenome polymorphism in a single branch sample revealed by SOLiD deep sequencing of the Lophelia pertusa coral genome. *Gene*, **506**(2),344-349.

4. Emblem A, Karlsen BO, Evertsen J, Johansen SD (2011) Mitogenome rearrangement in the cold-water scleractinian coral Lophelia pertusa (Cnidaria, Anthozoa) involves a long-term evolving group I intron. *Molecular phylogenetics and evolution*, **61**(2),495-503.

5. Salinas T, Duchene AM, Marechal-Drouard L (2008) Recent advances in tRNA mitochondrial import. *Trends in biochemical sciences*, **33**(7),320-329.

6. Martin RP, Schneller JM, Stahl AJ, Dirheimer G (1979) Import of nuclear deoxyribonucleic acid coded lysine-accepting transfer ribonucleic acid (anticodon C-U-U) into yeast mitochondria. *Biochemistry*, **18**(21),4600-4605.

7. Kolesnikova OA, Entelis NS, Mireau H, Fox TD, Martin RP, Tarassov IA (2000) Suppression of mutations in mitochondrial DNA by tRNAs imported from the cytoplasm. *Science*, **289**(5486),1931-1933.

8. Entelis NS, Kolesnikova OA, Dogan S, Martin RP, Tarassov IA (2001) 5 S rRNA and tRNA import into human mitochondria. Comparison of in vitro requirements. *The Journal of biological chemistry*, **276**(49),45642-45653.

9. Smirnov A, Comte C, Mager-Heckel AM, Addis V, Krasheninnikov IA, Martin RP, Entelis N, Tarassov I (2010) Mitochondrial enzyme rhodanese is essential for 5 S ribosomal RNA import into human mitochondria. *The Journal of biological chemistry*, **285**(40),30792-30803.

10. Smirnov A, Entelis N, Martin RP, Tarassov I (2011) Biological significance of 5S rRNA import into human mitochondria: role of ribosomal protein MRP-L18. *Genes & development*, **25**(12),1289-1305.

11. Kamenski P, Kolesnikova O, Jubenot V, Entelis N, Krasheninnikov IA, Martin RP, Tarassov I (2007) Evidence for an adaptation mechanism of mitochondrial translation via tRNA import from the cytosol. *Molecular cell*, **26**(5),625-637.

12. Karicheva OZ, Kolesnikova OA, Schirtz T, Vysokikh MY, Mager-Heckel AM, Lombes A, Boucheham A, Krasheninnikov IA, Martin RP, Entelis N, Tarassov I (2011) Correction of the consequences of mitochondrial 3243A>G mutation in the MT-TL1 gene causing the MELAS syndrome by tRNA import into mitochondria. *Nucleic Acids Res*, **39**(18),8173-8186.

13. Kolesnikova OA, Entelis NS, Jacquin-Becker C, Goltzene F, Chrzanowska-Lightowlers ZM, Lightowlers RN, Martin RP, Tarassov I (2004) Nuclear DNA-encoded tRNAs targeted into mitochondria can rescue a mitochondrial DNA mutation associated with the MERRF syndrome in cultured human cells. *Hum Mol Genet*, **13**(20),2519-2534.

14. Tarassov I, Entelis N, Martin RP (1995) An intact protein translocating machinery is required for mitochondrial import of a yeast cytoplasmic tRNA. *J Mol Biol*, **245**(4),315-323.

15. Baleva M, Gowher A, Kamenski P, Tarassov I, Entelis N, Masquida B (2015) A Moonlighting Human Protein Is Involved in Mitochondrial Import of tRNA. *International Journal of Molecular Sciences*, **16**(5),9354-9367.

16. Meyer M, Masquida B (2014) Cis-Acting 5' Hammerhead Ribozyme Optimization for In Vitro Transcription of Highly Structured RNAs. *Methods in molecular biology*, **1086**,21-40.

17. Meyer M, Masquida B (2016) Polyacrylamide Gel Electrophoresis for Purification of Large Amounts of RNA. *Methods in molecular biology*, **1320**,59-65.

18. Entelis NS, Krasheninnikov IA, Martin RP, Tarassov IA (1996) Mitochondrial import of a yeast cytoplasmic tRNA (Lys): possible roles of aminoacylation and modified nucleosides in subcellular partitioning. *FEBS letters*, **384**(1),38-42.

19. Gowher A, Smirnov A, Tarassov I, Entelis N (2013) Induced tRNA import into human mitochondria: implication of a host aminoacyl-tRNA-synthetase. *PloS one*, **8**(6),e66228.

20. Pancholi V (2001) Multifunctional alpha-enolase: its role in diseases. *Cellular and molecular life sciences : CMLS*, **58**(7),902-920.

21. Lu P, Vogel C, Wang R, Yao X, Marcotte EM (2007) Absolute protein expression profiling estimates the relative contributions of transcriptional and translational regulation. *Nature biotechnology*, **25**(1),117-124.

22. Entelis N, Brandina I, Kamenski P, Krasheninnikov IA, Martin RP, Tarassov I (2006) A glycolytic enzyme, enolase, is recruited as a cofactor of tRNA targeting toward mitochondria in Saccharomyces cerevisiae. *Genes & development*, **20**(12),1609-1620.

23. Kazakova HA, Entelis NS, Martin RP, Tarassov IA (1999) The aminoacceptor stem of the yeast tRNA(Lys) contains determinants of mitochondrial import selectivity. *FEBS letters*, **442**(2-3),193-197.

24. Milojevic T, Sonnleitner E, Romeo A, Djinovic-Carugo K, Blasi U (2013) False positive RNA binding activities after Ni-affinity purification from Escherichia coli. *RNA biology*, **10**(6),1066-1069.

## Figure legends

**Figure 1:** Scheme of the mechanism of mitochondrial import of the yeast lysine isoacceptor tRNA with a CUU anticodon (tRK1). tRK1 undertakes refolding through interaction with proteins including Eno2p. This complex shuttles tRK1 to the mitochondrial surface where it interacts with preMSK1p, which proceeds to import properly in a process that is neither fully understood nor characterized in yeast or human cells.

**Figure 2:** (A) Coomassie stained 10% SDS-PAGE of Ni-NTA-purified recombinant yeast Eno2p (MW ≈ 49 kDa). The lane on the left side presents the pattern of the PageRuler Prestained Protein Ladder (Fermentas) with the corresponding molecular weight scale. Lane 1 corresponds to the flow-through. For lane 2, loaded proteins were washed using a buffer containing 20 mM imidazole. Lanes 3 to 5 correspond to elutions at increasing imidazole concentrations 40, 80 and 150 mM, respectively. Fractions corresponding to lanes 4 and 5 were combined and underwent hydroxyapatite chromatography.

(B). EMSA between labeled tRK1 and Eno2p (wild type (WT) or H373F mutant). The results show how tRK1 binding is altered following hydroxyapatite chromatography of Eno2p. The previously characterized H373F mutation in Eno2p (21) prevents enzymatic activity while preserving the efficiency of *in vitro* import direction. The concentrations of Eno2p in each reaction are indicated on the top of each lane. (*) indicates samples subjected to an additional step of hydroxyapatite chromatography. Free and complex forms of tRK1 are explicitely indicated on the right side of the gel.

(C) Hydroxyapatite chromatography (CHT5-1 BioRad) of Ni-NTA purified recombinant yeast Eno2p. The trace of the optical density monitored at 280 nm presents a single peak corresponding to Eno2p. Fractions between 29 and 34 mL corresponding to the peak of retention volume (indicated with droplet) were analyzed by Coomassie-stained 10% SDS-PAGE (D); Lane 1 - fraction corresponding to 29 mL retention volume, lane 2 - 30 mL, lane 3 - 31 mL, lane 4 - 32 mL, lane 5 - 33 mL, lane 6 - 34 mL.

**Figure 3:** (A) Coomassie stained 10% SDS-PAGE of Ni-NTA purified *E.coli* proteins and recombinant Eno2p. Proteins from *E. coli* BL21 not expressing Eno2p were purified under the same conditions as Eno2p overexpressed in *E. coli* BL21. The patterns of migration of *E.coli* proteins eluted at imidazole concentrations of 20, 40, 60, 100 and 200 mM (lanes 1 to 5) show that some proteins possess strong affinity for the Ni-NTA resin. Lanes 6 to 9 represent the patterns of migration of recombinant Eno2p eluted at imidazole concentrations of 20, 40, 100 and 200 mM.

(B) A comparison between EMSA obtained using Ni-NTA-purified Eno2p and different fractions of Ni-NTA-purified *E. coli* proteins reveals comparable patterns. The interaction between tRK1 and Ni-NTA-purified *E. coli* proteins yields a band indicating a complex of about the same size as with the recombinant Eno2p. tRK1 alone in the EMSA buffer was used as a control. Fractions are labeled according to the imidazole concentration present in the elution buffer. Ten µL samples contained 1 µL of each protein fraction mixed with 3000 cpm of 5'-end labeled tRK1 in EMSA buffer (See Material & Methods section).

**Figure 4:** (A) Strategy of endogenous Eno2p purification from yeast extracts. The supernatant of an S100 fraction was obtained from total yeast (*ΔENO1*) extract. The S100 supernatant was successively subjected to 67% and 100% ammonium sulfate precipitation. The resuspended resulting pellet was fractionated by monoQ chromatography. The purification was polished by gel-filtration followed by hydroxyapatite chromatography.

(B) Representative UV traces obtained by gel-filtration (left side of panel B) followed by hydroxyapatite (right side of panel B) chromatography (UV traces monitored at 280 nm are scaled in milli absorbance units, mAU).

Coomassie-stained 10% SDS-PAGE of gel-filtration-collected fractions (C) and western blot (D) using SC-7455 antibodies allow to identify Eno2p-enriched fractions. PageRuler Prestained Protein Ladder (Fermentas) corresponds to the left lane. Lanes 1-8 present patterns of the 0.5 mL fractions collected at retention volumes (rV) between 12 to 16 mL. The western-blot of the corresponding fractions is shown in panel D.

**Figure 5:** Results of *in vitro* import assay. Recombinant Eno2p, yeast endogenous Eno2p and fractions of *E.coli* proteins active in EMSA were assayed for directing import of labeled tRK1 into isolated yeast mitochondria in the presence of preMSK1p. tRK1 input (lane 1) corresponds to 6% of the fraction that was used in mitochondrial *in vitro* import assay. Three control experiments were performed, without mitochondria (lane 2), or without adding any protein (lane 3), or using preMSK1p alone (lane 4). Other lanes correspond to tests of specific fractions (all reactions were performed in the presence of 60 nM preMSK1p): *E. coli* proteins eluted at 80 mM imidazole (lane 5); recombinant $His_6$-tagged Eno2p (lane 6); Eno2p-enriched fractions after purification from yeast cells prior to (lane 7) or after (lane 8) hydroxyapatite chromatography. The histogram reports the quantitation of gel lanes (in % from the total $^{32}P$ counts taken for each reaction).

**Figure 6:** (A) Coomassie-stained 10% SDS-PAGE of samples resulting from ammonium sulfate fractionation of yeast lysates. The PageRuler Prestained Protein Ladder (Fermentas) is represented on the left. Lane 1 - proteins precipitated at 0-30% ammonium sulfate (AS) saturation, lane 2 – 30-40%, lane 3 – 40-50%, lane 4 – 50-60%, lane 5 – 60-70%, lane 6 – 70-80%, lane 7 – 80-90%, lane 8 – 90-100% and lane 9 - fraction collected by gel filtration chromatography at rV 14 mL and further subjected to hydroxyapatite chromatography.

(B) Western blot of Eno2p allows identifying fractions enriched with Eno2p using the same antibody as in figure 4D.

(C) Fractions were tested in *in vitro* import assay in the presence of recombinant preMSK1p. tRK1 input (lane 1) corresponds to 2% of labeled tRNA that was used in each *in vitro* import assay. Two control experiments were performed, without adding any protein (lane 2) or without mitochondria (lane 3). Other tests were all done in the presence of preMSK1p: lane 4 - preMSK1p alone, lane 5 – fraction 30-40% AS saturation, 6 – 40-50%, 7 – 50-60%, 8 – 60-70%, 9 – 70-80%, 10 – 80-90%, 11 – 90-100% and lane 12 - endogenous yeast Eno2p-enriched prior to hydroxyapatite fractionation. The histogram below the gel shows the quantitation of gel lanes (in % from the total $^{32}P$ counts taken for each reaction). Only fractions 6 to 8 from panel A could direct import of tRK1 (corresponding to lanes 9 to 11 in panel C).

(D) *In vitro* import of tRK2 transcript ($tRNA^{Lys}$ with anticodon UUU) was also assayed to evaluate the specificity of the *in vitro* import test. Lanes 1-4 are the same as in panel C. Lane 5 – fraction of proteins precipitated at 50-60% and lane 6 – 90-100% AS saturation. The ability to direct tRK2 *in vitro* import were tested for 67%-100% AS-saturated Eno2p-enriched fractions prior to and after hydroxyapatite chromatography (lanes 7 and 8, respectively), recombinant Eno2p fractions eluted at 80 and 200 mM

imidazole concentrations (lanes 9 and 10) and *E.coli* proteins fraction eluted at 200 mM imidazole concentration (lane 11; See Figure 3A).

(E) Comparison of tRK1 and tRK2 in vitro mitochondrial import for two samples - fraction 90-100% saturation of ammonium sulfate and yeast protein fractions containing significant amounts of Eno2p prior to hydroxyapatite chromatography.

**Figure 7:** (A) Coomassie-stained 10% SDS-PAGE of of yeast protein extract fractions (S100) fractionated by heparin chromatography. Ten μg of protein (as determined by Bradford assay) were loaded per lane. Lane 1 – recombinant Eno2p, lane 2 - PageRuler Prestained Protein Ladder (Fermentas), lane 3 – HP-500 (500 mM NaCl in elution buffer), lane 4 – HP-200 (200 mM NaCl), lane 5 – HP-100 (100 mM NaCl), lane 6 – HP-0 (no NaCl), lane 7 – S100.

(B) The western blot analysis of fractions obtained by heparin chromatography using the same antibodies as in figure 4D indicates that most Eno2p remains in the flow-through (HP-0, lane 6). Recombinant yeast Eno2p was used as a control (lane 1). No significant signal could be detected for other fractions.

**Figure 8:** Analysis of tRK1-protein interaction. $^{32}$P-5' end labeled tRK1 was incubated in the presence of protein fractions after heparin chromatography (5 μg of total protein per reaction as determined by Bradford assay). Each reaction was fractionated both by EMSA on native 8% PAGE (A) and by denaturing 8% PAGE (B). Lanes 2 - HP-0, lanes 3 – HP-100, lanes 4 – HP-200 and lanes 5 – HP-500. The sample containing tRK1 in the reaction buffer without proteins was used as a control (lanes 1).

(C) The tRK1 import ability of the protein fractions assayed in EMSA was evaluated by *in vitro* import assay of $^{32}$P-5' end labeled tRK1 transcripts into yeast mitochondria. Lane 1 – 1% of tRK1 input, lane 2 - control without any protein, lane 3 - preMSK1p alone, lane 4 - S100. All other reactions were performed in the presence of preMSK1p: lane 5 - HP-0, lane 6 - HP-100, lane 7 - HP-200, lane 8 - HP-500, lane 9 - human KARS2 and alpha enolase, and lane 10 - HP-900.

**Figure 1.**

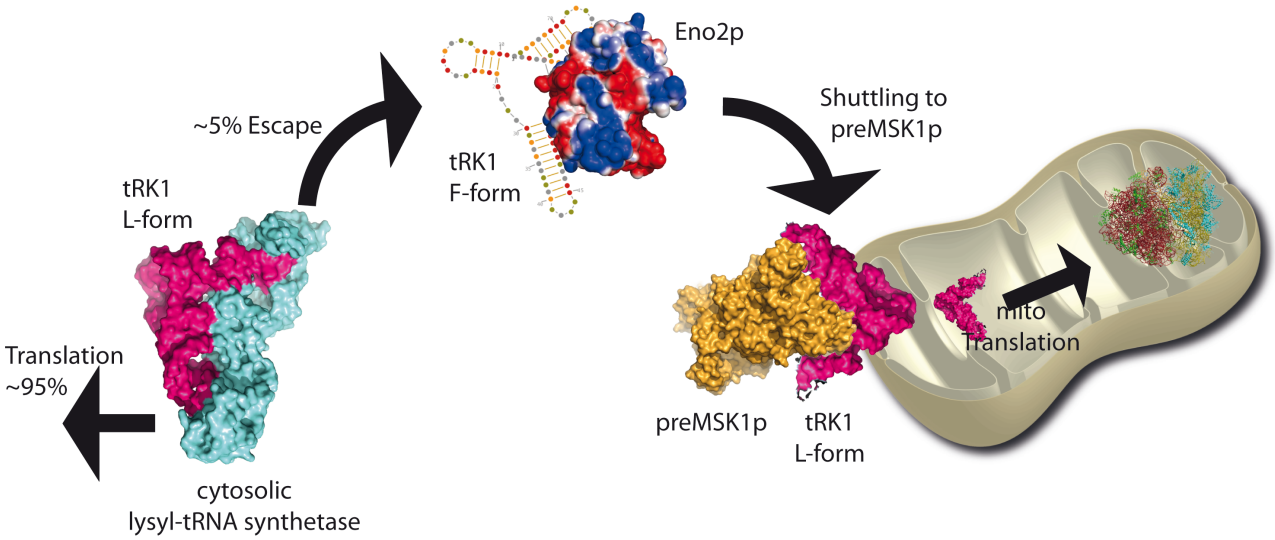
Eno2p
~5% Escape
tRK1
L-form
tRK1
F-form
Shuttling to
preMSK1p
Translation
~95%
cytosolic
lysyl-tRNA synthetase
preMSK1p
tRK1
L-form
mito
Translation

**Figure 2.**

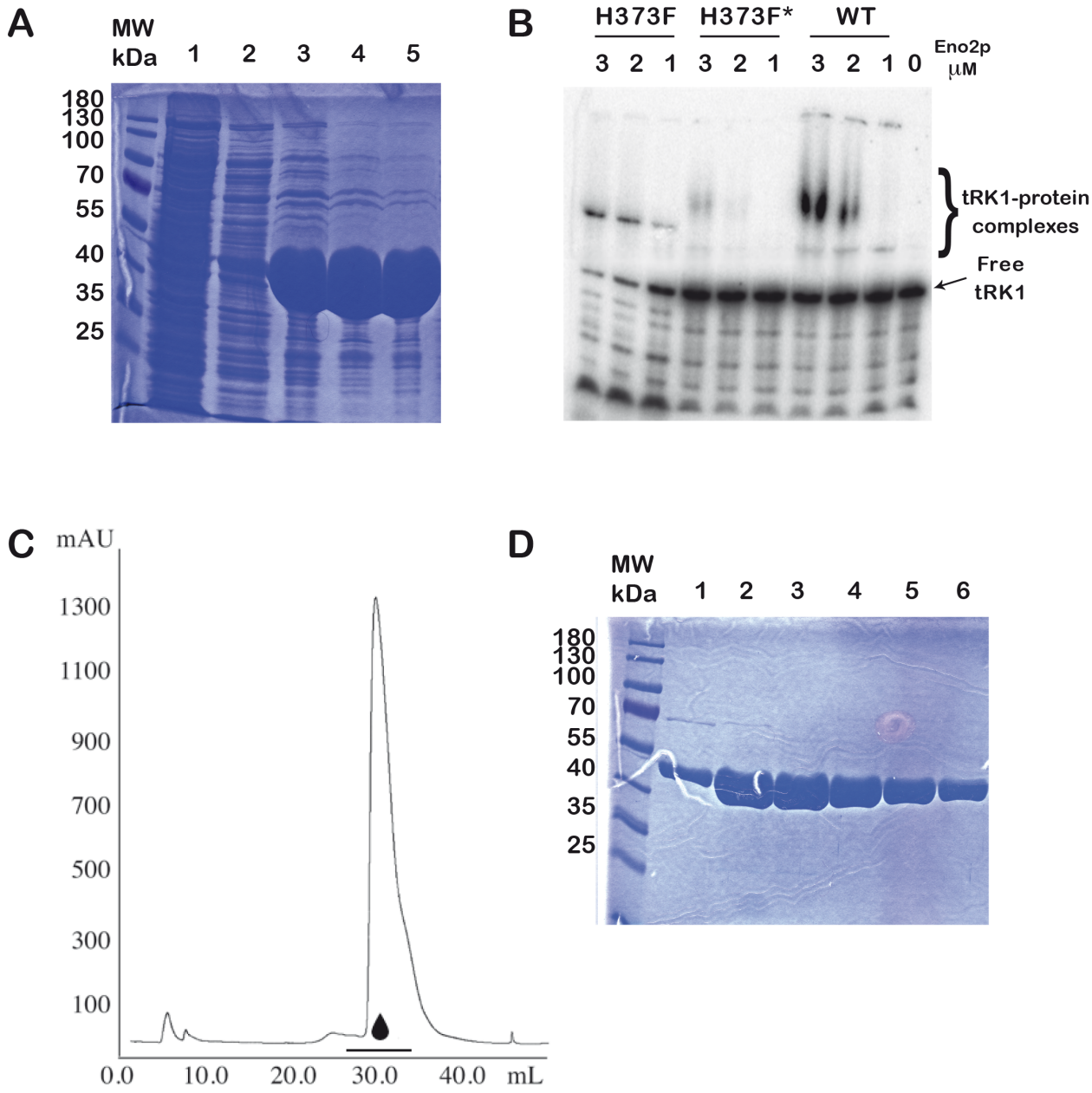
A
MW
kDa
1
2
3
4
5
180
130
100
70
55
40
35
25
B
H373F
H373F*
WT
3 2 1 3 2 1 3 2 1 0
Eno2p
μM
tRK1-protein
complexes
Free
tRK1
C
mAU
1300
1100
900
700
500
300
100
0.0
10.0
20.0
30.0
40.0
mL
D
MW
kDa
1
2
3
4
5
6
180
130
100
70
55
40
35
25

**Figure 3.**

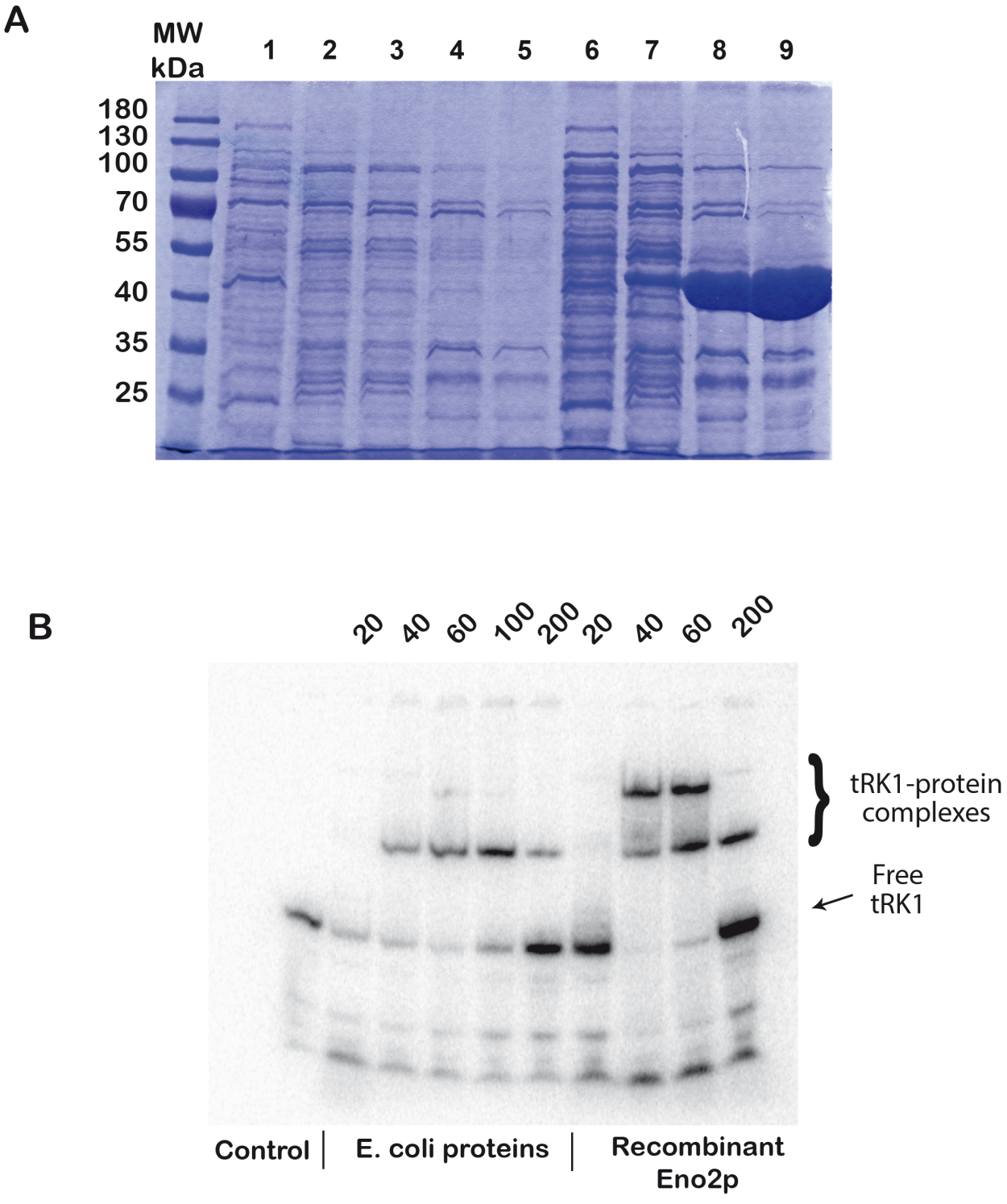
A
MW
kDa
1
2
3
4
5
6
7
8
9
180
130
100
70
55
40
35
25
B
20
40
60
100
200
20
40
60
200
tRK1-protein
complexes
Free
tRK1
Control
E. coli proteins
Recombinant
Eno2p

**Figure 4.**

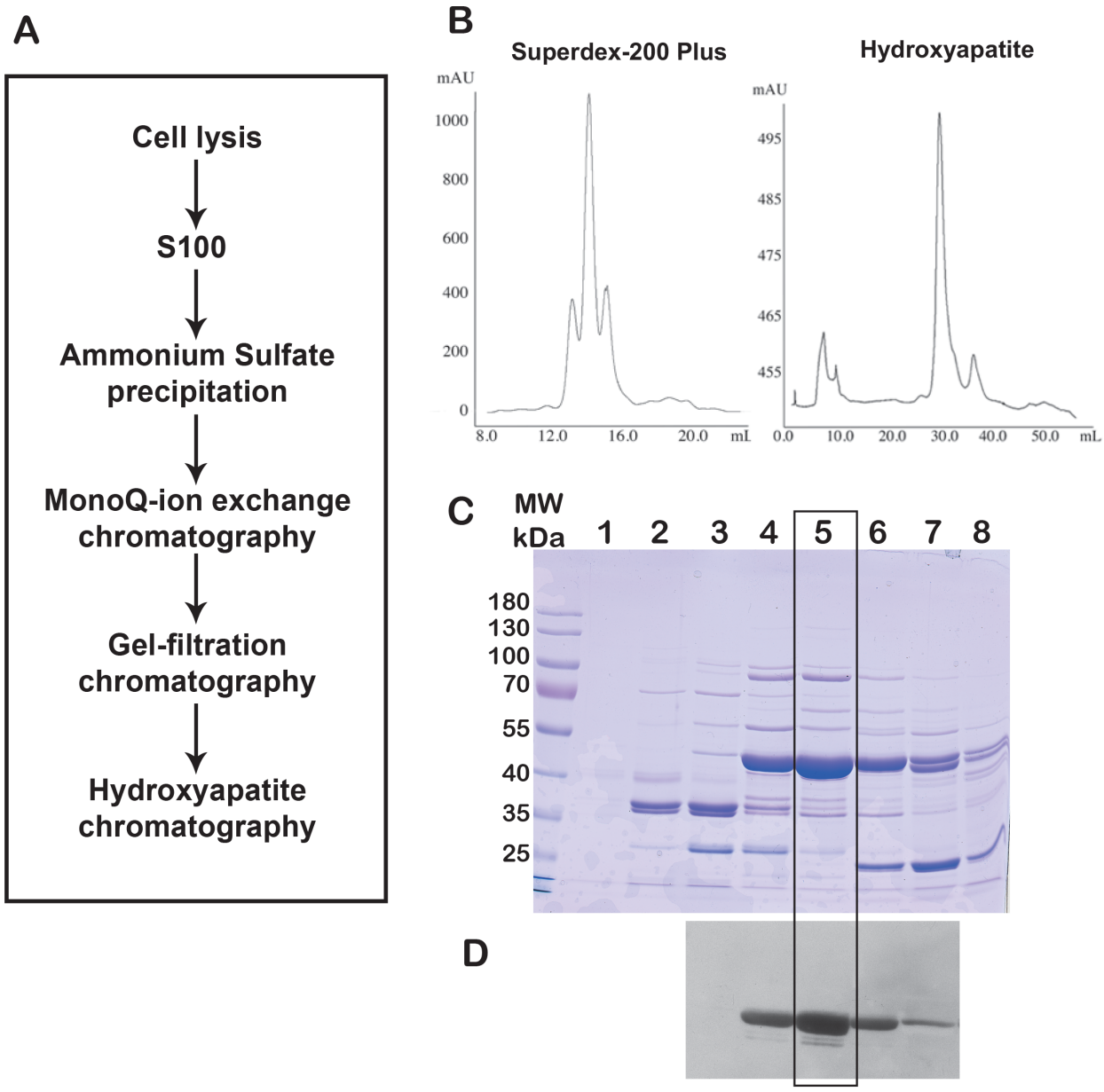
A
Cell lysis
S100
Ammonium Sulfate precipitation
MonoQ-ion exchange chromatography
Gel-filtration chromatography
Hydroxyapatite chromatography
B
Superdex-200 Plus
Hydroxyapatite
mAU
mL
C
MW kDa
1 2 3 4 5 6 7 8
180
130
100
70
55
40
35
25
D

**Figure 5.**

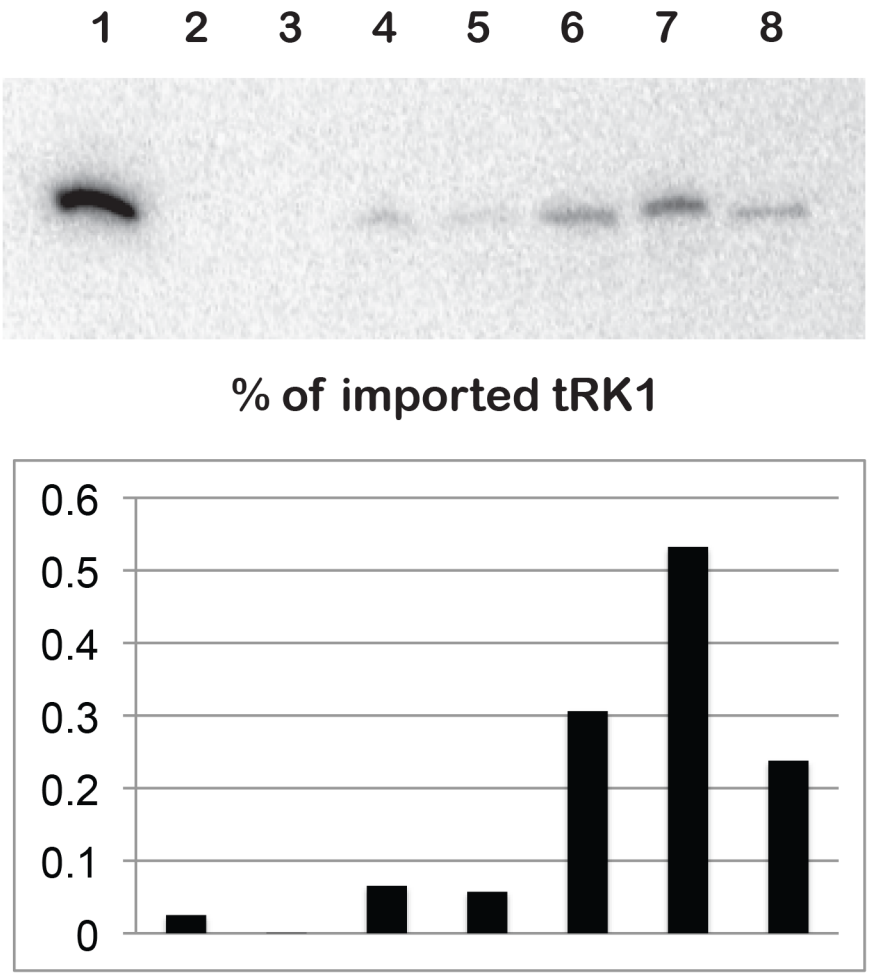

**Figure 6.**

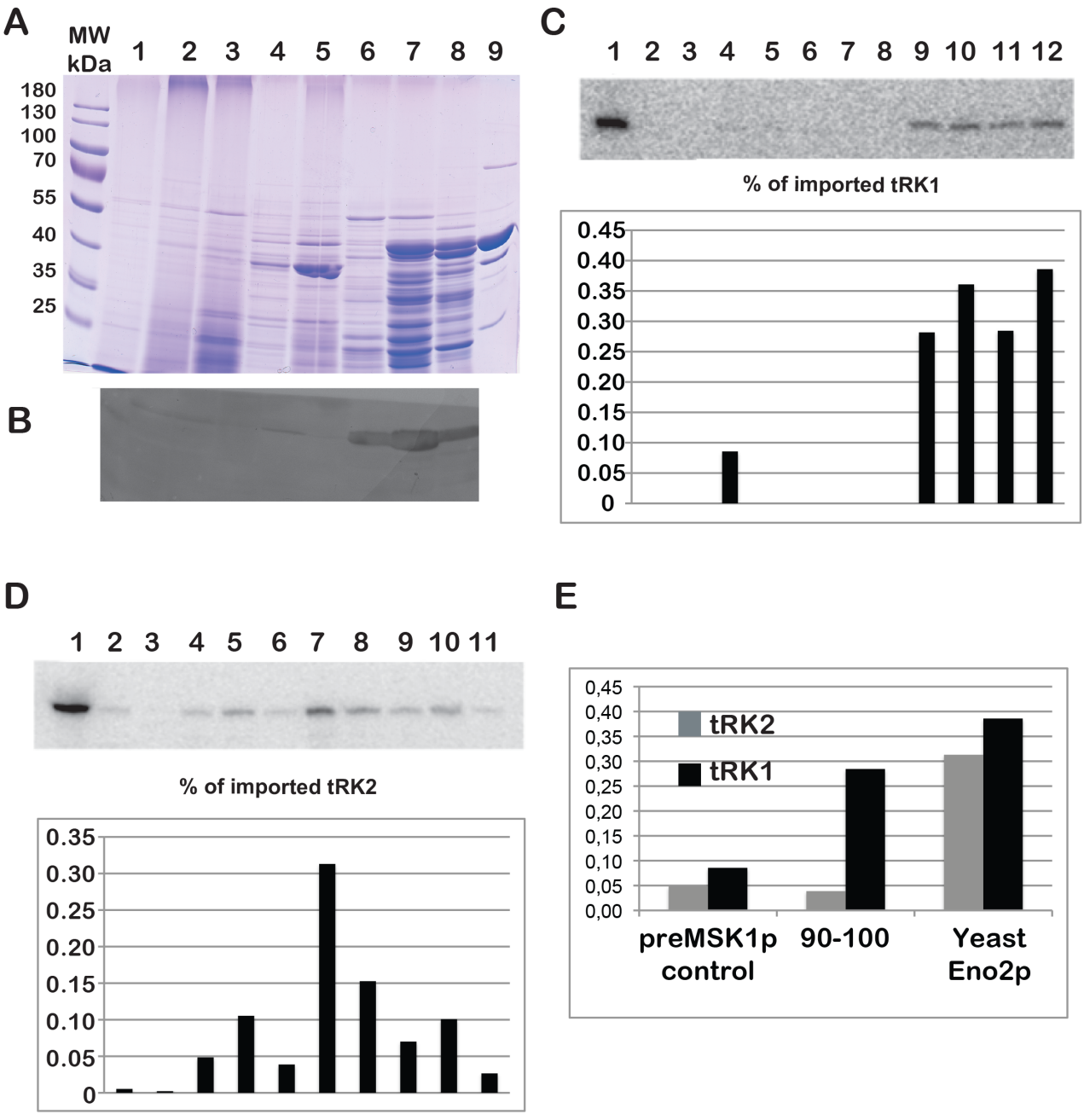
A
MW kDa
1 2 3 4 5 6 7 8 9
180
130
100
70
55
40
35
25
B
C
1 2 3 4 5 6 7 8 9 10 11 12
% of imported tRK1
0.45
0.40
0.35
0.30
0.25
0.20
0.15
0.10
0.05
0
D
1 2 3 4 5 6 7 8 9 10 11
% of imported tRK2
0.35
0.30
0.25
0.20
0.15
0.10
0.05
0
E
0,45
0,40
0,35
0,30
0,25
0,20
0,15
0,10
0,05
0,00
tRK2
tRK1
preMSK1p control
90-100
Yeast Eno2p

**Figure 7.**

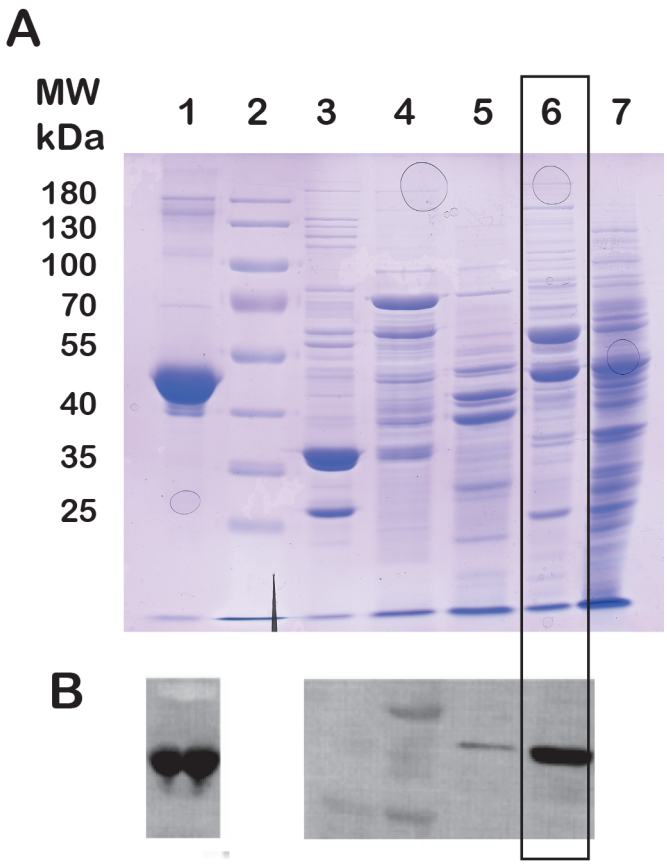

**Figure 8**

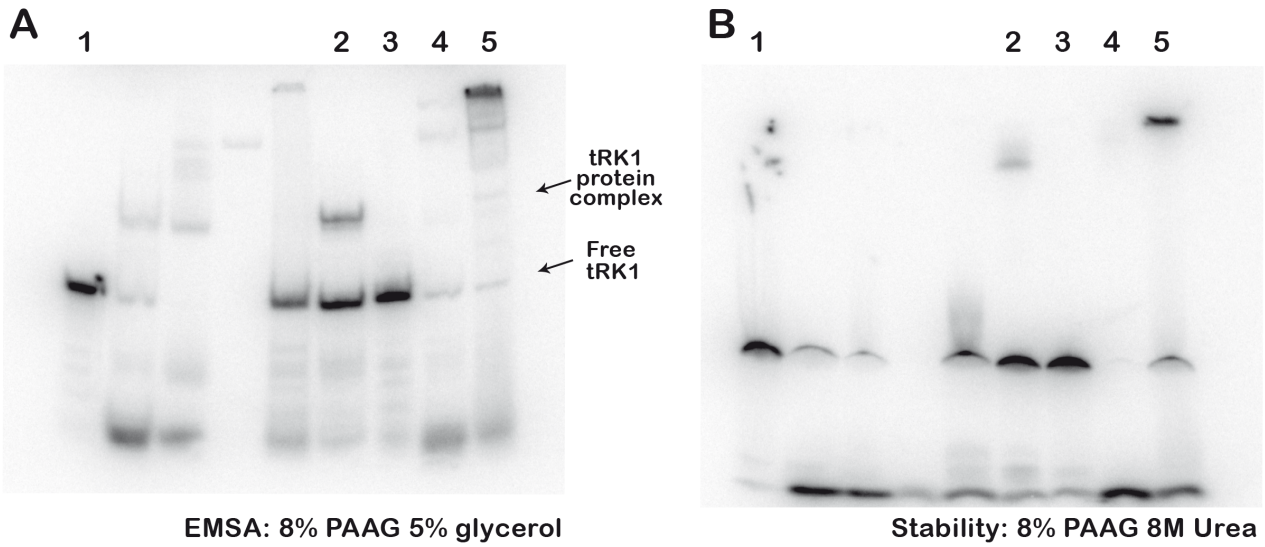
A
1
2
3
4
5
tRK1
protein
complex
Free
tRK1
EMSA: 8% PAAG 5% glycerol
B
1
2
3
4
5
Stability: 8% PAAG 8M Urea

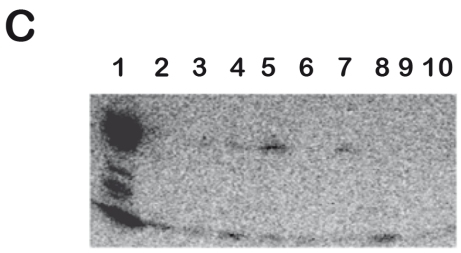
C
1 2 3 4 5 6 7 8 9 10

## The analysis of protein content of Eno2p-containing samples

The protein content of Eno2p-enriched fractions (obtained by ammonium sulfate precipitation at 50-60%, 70-80% and 90-100% saturation as well as endogenous yeast Eno2p-enriched sample obtained by gel-filtration) was analysed by mass-spectrometry. Proteins presented in Table 1 were found in all fractions.

| | Description | kDa | pI | Native yeast Eno2p | | | | Rec. Eno2p F80 |
|---|---|---|---|---|---|---|---|---|
| | | | | 50-60 | 70-80 | 90-100 | 67-100 followed by chromato graphy | |
| | | | | #Spectra | #Spectra | #Spectra | #Spectra | #Spectra |
| APE2 | Aminopeptidase 2, mitochondrial | 107,7 | 8,8 | 9 | 78 | 34 | 29 | |
| MET6 | 5-methyltetrahydropteroyltriglutamate--homocysteine methyltransferase | 85,8 | 6 | 90 | 405 | 102 | 287 | |
| TKL1 | Transketolase 1 | 73,8 | 6,5 | 283 | 439 | 24 | 6 | |
| PGI1 | Glucose-6-phosphate isomerase | 61,3 | 6 | 281 | 761 | 60 | 96 | |
| THR4 | Threonine synthase | 57,4 | 5,3 | 2 | 33 | 27 | 10 | |
| HXK2 | Hexokinase-2 | 53,9 | 5 | 12 | 84 | 6 | 10 | |
| ENO2 | Enolase 2 | 46,9 | 5,6 | 127 | 1269 | 1568 | 3722 | |
| ENO1 | Enolase 1 | 46,8 | 6,2 | 138 | 1220 | 1277 | 1930 | |
| OYE2 | NADPH dehydrogenase 2 | 45 | 6,1 | 403 | 927 | 34 | 121 | |
| PGK1 | Phosphoglycerate kinase | 44,7 | 7,8 | 188 | 822 | 2176 | 6 | |
| ETR1 | Enoyl-[acyl-carrier protein] reductase [NADPH, B-specific], mitochondrial | 42 | 9,5 | 1 | 29 | 5 | 5 | |
| ERG2 | Farnesyl pyrophosphate synthase | 40,5 | 5,2 | 6 | 19 | 1 | 2 | |
| HOM2 | Aspartate-semialdehyde dehydrogenase | 39,5 | 6,3 | 85 | 417 | 52 | 5 | |
| GRE3 | NADPH-dependent aldose reductase | 37,1 | 6,7 | 3 | 25 | 8 | 6 | |
| TDH3 | Glyceraldehyde-3-phosphate dehydrogenase 3 | 35,7 | 6,5 | 2 | 13 | 58 | 32 | |

| | | | | | | | | |
|---|---|---|---|---|---|---|---|---|
| MDH1 | Malate dehydrogenase, mitochondrial | 35,6 | 9,2 | 24 | 50 | 1 | 9 | |
| IPP1 | Inorganic pyrophosphatase | 32,3 | 5,3 | 109 | 288 | 7 | 55 | |
| GPM1 | Phosphoglycerate mutase 1 | 27,6 | 9,3 | 172 | 400 | 29 | 97 | |
| TPI1 | Triosephosphate isomerase | 26,8 | 5,7 | 22 | 132 | 360 | 3 | 6 |
| SOD2 | Superoxide dismutase [Mn], mitochondrial | 25,8 | 9,1 | 5 | 37 | 5 | 14 | |

**Table 1. The results of mass-spectrometry analysis of protein content of Eno2p-enriched fractions**

The sample of recombinant Eno2p eluted by 80 mM imidazole in the buffer (Rec. Eno2p F80) was also subjected to mass-spectrometry analysis. In addition to its ability to bind tRK1, Rec. Eno2p F80 directed import of tRK1 into isolated yeast mitochondria in the presence of recombinant preMSK1p. That fact indicated that it should contain proteins required for the import. The analysis of Rec. Eno2p F80 revealed the same protein - triosephosphate isomerase (yeast TPI 1 and *E. coli* TpiA) – presented in Rec. Eno2p F80 sample as well as in Eno2p-containing fractions extracted from yeast. Triosephosphate isomerase is a glycolitic enzyme also involved in the gluconeogenesis. It was reported that quinolinate synthase (NadA), a $Fe_4S_4$ clustercontaining dehydrating enzyme involved in the synthesis of quinolinic acid, exibited TPI activity (Reichmann et al, 2015). Nevertheless, not much known about tRNA binding activity of this protein. The analysis of RNA-binding proteins of HeLa cells based on "interactome capture" proposed triosephosphate isomerase as a cadidate of mRNA-binding protein (Castello et al, 2012).

RNA-binding protein YbiB was found in the sample of recombinant Eno2p . YbiB is a member of the uncharacterized TrpD2 protein family. It was reported that YbiB binds with high affinity ($K_d$ = 10–100 nM) to nucleic acids without detectable sequence specificity in a cooperative manner (Schneider et al, 2015). It is possible that YbiB co-purified with recombinant Eno2p and provided tRK1 retardation in EMSA.

## Analysis of Eno2p structure by SAXS and X-ray crystallography

In parallel with previous experiments, we attempted to solve the structure of the complex forming between recombinant Eno2p and tRK1 transcript. We planned to do this by

two methods - by small-angle X-ray scattering (SAXS) and by X-ray crystallography. While X-ray crystallography supplies the atomic resolution structures, SAXS offers information about the shape, folding and assembly state of macromolecules in solution. Together these techniques allow creating complete and accurate models for studied macromolecules or macromolecular complexes.

We used SAXS coupled with high-performance liquid chromatography (HPLC) to study shapes of Eno2p and tRK1 transcript as well as their complex in solution under native conditions (Figure 17). tRK1 transcript was refolded by heating at 95°C during 1 min followed by mixing with recombinant Eno2p (eluted at 80 mM imidazole) in the buffer routinely used for EMSA. The complex was formed at room temperature for 15-30 min and was applied onto the column. The individual components were analyzed under the same conditions.

The scattering pattern from Eno2p as well as for tRK1 and the complex are presented in Figure 17B. The volume of the scattering solutes is 83247 $Å^3$ corresponding to a molecular mass of ~ 48,9 kDa (46,9 kDa from uniprot database), which was consistent with monomeric state of Eno2p in solution. The experimental radius of gyration *Rg* and the maximum size $D_{max}$ of Eno2p were 23 and 75 Å. The fit between the Guinier curve derived from the available crystal structures of Eno1p and the experimental SAXS curve for Eno2p was better in the case of the monomeric form ($\chi^2$ = 5,97) than in the case of dimeric ($\chi^2$ > 10). Nevertheless, the conformation of Eno2p monomer should significantly differ from the conformation of the crystallographic Eno1p monomer (Figure 17C, E).

Under the experimental conditions defined above, tRK1 adopted the classical L shape ($\chi^2$ = 2.1) (Figure 17D) with *Rg* 24.2 and $D_{max}$ 85 Å. Molecular shapes calculated *ab initio* from the SAXS data obtained from samples containing both Eno2p and tRK1 revealed an elongated rod-like complex with *Rg* 37.2 and $D_{max}$ 130 Å. The model presented two lobes that could accommodate the conformational rearrangement protein and RNA parts folded as an F-form.

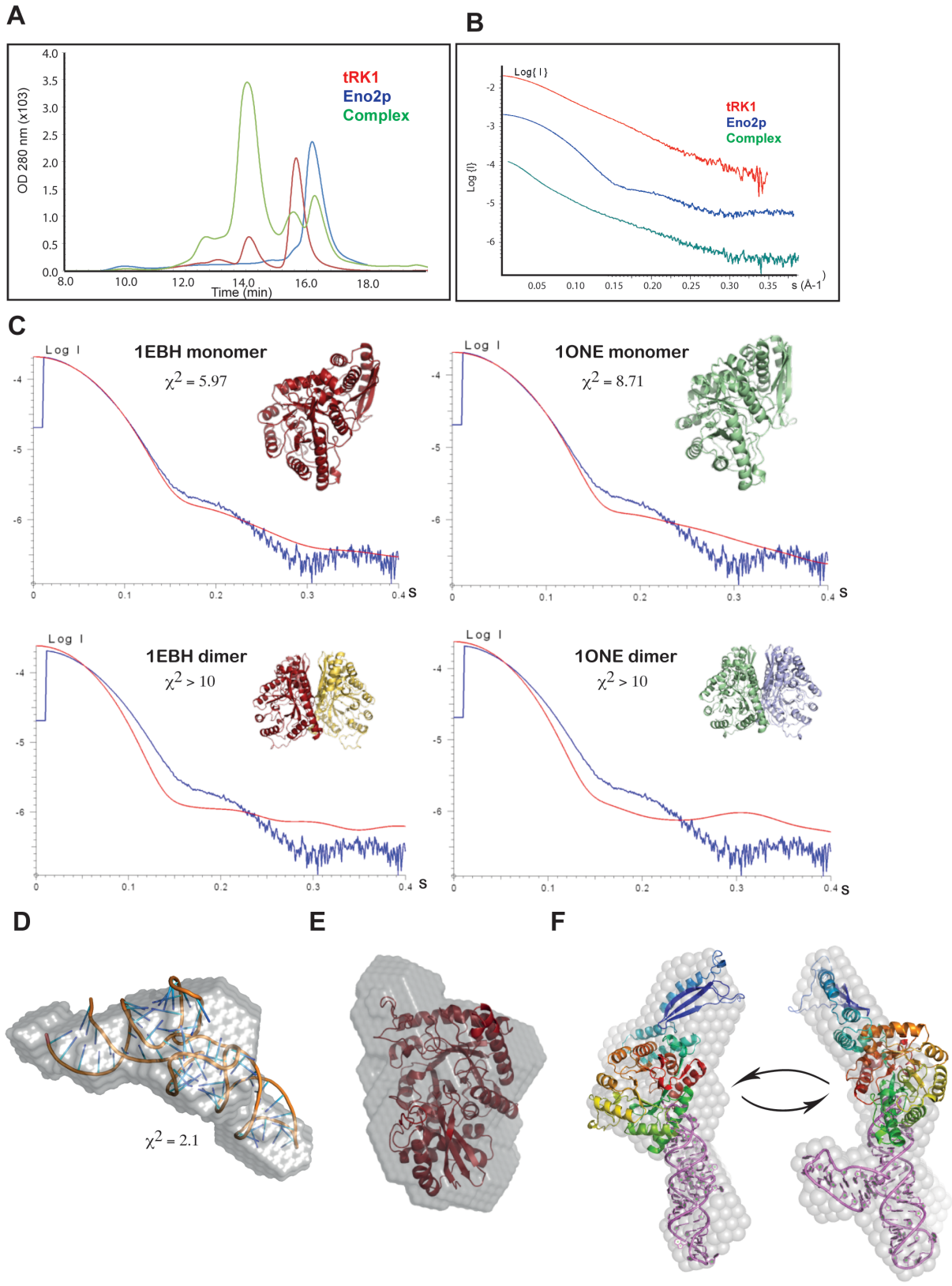
A
B
tRK1
Eno2p
Complex
OD 280 nm (x103)
Time (min)
Log{I}
Log {I}
s (Å-1)
C
1EBH monomer
χ2 = 5.97
1ONE monomer
χ2 = 8.71
1EBH dimer
χ2 > 10
1ONE dimer
χ2 > 10
Log I
s
D
E
F
χ2 = 2.1

**Figure 17.** (A) An elution profile of gel filtration of Eno2p, tRK1 and complex. (B) Logarithmic plot of the scattering intensity $I(s)$ (in arbitrary units) *vs.* $s$ ($Å^{-1}$). The logarithms of the scattering intensity were a function of the momentum transfer $s= 4\pi\sin\theta/\lambda$, where $2\theta$ is the scattering angle and $\lambda$ is the X-ray wavelength. (C) The comparison analysis of crystallography data and SAXS data for enolase. (D) A shape of tRK1 transcript in solution. (E) A shape of Eno2p in solution. (F) A shape of complex formed between the Eno2p recombinant sample and tRK1 transcript.

The crystal strycture of Eno2p represented organization similar to Eno1p structure. The Eno2p is a dimer. The Eno2p monomer (Figure 18) is built of two domains – N-terminal having the α+β structure and C-terminal 8-folded α+β barrel.

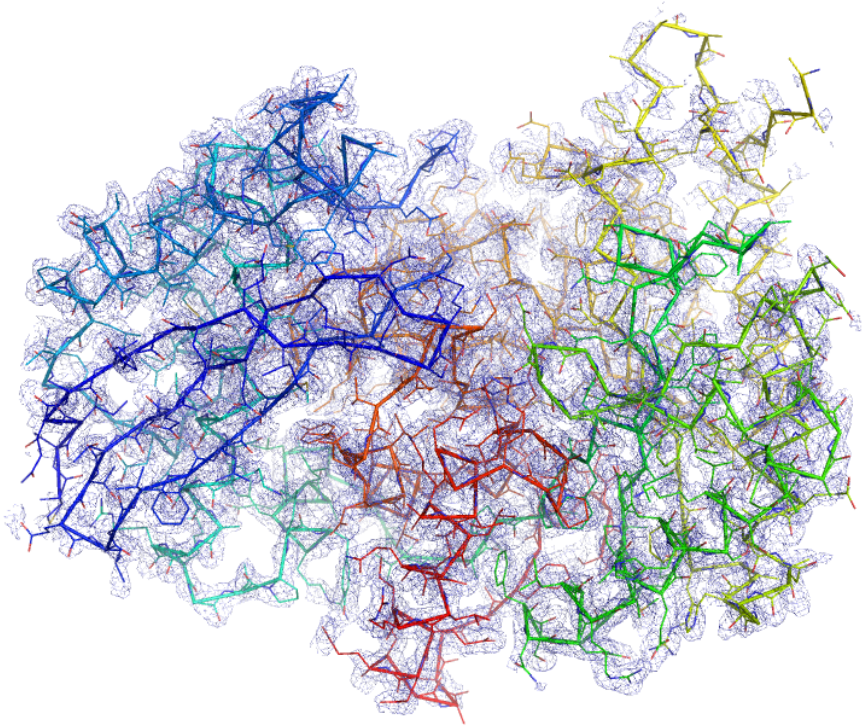

**Figure 18. The preliminary structure of Eno2p (monomer).** R-work = 0.3164 R-free = 0.3624

## Analysis of tRK1-protein complexes purified from yeast

To search for factors that might interact with tRK1 in yeast, we used an affinity chromatography approach based on the ARiBo1 tag (Figure 19) (Di Tomasso et al, 2010). This tag was initially developed for large-scale purification of T7 RNA transcripts. We adapted this tag to search for potential tRK1 interactors in yeast.

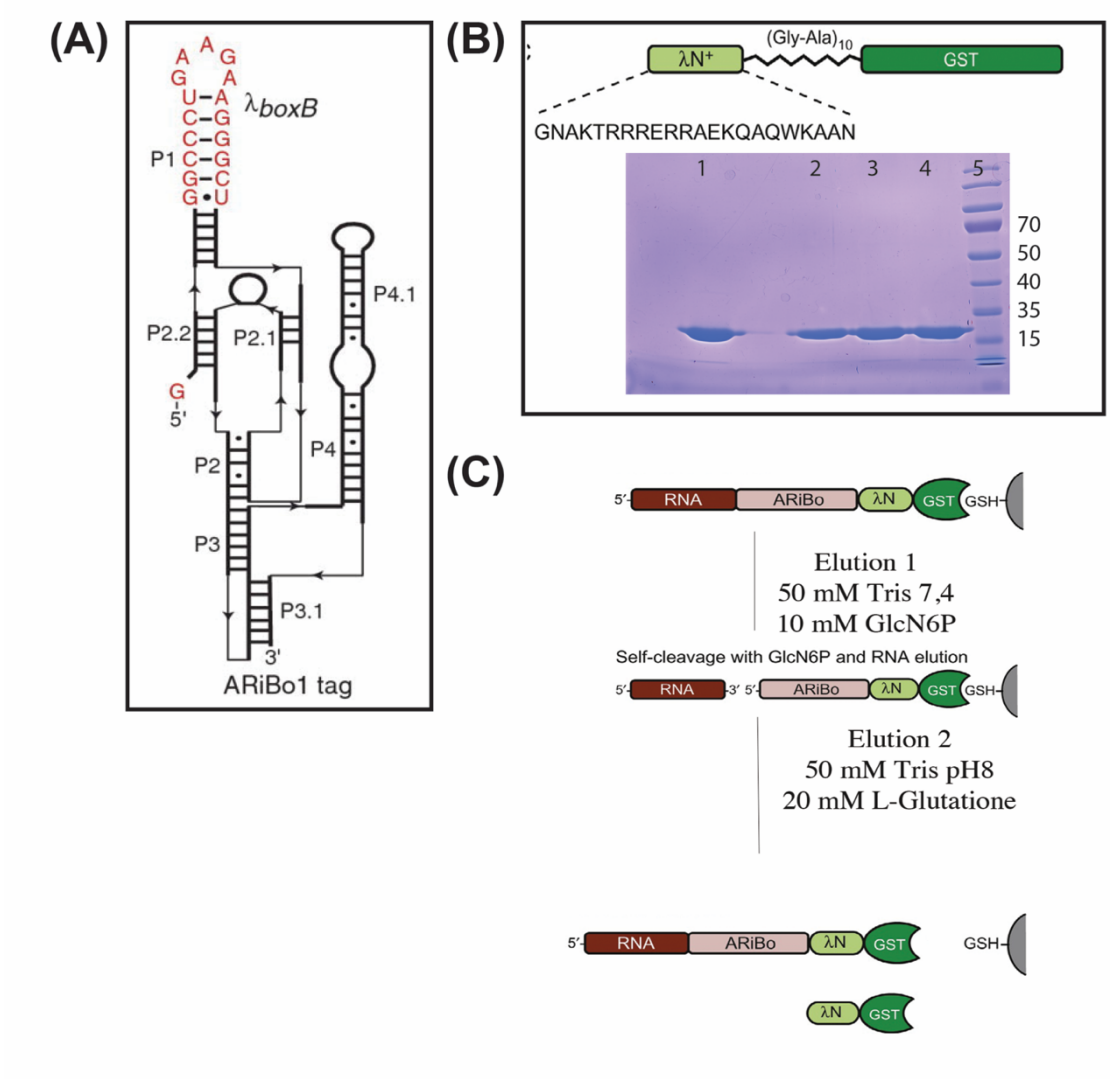


**Figure 19. ARiBo1-based affinity chromatography.** A) Structure of ARiBo1 tag. The ARiBo1 tag contains the λ*BoxB* RNA incorporated in the P1 stem-loop of the *glmS* ribozyme (red). In the ARiBo1 fused RNAs, the CCA at the 3'-end of tRNA connects to the G at the 5'-end of ARiBo1 tag (green). B) Schematic diagram of GST/λN⁺ fusion protein derived by G1N2K4 triple mutation (red) of the λN peptide and Coomassie stained 10% SDS-PAGE of GST/λN⁺ fusion protein (≈ 30 kDa) purification. Lanes 1-4 – different GST/λN⁺ fusion protein containing samples, lane 5 - PageRuler Prestained Protein Ladder. C) General strategy for affinity chromatography based on λ*BoxB*/λN⁺ peptide interaction. After incubation of RNA fused to ARiBo1 tag with yeast lysates, RNA-associated complexes were captured on GSH-Sepharose beads via binding to a GST protein fused to a λN⁺ peptide. The first elution of RNA-associated complexes was triggered by glucosamine-6-phosphate (GlcN6P) followed by the second elution by 20 mM reduced L-Glutathione.

The ARiBo1 tag (Activatable Ribozyme with the λ*BoxB* RNA) is comprised of several functional domains. The *BoxB* RNA from bacteriophage λ is fused with *glmS* ribozyme that self-cleaves upon activation by glucosamine-6-phosphate (GlcN6P). The RNA was immobilized on Glutathione-Sepharose (GSH-Sepharose) resin via a Glutathione-S-Transferase (GST) fusion with λN⁺ peptide. The general strategy is outlined in Figure 19C. The

tRK1 was first transcribed with an AriBo1 tag at its 3′-end and bound with the GST/λN$^+$-fusion protein. After incubation with yeast lysates, the tRK1-associated complexes were captured on GSH-Sepharose resin. After washing to remove impurities, the possible complexes were eluted by self-cleavage of the *glmS* ribozyme upon activation by GlcN6P. Following the same protocol, we analyzed proteins of yeast lysate possessed affinity to GSH-Sepharose matrix or ARiBo1 tag not fused with tRK1. We used tRK40 fused with ARiBo1 tag to define proteins associated with non-imported tRNA and to figure out candidates enriched in tRK1 sample. A transcript of tRK40 exhibited less than 5% of import efficiency (compared to tRK1) in previous experiments due to mutations in tRK1 at positions 67-69 (CAG→UGA) (Entelis et al, 1998).

Loading, wash and elution fractions were collected and analyzed by various methods. Proteins were analyzed by silver-stained 10% SDS-PAGE (Figure 20A). The RNAs were analyzed on 8% denature PAGE (Figure 20B) and subsequently analyzed by Northern blot hybridization (Figure 20C). The same experiments were performed for the fraction of yeast proteins without heparin-binding capacity (HP-0), which was active in both EMSA and mitochondrial *in vitro* import assays according to results of previous experiments.

Fractions eluted upon activation of *glmS* ribozyme were analyzed by mass-spectrometry (LC-MS/MS). All spectral counts were normalized to the total number of spectra observed in the sample. Selected candidate proteins showed a two-fold enrichement factor as compared to control experiments performed with tRK40 fused with ARiBo1 tag as well as ARiBo1 tag RNA or without RNA.

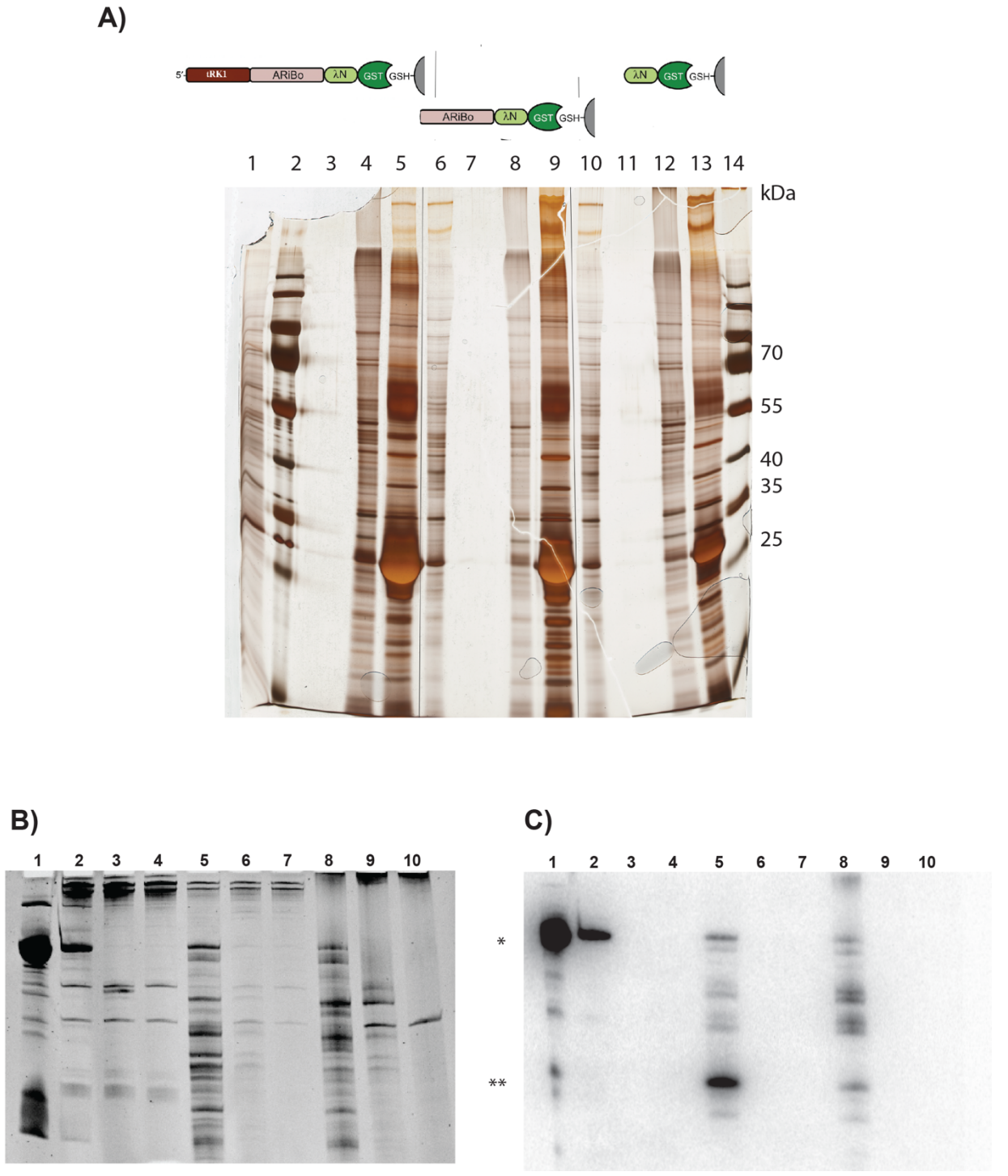


**Figure 20. ARiBo1 tag based affinity chromatography.** A) Silver stained 10% SDS-PAGE of fractions: last washing (3, 7, and 11), first elution (4, 8, and 12), second elutions (5, 9, and 13) and initial lysates (1, 6, and 10). Lanes 2 and 14 correspond to PageRuler Prestained Protein Ladder. B) Ethidium bromide stained 8% denature PAGE and (C) Northern blot analysis with anti-tRK1 probe of fractions. Lanes 1 - T7 tRK1-ARiBo1. Initial lysates: 2 – with T7 tRK1-ARiBo1, 3 – with T7 AriBo1, 4 – without tRK1 or ARiBo1; first elution: 5– with T7 tRK1-ARiBo1, 6 – with T7 AriBo1, 7 – without tRK1 or ARiBo1; second elution: 8– with T7 tRK1-ARiBo1, 9 – with T7 AriBo1, 10 – without tRK1 or ARiBo1. The level of tRK1-ARiBo1 is indicated by *, tRK1 - **

Proteins enriched in several experiments presented in Table 2.

| | Name | kDa | pI | Function |
|---|---|---|---|---|
| NPL3 | Nucleolar protein 3 | 45,4 | 5,3 | Npl3p mediates the export of mature mRNA from the nucleus as well as a cytoplasmic transport of mRNA. Moreover, the mutation in Npl3p affect the mitochondrial protein import by increasing half-life of some polysome complexes. |
| IF2G | Eukaryotic translation initiation factor 2 subunit gamma | 57,8 | 6,4 | IF2G participates in the early stage of protein synthesis by formation a complex with GTP and initiator tRNA. It also required for the 80S initiation complex formathion. |
| TRM2 | tRNA (uracil(54)-C(5))-methyltransferase | 72,8 | 9,6 | forms T in the highly conserved TΨC loop of tRNAs |
| PUS4 | tRNA pseudouridine synthase 4 | 45,2 | 6,2 | catalyzes $\Psi_{55}$ formation in both cytoplasmic and mitochondrial tRNA |
| IMDH3 | Inosine-5'-monophosphate dehydrogenase 3 | 56,5 | 7,7 | Involved in the amino acid biosynthesis pathway |

**Table 2. The results of mass-spectrometry analysis of proteins associated with tRK1**

We could not observe the enrichment of neither Eno2p as we expected nor cytosolic lysyl-tRNA synthetase or triosephosphate isomerase (see above). Those proteins exhibited affinity to GSH-Sepharose matrix so minor specific enrichment could be lost. Essential import factor preMSK1p was not detected also. This can be explained that the detection of some low-abundance proteins can be masked by peptides from high-abundance proteins in rather complex sample. Nevertheless, this method required optimization to be applied for the searching of import factors.

# DISCUSSION

## Enolase is a factor of tRK1 mitochondrial import in yeast

Yeast cells possess the mechanism of tRNA mitochondrial targeting. This process is highly selective as only a small subpopulation of $tRNA^{Lys}_{CUU}$ (tRK1) is found within the mitochondria while another $tRNA^{Lys}$ with anticodon UUU shows an exclusive cytosolic localization (Tarassov and Entelis, 1992). The tRNA mitochondrial import in yeast relies on the cooperative work of several protein factors. Thus, the cytosolic lysyl-tRNA synthetase (KRS1p) amynoacylates tRK1 whereas the precursor of mitochondrial lysyl-tRNA synthetase (preMSK1p) is required for translocation of tRK1 through the mitochondrial membrane (Tarassov et al, 1995b). Eno2p has been also identified as a necessary factor for the initial step of tRK1 mitochondrial import in yeast. While, yeast have two isoforms of enolase, Eno1p shows low import directing capability as compared to Eno2p (Entelis et al, 2006). It was supposed that Eno2p specifically binds aminoacylated tRK1 in cytosol to make it escape from the cytosol and to deliver it towards mitochondria. On the mitochondrial surface, Eno2p passes tRK1 to another import factor, preMSK1p, which is synthesized mainly on mitochondria-attached polysomes (Entelis et al, 2006) and integrates into a mitochondrial multiprotein complex on the mitochondrial outer membrane (Brandina et al, 2006).

## Yeast Eno2p does not bind tRK1 *in vitro*

The suggestion that Eno2p is the RNA-binding protein, which delivers tRK1 to its carrier protein, was based mainly on the observation that recombinant Eno2p makes a stable complex with tRK1 in EMSA with apparent $K_d$ = 2.5±0.2 μM (Entelis et al, 1996). It was also supported *in vivo* by the results of three-hybrid approach (Entelis et al, 2006). We found that additional purification steps significantly decrease the interaction between tRK1 and Eno2p in EMSA. This observation was confirmed by thermodynamic studies performed by isothermal titration microcalorimetry. It is suggested that Eno2p is implicated in the mitochondrial import as RNA-binding protein. However, classical RNA binding proteins present large positively charged electrostatic surfaces and isoelectric point (pI) usually

beyond 8.0. Eno2p is rather acidic protein with pI ≈ 5.88, certainly not favorable for interacting with negatively charged nucleic acids. It was reported about the capability of Eno1p to bind either DNA or RNA molecules under specific conditions of pH <5.5 and low ionic strength (Al-Giery and Brewer, 1992). Nevertheless, such interaction is conditional and seems to be rather unlikely in cell at physiological pH as the normal tissue has a pH ≈ 6.9-7.4.

There is not a lot of evidence supporting enolase RNA-binding capabilities *in vivo*. The product of the alternative translation of the human α-enolase lacking the N-terminus 96 aminoacids, was found as a repressor of the c-myc promoter transcriptional activity (Feo et al, 2000). This protein product presents affinity to *c-myc* P2-promoter in EMSA and can down-regulate its activity. The full-lenght α-enolase was also proposed to be a DNA-binding protein due to its presence in a complex with affinity for a specific double-stranded oligonucleotide (Wang, 2005). But in this situation enolase might be a structural component and not DNA-binding like *E. coli* enolase in the RNA degradosome (Nurmohamed et al, 2010). Enolase interacts mainly with C-terminus of RNase E and might play an important functional role in degradosome assembly serving as a link between cell metabolism and regulation at the post-transcriptional level.

Lack of interaction between Eno2p and tRK1 *in vitro* could be attributed to the absence of chemical modifications of tRK1 T7 transcripts or post-translational modifications of Eno2p. Nevertheless, it was observed in previous study (Entelis et al, 1996) and confirmed by recent data that transcripts can be successfully imported into mitochondria. Furthermore, samples of recombinant Eno2p do not present eukaryotic-specific modifications while they can direct the mitochondrial import of tRK1 *in vitro*. Thus, we conclude that while enolase is necessary to promote tRK1 mitochondrial import its role in this process needs to be defined more accurately.

We supposed that Eno2p requires help from additional factor(s) to interact with tRK1 transcripts. Our study indicates that fractions enriched either with recombinant Eno2p over-expressed in *E. coli* or Eno2p directly purified from yeast are able to direct mitochondrial import, in agreement with previously published results. It suggests that contaminants contained in Eno2p-enriched samples favor the mitochondrial import, whether they originate

from *E. coli* or yeast proteins. Enolases from these organisms share 46% of identity (Pancholi, 2001), which may partially rationalize why *E. coli* factor(s) might affect the import capabilities of recombinant Eno2p as would do those in Eno2p-enriched fractions directly obtained from yeast.

The existence of a limiting protein co-factor for the regulation of this process is indeed very likely. Eno2p is an abundant cytosolic protein while no more than 5% of the tRK1 pool follows the mitochondrial import pathway *in vivo* (Entelis et al, 2006; Tarassov and Entelis, 1992). We assume that a limiting protein co-factor might have an important role in maintaining the escape rate in the 5% range to keep up the level of cytosolic translation. The ubiquitin/26S proteasome system (UPS) demonstrated the capability to regulate the efficiency of import possibly by degradation of certain factors involved in either translation or mitochondrial import (Brandina et al, 2007). The regulation of abundant proteins would have minor effects as compared to rather rare proteins. Also enolase activity is coupled to many mechanisms (degradosome, glycolysis, import). Hence it is difficult to study one process without affecting the others. The data are necessarily very complex to interpret since they reflect the potential perturbations introduced by our experimental set-ups.

## Overexpression or down-regulation of human enolases does not change the efficiency of tRK1 import into mitochondria of human cells

This hypothesis may explain the experimental results of over-expression and down-regulation of human enolases. We suggested that cryptic mechanisms of tRK1 targeting in human cells are similar to that mechanism in yeast cells. Thus, this process in human cells involves the precursor of mitochondrial lysyl-tRNA synthetase (preKARS2p) (Gowher et al, 2013), the homologue of yeast preMSK1p. Nevertheless, *in vitro* import into isolated human mitochondria cannot be induced without yeast enolase or rabbit muscle enolase even in presence of preKARS2p (Gowher et al, 2013). It is thus reasonable to expect that human enolase is involved in mitochondrial import mechanism. There are three isoforms of this protein in human cells including α-enolase as the main form and two tissue-specific forms (β and γ-enolase). Sequence comparisons show that human enolases present from 62% to 83% identity with yeast Eno2p.

The results of *in vitro* RNA mitochondrial import experiments demonstrated that all human enolases direct tRK1 mitochondrial import in presence of preKARS2p. Similar to yeast Eno2p, human enolases facilitate the formation of tRK1-preKARS2p complex by decreasing ~10 fold the apparent $K_d$ from 300 nM to 10-20 nM, hence contributing to the import process. This suggestion was based on EMSA data. However, the down-regulation of enolase in human cells demonstrated slight decrease of 30% in amount of tRK1 recovered in mitochondria, while the overexpression of two isoforms of human enolase had no effect on the amounts of tRK1 associated with mitochondria. If we assume the implication of an additional limited factor in the mitochondrial import process, these results are not surprising. The amount of protein remaining in down-regulating cells might be enough to cooperate with minor factors and to fulfill import. In the case of enolase overexpression, an additional factor could still be limiting, implying unchanged import efficiency.

The work with the samples of recombinant protein brings numerous pitfalls. Certain modifications could change the protein properties and switch between moonlighting functions (Jeffery, 2016). The similar capacities of recombinant Eno2p and Eno2p purified from yeast to direct tRK1 mitochondrial import present evidence against this case. *E. coli* contaminated proteins also might be responsible for the false positive results of EMSA. An example describes an interaction artifact between bacterial non-coding RNAs and Hfq, which was co-purified in Ni-NTA-protein samples certainly due to the presence of histidine residues (Milojevic et al, 2013). We found that Ni-NTA purified recombinant Eno2p presents a pattern of tRK1 retardation in EMSA similar to that from *E. coli* proteins obtained by applying the recombinant Eno2p purification protocol to BL21 cells, containing a plasmid without the ENO2 insert. This mean that EMSA with contaminated recombinant Eno2p sample can lead to a wrong picture concerning the interaction between Eno2p and tRK1. After mass-spectrometry analysis of the protein content of one of the samples containing the recombinant Eno2p, we found *E. coli* YbiB, which was not characterized by sequence specificity, but showed high affinity to nucleic acids (Schneider et al, 2015). Nevertheless, we cannot rule out the participation of *E. coli* enolase in tRK1 retardation. However, it must be noted that *E. coli* proteins presented affinity to tRK1 transcripts did not show significant ability to promote mitochondrial import *in vitro* in the presence of preMSK1p.

## The conformation of tRK1 ans tRK2 conformation in the solution

In yeast, tRK1 only is imported into mitochondria while the second isoacceptor tRK2 is retained in cytosol. The same is true for T7 transcripts of those tRNAs (Entelis et al, 1996). Moreovere, the aminoacylated tRNAs T7 transcripts appeared to be better substrate for mitochondrial import than modified tRNAs. The SELEX experiments and FRET analysis gave rise to the hypothesis about an alternative F-form tRNA which would determine mitochondrial import (Kolesnikova et al, 2010). In other words, only tRNA molecules able to form a stable F-stem follow the mitochondrial import pathway. But synthetic molecules, which were built only from F-stem were imported with low efficiency while a fusion between the D-arm and the F-stem increases its own import 5 fold greater that tRK1 import (Kolesnikova et al, 2010). The synthetic transcript of yeast mitochondrial $tRNA^{Lys}$ was imported into mitochondria two fold more efficiently than tRK1 although the presence of the F-stem could not be assessed by means of secondary structure prediction programs (Mfold RNA folding form ver. 2.3 energies). However, in human cells, several distinct pathways of mitochondrial import seem to exist. Thus, short molecules containing either D-arm or F-stem as import determinants exploit the import mechanism that differ from preKARS2-dependent used by longer RNAs containing both (D and F) determinants (Gowher et al, 2013). All this indicates that the mechanism of determination of substrate import is complex that raises a lot of questions. We tested the conformation of tRK1 and tRK2 transcripts in solution by RNases T1 and V1 and In-line probing. Both transcripts exist in various conformations, which are hard to decipher in probing assays. In general, tRK2 possessed more “open” regions than tRK1, but in both cases the contribution of two sets of conformations with free anticodon or with anticodon involved in stem structure is observed. The signatures of several likely conformations can be distinguished. Thus we detected a tRK1 rod-like conformation presenting an aminoacceptor stem similar to the conformation predicted for synthetic tRK3. It is possible to suggest that the ratio between different conformations *in vitro* as well as *in vivo* could serve as an additional factor that determines the efficiency of import.

## Eno2p structure

Enolase is responsible for the reversible conversion of 2-phosphoglycerate into phosphoenolpyruvate that is one of the common reactions of glycolysis and gluconeogenesis. Yeast possesses two isoforms of the glycolytic enzyme enolase – Eno1p and Eno2p. Both

proteins are strongly regulated by the availability of carbon source. While Eno1p is a constantly expressed protein the presence of Eno2p increases 20-fold on glucose as a carbon source (Mcalister and Holland, 1982).

There is a suggestion that enolase may not only link glycolysis and gluconeogenesis but may separate them through specialization of functions of isozymes. While Eno1p is inhibited by the glycolytic substrate 2-phosphoglycerate, phosphoenolpyruvate appears to inhibit Eno2p, even though the differences of their kinetic properties are rather small and cannot fully explain the reason for the isoenzyme carbon source-dependent regulation (Entian et al, 1987).

The Eno1p crystal structure presents an α2 dimeric organization (Lebioda et al, 1989). This was confirmed by gel filtration (Folta-Stogniew and Williams, 1999). The structure of Eno2p has not been studied until now. Nevertheless, Eno2p was suggested to exist as a dimer in solution as Eno1p.

We studied the structure of Eno2p by SAXS and X-ray crystallography. The crystal structure of Eno2p is similar to the ones obtained for Eno1p. Although both proteins form dimers in the crystal, unexpected results were obtained by SAXS. The comparison of crystal structure of Eno1p monomer and SAXS shapes calculated for Eno2p showed that Eno2p is actually monomeric in solution. Moreover, a relatively poor fit ($\chi^2 > 5$) between the SAXS shapes calcultate for the Eno2p structure model and the shapes derived from the crystallographic monomer of Eno1p indicated that these proteins present significantly different conformations. Nevertheless, such data are not unusual; since the crystal structure represents an energetically optimal packing, which may favour dimerization (Krissinel, 2010). SAXS allows studying molecules in unbiased environment and possibly better reflects the biological macromolecule interactions.

Eno1p and Eno2p are closely related proteins differing in only 20 out of 437 aminoacids that presents 95% identity (Baleva et al, 2015). The enzymatic properties of both enzymes are similar while their additional functions differ. For instance, Eno2p is more efficient in directing mitochondrial import of tRK1 with respect to Eno1p (Entelis et al, 2006). Hence, the two isoforms of yeast enolase seem to have different oligomeric states; it is tempting to

speculate that oligomerization may influence the functions of enolases. The enzymatic function of Eno1p does not depend on enolase dimerization since Eno1p can be dissociated into active monomers (Holleman, 1973; Keresztes-Nagy and Orman, 1971). However, Eno2p is more sensitive to oxidation (Reverter-Branchat et al, 2004) glycosylation modifications (Gomes et al, 2008) that is consistent with its structure. Thus, Eno2p dimer dissociation results in increasing the part of its surface accessible to the cellular environement, and consequently which could be involved in intermolecular contacts. This surface may serve as a regulation platform by modification. Hence, this suggests that the conformational difference between Eno1p and Eno2p could allow tRK1 import, a moonlighting function of Eno2p.

The results of potential tRK1-Eno2p complex obtained by SAXS should be critically revisited in the light of results of the present work indicating that *E. coli* contaminant proteins present significant affinity to tRK1. While we studied the shape of this complex, the components of this complex have not been precisely identified since the participation of other molecules is expected.

## RNA Affinity chromatography based on ARiBo1 tag

Affinity chromatography is a reliable tool both for protein and RNA purification and for identifying both simple biomolecular interactions and the members of large complexes. There are numerous strategies relying on different tags. We developed an affinity chromatography method to search for proteins binding tRK1 using an ARiBo1 tag. ARiBo1 tag is based on two functional modules and provides a certain advantage compared to the MS2 tag. The λ*boxB* RNA enables the attachment to GST-$\lambda N^+$ fusion protein captured on glutathione resin while the *glmS* ribozyme allows eluting the tRNA associated complexes by self-cleavage of *glmS* ribozyme upon activation by GlcN6P. The absence of the tag in eluted samples potentially improves successful identification of peptides by mass-spectrometry and further facilitates handling of samples enriched with complex of interest.

We fused tRK1 with ARiBo1 tag in order to search the cytosolic partners of tRK1. Since the method is novel, protocol optimization is required. Our data did not contain any factors of mitochondrial import identified previously such as KRS1p or preMSK1p. This can be attributed to poor detection of these low-abundance proteins. Enolase, instead, is an abundant

protein, although we detected only minor enrichment of enolase in tRK1 samples. In addition, it binds to GSH-Sepharose resin. Since we search a limiting factor, it might be lost as known import factors. All proteins enriched in tRK1 fractions were not identified in Eno2p-enriched fractions. While their relationship to the mitochondrial import process requires verification, they might reflect the involvement of tRK1 in other cellular processes.

# CONCLUSIONS AND PERSPECTIVES

The results obtained during this work permitted to draw the following conclusions:

- ✓ Confirmation that both recombinant and yeast purified Eno2p direct the import of tRK1 *in vitro* in presence of preMSK1p
- ✓ *E. coli* proteins co-purified with recombinant Eno2p possess affinity to yeast tRK1 transcript of in EMSA but do not capable to direct tRK1 *in vitro* import in the presence of preMSK1p.
- ✓ Additional factor(s) may contribute to the structure of tRK1-Eno2p complex as well as to the selectivity of tRK1 mitochondrial import in yeast.

Our work exposed the need to review the tRNA targeting process in yeast. An important direction of future studies would be identification of missing factor(s) that together with Eno2p interact(s) with tRK1 to direct it into the mitochondrial import pathway.

The experimental strategy developed in the present work yielded promising results but some improvements are required. In particular, the complexity of the pool of potential «prey» proteins needs to be decreased (e.g. by introduction of additional fractionation steps) to increase chances of detection of low-abundant import factors.

Once the missed targeting factors have been identified, a crystal structure of the tRK1-targeting complex may be obtained. This would help to better understand its organization and functioning and shed light on questions concerning the selectivity and regulation of the tRNA import process.

# MATERIAL AND METHODS

## 1. Strains

### 1.1. *E. coli* strains

XL-1 Blue: (*recA1 endA1 gyrA96 thi-1 hsdR17 supE44 relA1 lac [F' proAB lacIqZ.M15 Tn10 (Tet$^T$)]]) (Stratagene)*

BL21: F$^-$*ompT hsdS*$_B$($r_{B^-}$ $m_{B^-}$) *gal dcm* pRARE ($Cam^R$)

### 1.2. Yeast strains

W303: *MAT*a {*leu2-3; 112; trp1-1; can1-100; ura3-1; ade2-1; his3-11,15*}

Δ*ENO1*: was obtained from W303 by *KanMX4*-casette replacement of *ENO1* gene

YPH499*: MAT*a *ura3-52 lys2-801_amber ade2-101_ochre trp1-Δ63 his3-Δ200 leu2-Δ1*

### 1.3. Human cell lines

For overexpression and down-regulation experiments, human hepatocarcinoma (HepG2) and human embryonic kidney (HEK293T) cells were used.

Monolayer cultures were grown at 37°C in DMEM (Dulbecco's Modified Eagle's Medium) (Sigma) or on the MEM (Minimum Essential Medium Eagle) (Sigma) supplemented with 10% fetal calf serum, 100 μg/ml streptomycin and 100 μg/ml penicillin (Gibco). The cells were cultivated at 37 °C in a humidified atmosphere with 5% $CO_2$.

### 1.4. Media

LB (Biomedicats): 1% tryptone, 0.5% yeast extract, 1% NaCl

LB with agar (Difco): 1% tryptone, 0.5% yeast extract, 0.5% NaCl, 1.5% agar

YPD: 2% dextrose, 2% peptone, 1% yeast extract

YPCly: 2% peptone, 1% yeast extract, 2% glycerol

Solid YPD and YPGly media is supplied with 1,5% agar

### 1.5. Preparation of competent *E. coli* cells

All materials and solutions were pre-chilled, and all work was carried out in cold room. Temperature increase significantly affects the competence of cells.

A starter culture was prepared by inoculation of 3 ml of LB/Ampicilline (100 μg/ml) with a 50 μl aliquot of initial competent cells and incubated at 18°C for 6 hours.

250 ml of LB/Amp (100 μg/ml) was inoculated by 3 ml of the starter culture and incubated at 18°C until the $OD_{600}$ reached 0.55.

The bacterial cells were harvested by a 10 min centrifugation step at 2 500 *g* at 4°C. The supernatant was discarded carefully and cell pellet was gently re-suspended in 80 ml of TBjap buffer (10 mM PIPES, 15 mM $CaCl_2$, 250 mM KCl, 55 mM $MnCl_2$, pH 6.7) supplemented with DMSO up to 1.96% and incubated 10 min on ice.

The bacterial cells were harvested by a 10 min centrifugation step at 2 500 *g* at 4°C. The supernatant was discarded. Pellets of cells were resuspended in 18.6 ml of TBjap buffer. DMSO was slowly added up to 7%. The cells suspension was stored 10 min on ice. Competent cells were delicately aliquoted 200 μl per tube and immediately frozen in liquid nitrogen. Tubes were stored at -80°C

### 1.6. *E. coli transformation*

An 200 μl aliquot of competent XL1Blue cells was incubated with ligation mixture (10 μl) or DNA (usually 50 pg -1 ng) for 30 min on ice, for 35 s at 42 °C and for 5 min on ice. Then 1 ml liquid LB was added to cells further incubated for 30-60 min at 37 °C for cell recovery and for expression of antibiotic resistence. Finally, 300 μl bacteria suspention was seeded to LB-agar/antibiotic(s) plates for the selection.

### 1.7. *Glycerol stocks*

The glycerol stocks of the clones containing the desired sequences were prepared by mixing of 1 ml of overnight bacterial culture to 600 μl of sterilized 50% glycerol in 2 ml screw cap tubes. The tubes were stored at -80 °C.

## 2. Plasmids

The high-copy prokaryotic pUC19 plasmid was used for cloning of tRK1 or tRK2 genes flanked by HMH and HdV ribozyme genes:

**HMH-tRK1-HdV**

5'GACGGCCAGTGAATTCTAATACGACTCACTATAGGGCGCCACCAAGGCCTGACGAGTCTCTGA
GATGAGACGAAACTCTTCGCAAGAAGAGTCGCCTTGTTGGCGCAATCGGTAGCGCGTATGACTCTTA
ATCATAAGGTTAGGGGTTCGAGCCCCCTACAGGGCTCCAGGCGGCCATGGTCCCAGCCTCCTCGCTG
GCGGCCGCTGGGCAACATTCCGAGGGGACCGTCCCCTCGGTAATGGCGAATGGGACA
AGGTCGACTCTAGAGGATCC 3'

**HMH-tRK2-HdV**

5'GACGGCCAGTGAATTCTAATACGACTCACTATAGGGTGAGCATACCAAGGACTGACGAGTCTC
TGAGATGAGACGAAACTCTTCGCAAGAAGAGTCTCCTTGTTAGCTCAGTTGGTAGAGCGTTCGGCT
TTTAACCGAAATGTCAGGGGTTCGAGCCCCCTATGAGGAGCCAGGCGGCCATGGTCCCAGCCTCCTC
GCTGGCGGCCGCTGGGCAACATTCCGAGGGGACCGTCCCCTCGGTAATGGCGAATGGGACA
AGGTCGACTGCAGAGGATCC 3'

The plasmids containing tRK1 and tRK2 sequences were kindly provided by Kamenski Piotr (MSU, Moscow). For affinity chromatography with *in vitro* transcribed ARiBo1-tagged tRNAs, we used the pET42a-λN$^+$-L$^+$-GST and ARiBo1 based pTZ19R-derived pTR-4 vectors kindly provided by (Di Tomasso et al, 2010)

Recombinant human enolases, yeast enolase 2 and mutant Eno2p H373F were prepared from cDNAs cloned in pET3a expression plasmid. Plasmid pDEST17 expressing human mitochondrial lysyl-tRNA synthetase, KARS2, was kindly provided by A. Gowhar. Plasmids

pCMV6-XL5 containing human α-enolase and pCMV-AC containing human β and γ-enolase genes used for overexpression of certain enolases in human cells were purchased from Origen.

***Plasmid DNA preparation.*** Plasmid Miniprep (midi or maxiprep) kit (QIAgen) was used for plasmid DNA extraction according to the provider's protocol.

## 3. Primers

| | | Sequence (5'-3') |
|---|---|---|
| ***For PCR of tRK1 gene:*** | | |
| **1.** | HindIII_T7 | GGCCAGTAAGCTTTAATACGACTCACTATAGGG |
| 2. | ApaI_ARiBo | TCTTCAGGGCCCAGTTCGGCGCGGAAGCC |
| ***For PCR of tRK1 gene flancked by HMH and HdV:*** | | |
| **3.** | F-HMH-tRK1-PCR2 | GACGGCCAGTGAATTCTAATACGACTCACTATAGGGCGCCACCAAGGCC TGACGAGTCTCTGAGATGAGA |
| **4.** | F-HMH-tRK1-PCR1 | GAGTCTCTGAGATGAGACGAAACTCTTCGCAAGAAGAGTCGCCTTGTTG GCGCAA |
| **5.** | R-tRK1-HdV-PCR2 | GGATCCTCTAGAGTCGACCTTGTCCCATTCGCCATTACCGAGGGGACGG TCCCCTCGGAATGTT |
| **6.** | R-tRK1-HdV-PCR1 | GTCCCCTCGGAATGTTGCCCAGCGGCCGCCAGCGAGGAGGCTGGGACCA TGGCCGCCTGGAGCCCTGTAGGG |
| ***For PCR of tRK2(CUU) gene gene flancked by HMH and HdV:*** | | |
| **7.** | R-tRK2-HdV-PCR1 | GTCCCCTCGGAATGTTGCCCAGCGGCCGCCAGCGAGGAGGCTGGGACCA TGGCC |
| **8.** | F-HMH-tRK2-PCR1 | GAGTCTCTGAGATGAGACGAAACTCTTCGCAAGAAGAGTCTCCTTGTTA GCTCAG |
| **9.** | R-tRK2-HdV-PCR2 | GGATCCTCTGCAGTCGACCTTGTCCCATTCGCCATTACCGAGGGGACGG TCCCCTCGGAA |
| **10.** | F-HMH-tRK2-PCR2 | GACGGCCAGTGAATTCTAATACGACTCACTATAGGGTGAGCATACCAAG GACTG |
| ***For QuickQange for constraction of tRK2(UUU) gene*** | | |
| **11.** | QCtRK2-F | GCTCAGTTGGTAGAGCGTTCGGCTTTTAACCG |
| **12.** | QCtRK2-R | CGGTTAAAAGCCGAACGCTCTACCAACTGAGC |
| ***For QuickQange for construction of tRK40 gene (substitution of $C_{67}$, $A_{68}$, $G_{69}$ of tRK1 to $U_{67}$, $G_{68}$, $A_{69}$)*** | | |
| **13.** | QCtK40Fwd | GGGGTTCGAGCCCCCTATGAGGCTCCAGCGCCGAACTGG |

| | | |
|---|---|---|
| **14.** | QCtK40-Rev | CCAGTTCGGCGCTGGAGCCTCATAGGGGGCTCGAACCCC |
| ***For QuickQange for substitution of aminoacids K377 K378 →A377 A378 in Eno2p*** | | |
| **15.** | K377(378)Aeno2Fwd | GCTACCGCCATCGAAGCGGCGGCTGCTGACGC |
| **16.** | K377(378)Aeno2Rev | GCGTCAGCAGCCGCCGCTTCGATGGCGGTAGC |
| ***Oligonucleotides for Nothern blot*** | | |
| **17.** | anti-tRK1 probe (1-34) | GAGTCATACGCGCTACCGATTGCGCCAACAAGGC |
| **18.** | anti-mito $tRNA^{Val}$ | GTTGAAATCTCCTAAGTG |
| **19.** | anti-cyt 5.8S rRNA | GGCCGCAAGTGCGTTCGAAG |
| **20.** | anti-mito $tRNA^{Lys}$ | GGTTCTCTTAATCTTTAAC |

# 4. Preparation of T7 transcripts of tRNAs

## 4.1. Preparation of DNA templates for T7 transcription of tRK1 and tRK2

The forward primers were designed to contain an EcoRI restriction site, a T7 promoter, the sequence of the HMH ribozyme and the 5' sequence of tRNA. The reverse primers contained a Sal I restriction site, the sequence of the HdV ribozyme and the 3' sequence of tRNA.

50 μl of PCR1 reaction contained 50 pg of template plasmid DNA, per 1.2 μl of forward and reverse primers, 400 μM dNTP mixture, 10 μl 5x Phusion HF Buffer (New England Biolabs), 0.5 μl Phusion High-Fidelity DNA polymerase (2 000 U/μl) (New England Biolabs) in milliQ water.

Conditions of PCR: 95°C – 3 min

denaturation/ 95°C – 30 s
hybridization of primers/ 50°C – 60 s } 30 cycles
elongation/ 72°C – 60 s
4°C – 10 min.

The PCR1 product was purified by 1% agarose gel following extraction by QIAquick gel extraction kit (Qiagen).

PCR2 was performed under the same conditions as PCR1 using as a template 50 pg of PCR1 product. Purified PCR2 product was double diested by EcoRI and Sal I FastDigested

enzymes (Termo Fisher Scientific) according to the provider's protocol and inserted into pUC19 vector double digested by the same enzymes (a molar ratio of vector/insertion was 1/2). Ligation of digested PCR2 product with plasmid was carried out for 10 min at 22 °C in 1x FastDigest buffer supplied with 5 U T4 DNA ligase (Termo Scientific) and 0.5 mM ATP in. The reaction mixter was transformed into 200 µl aliquot of XL1Blue competent cells. For screening, cells were seeded on LB–ampicillin (100 µg/ml) agar plates and incubated overnight at 37 °C. The resulting colonies were used by isolation of plasmid DNA. The plasmids were sequenced.

### 4.2. Large scale *in vitro* transcription of tRNA

Plasmid DNA templates were typically obtained from XL-1 Blue cells using the QIAGEN Plasmid Maxi Kit. The plasmids were linearized by MvaI (BstNI) (Fermentas, ThermoFisher Scientific). A typical 300 µl reaction mixture contained 300 µg of plasmid DNA, 30 µl 10x FastDigest buffer, 30 µl (10 U/µl) FastDigest MvaI (BstNI) in milliQ water. The reaction was carried out at 37 °C for 2-3 h.

***Transcription reaction contained****:* 50 µg/ml of linearized plasmid DNA, 1x HMSDT buffer (200 mM HEPES pH 8.0, 125 mM $MgCl_2$, 5 mM spermidine; 250 mM DTT, 0.5% Triton 100-X), 5 mM ATP, 5 mM GTP, 5 mM CTP, 5 mM UTP, 1 U /ml of *E. coli* inorganic phosphatase, T7 RNA polymerase (according provider's recommendation or 10 µl/ml prepared in our laboratory).

The reaction was carried out at 37 °C for 4 h, then transcribed RNA was precipitated.

### 4.3. Purification of T7 tRNA*s:*

Transcribed RNA was precipitated with 3 volumes of 100% ethanol and collected by centrifugation for 30 min at 30 000 *g* 4°C. Supernatant was discarded. Pellet was re-suspended in appropriate volume of milliQ water and the same volume of urea blue loading buffer (8M urea, 0.025% bromophenol blue) was added.

Mixture was loaded on 8% denaturing PAGE (8% acrylamide/bis-acrylamide (19:1), 8M urea, 0.5x TBE). Gel size: 35 cm width/ 42 cm lenth/ 1 mm thickness. The gel was run at 50 W until the bromophenol blue reached the bottom of the gel.

The gel was placed on a silica plate. RNA band was cut out of the gel under UV shadowing. The RNA band was cut out of the gel and crushed through a syringe. RNA was passively eluted from the gel by milliQ water over-night at 4°C on a roller mixer.

Next day, the mixture was filtered through an Analytic Filtration Unit (Nalgene). RNA was precipitated by 0.9 volume of isopropanol and centrifugated at 30 000 *g* for 30 min at 4°C. Pellet was washed with 80% ethanol, centrifugated under the same conditions for 10 min and resuspended in 50-100 µl of milliQ water. The RNA concentration was determined by $OD_{260}$ measurement on NanoDrop ND-1000 Spectrophotometer (NanoDrop Technologies).

# 5. Preparation of enolase 2

## 5.1. Preparation of recombinant enolases

### 5.1.1. Expression and purification of recombinant yeast enolases and human enolases

Native wild type or mutant yeast eno2p with a C-terminal $His_6$-tag was expressed from a plasmid pET-3a derivative transformed in *E. coli* BL21. Plasmids containing human cDNAs encoding enolase isoforms enolase 1 (α), enolase 2 (γ, neuronal) or enolase 3 (β, muscle) were purchased from OriGene (Rockville, MD, USA). Coding regions with a C-terminal $His_6$-tag were inserted into pET30a expression vector. Plasmids were transformed in *E. coli* BL21.

Bacteria were grown at 37°C in LB/Ampicilline (100 µg/ml) until $OD_{600}$ reached 0.6.

*Induction of protein expression*

Protein expression was induced by 0.5 mM IPTG for 2-3 h at 30°C. Cells were harvested by centrifugation at 4 000 *g* for 15 min. Cells were frozen at -80 °C.

*Cell lysis*

The cell pellet was thawn on ice and resuspended in NP buffer (50 mM $NaH_2PO_4$, 300 mM NaCl, pH 8.0) supplemented with Complete EDTA-free protease inhibitor tablets (Roche). Cell suspention was incubated with lysozyme (1 mg/ml) for 30 min on ice. Cells were lysed by sonication for 10 min (Amplitude 37%, pulse on 8 s, pulse off 8 s) on ice. The cellular debris were pelleted by centrifugation at 20 000 *g* for 1 h at 4°C. The supernatant was incubated overnight at 4°C with Ni-NTA slurry (Qiagen) (1 ml per 10 mg of proteins) in presence of 10 mM imidazole.

*Recombinant protein purification using Ni-NTA resin.*

The lysate-Ni-NTA mixture was loaded into a column the bottom outlet capped. The Ni-NTA resin with bound proteins was washed with NP-buffer containing 10, 20 and 30 mM imidazole. The bound protein was eluted from the resin with NPI-buffer (NP buffer supplemented with imiadazole) with imidazole concentrations increasing from 60 mM to 200 mM.

The protein samples were dialyzed at 4°C against a buffer containing 50 mM HEPES-KOH, 100 mM KCl, 1 mM $MgCl_2$, pH 7.5. The protein was stored at +4. The concentration of protein was estimated by measuring $A_{280}$ (Mass extinction coefficient = 8.95 $L*g^{-1}*cm^{-1}$) on NanoDrop ND-1000 Spectrophotometer (NanoDrop Technologies). The purity of the protein was assessed by 10% SDS-PAGE.

### 5.1.2. Protein purification by hydroxyapatite chromatography

CHT5-1 column (BioRad) was used. Protein samples were dialyzed against buffer A (5 mM $NaPO_4$, 150 mM NaCl, pH 6.8) and loaded onto the column pre-equilibrated with the same buffer. The protein was eluted using a linear gradient of phosphate buffer (5-500 mM sodium phosphate) pH 6.8. The flow rate was 1 ml/min. The elution of proteins was monitored by measuring the optical density at 280 nm. The purity of the protein was assessed by 10% SDS-PAGE.

## 5.2. Preparation of native endogenous yeast enolase 2

Native enolase 2 (Eno2p) was purified from Δ*ENO1* yeast cells at the end of the exponential phase of growth. Yeast was grown in liquid YPD medium supplemented with 0.2 mg/ml of G418 and 0.1 mg/ml ampicilline at 30°C in a shaking incubator (Infors HT Multitron) at 250 rpm for 18 h. The cells were harvested by 15 min centrifugation at 5 000 *g* at 4°C and washed by pre-chilled milliQ water.

Cells were resuspended in 2 volumes of breakage buffer (0.6 M Sorbitol, 10 mM Tris-HCl, pH 7.5, 1 mM EDTA and complete proteases inhibitors cocktail (Roche) with 2 volumes of glass beads (d = 0.25-0.5 mm). Disruption of cells was performed using a FastPrep-24 instrument (MP Biomedical). Five runs of 30 s interspersed by 5 min cooling on ice were done.

The cell extract was centrifuged for 30 min at 40 000 *g* at 4 °C to remove the cellular debris. The supernatant was transferred to a fresh tube and saturated to 67% of ammonium sulfate by adding solid ammonium sulfate. After centrifugation at 40 000 *g* at 4°C for 30 min, the supernatant was saturated to 100% and centrifuged again under the same conditions.

The supernatant was discarded and the pellet was resuspended in 20 mM Tris–HCl buffer, pH 8.3, containing 5 mM $MgSO_4$, 1 mM EDTA. The sample was dialyzed overnight against the same buffer to remove ammonium sulfate and applied to a mono-Q column (HiTrap Q XL, GE Healthcare) equilibrated with 20 mM Tris–HCl buffer, pH 8.3, containing 5 mM $MgSO_4$, 1 mM EDTA. Proteins were eluted with a linear NaCl gradient (0-1 M) at a flow rate of 1 ml/min and the eluate was monitored at 280 nm.

Eno2p-enriched fractions were applied to a Superdex-200 Increase 10/300 GL column (GE Healthcare) equilibrated with 50 mM HEPES-KOH, pH 7.5, 150 mM KCl, 5 mM $MgSO_4$ and 1 mM EDTA.

At each purification step, protein-containing fractions were analyzed on 10% SDS-PAGE and probed by dot-blot analysis or by Western-blot using an anti-enolase antibody (C-19: sc-7455, Santa Cruz Biotechnology). The protein sample was stored at +4.

### 5.3. Preparation of enolase-enriched fraction by ammonium sulfate precipitation

The extract of yeast Δ*ENO1* cells was prepared as described at paragraph 4.2 and centrifuged for 30 min at 40 000 *g* at 4°C. The extracted proteins were subjected to differential ammonium sulfate precipitation. Fractions were dialyzed against 50 mM HEPES-KOH, pH 7.5, 150 mM KCl, 5 mM $MgSO_4$ and 1 mM EDTA to remove ammonium sulfate.

### 5.4. Fractionation of yeast protein extract by heparin chromatography

Yeast W303 cells were grown in liquid YPD medium at 30°C in a shaking incubator (Infors HT Multitron) at 250 rpm overnight ($OD_{600} \cong 1$). Cells were harvested by 5 min centrifugation at 3 500 *g* 4°C and washed in pre-chilled milliQ water.

Cell pellet was resuspended in 3 volumes of buffer (10 mM HEPES-KOH, pH 6.8, 50 mM KCl, 1 mM EDTA, 5 mM DTT, 10% glycerol supplemented with complete protease inhibitor cocktail (Roche), mixed with 1 volume of glass beads (d = 0.25-0.5 mm). Disruption of cells was performed using a FastPrep-24 instrument (MP Biomedical). Six cycles of 20 s of run time with 5 min cooling on ice were done. Glass beads and cell debris were removed by centrifugation for 5 min at 500 *g*. The S-100 fraction was prepared by centrifugation at 100 000 *g* for 30 min at 4°C.

The supernatant of the S-100 fraction was dialyzed against 20 mM HEPES-KOH, pH 6.8, 10 mM NaCl, 0,5 mM PMSF, 1 mM DTT and 10% glycerol, and applied to a heparin-sepharose column (Hi Trap Heparin HP 1 mL, GE Healthcare) equilibrated with the same buffer. Proteins were eluted by a step gradient of sodium chloride (0-900 mM).

Fractions were analyzed on 10% SDS-PAGE and checked for the presence of Eno2p by western blot with anti-enolase antibody (4.5.). Then they were dialyzed against 20 mM HEPES-KOH, pH 6.8, 1 mM DTT, 10 mM KCl and 50% glycerol and complete protease inhibitor cocktail (Roche), and stored at -20°C.

### 5.5. Western blot analysis (Sambrook and Russel)

***Protein SDS-PAGE.*** Protein sample in Laemmli buffer (50 mM Tris-HCl pH 6.8, 2% SDS, 10% glycerol, 1% β-mercaptoethanol, 12.5 mM EDTA, 0.02 % bromophenol blue) is heated at 90°C for 5 min and cooled down to room temperature.

Concentration gel – 4% PAAG, 1x Upper Tris buffer (15 g/l Tris; 0.1%SDS) pH 6.8. Separation gel – 10% PAAG, 1x Lower Tris buffer (45 g/l Tris; 0.1%SDS) pH 8.8. The gel was polimerized by addition of 0.1% ammonium persulfate and 0.2% TEMED. Electrophoresis buffer is Tris-Glycine buffer (25 mM Tris-HCl, 195 mM glycine, 0.1% SDS, pH 8.3-8.5).

Protein samples and Pageruler Prestained Protein Ladder (Thermo Fisher Scientific) were loaded onto the gel and run at 10-15 V/cm.

***Electrotransfer of proteins on Protran membrane.*** The wet transfer method was used. The gel and the Protran 0.45μm membrane (Amersham) were sandwiched between sponge and paper. The transfer was carried out in the Mini Trans-Blot cell (Bio Rad) in Tris-glycine buffer (used for protein gel) with 20% ethanol for 1.5 h at 90 V.

***Western blot.*** The membrane was washed in water and stained with Ponceau S solution (0.2% (w/v) Ponceau S, 5% acetic acid) to check the efficiency of transfer. The stain was removed by washing with 1x PBS buffer (Euromedex). The membrane was blocked in 5% non-fat milk in PBS buffer for 1 h at room temperature. The membrane was washed with PBS-Tween buffer (PBS buffer supplemented with 0.5% Tween-20) 3 times for 10 min and incubated with primary antibodies for 2 h at room temperature or overnight at 4°C at constant stirring. The blot was washed with PBS-Tween buffer 3 times for 10 min and incubated with corresponding secondary antibodies for 1-2 h at room temperature. The membrane was washed with PBS-Tween buffer 3 times for 10 min and developed using the ECL detection system. For 2 ml of the ECL solution 200 μl of 1M Tris-HCl, pH 8.5, 0.6 μl of 30% $H_2O_2$, 10 μl of 250 mM luminol , and 5 μl of 90 mM *p*-coumaric acid were mixed. Luminescent signal was detected using G-box (Syngene) or Amersham hyperfilm ECL.

***Stripping and reprobing.*** The membrane was incubated in 62.5 mM Tris-HCl, pH 6.7, 2% SDS, 100mM β-mercaptoethanol at 50°C for 30 min. Then the membrane was washed thoroughly with PBS buffer to remove traces of β-mercaptoethanol that can damage the antibodies, and used for blocking step.

### 5.6. Purification of recombinant preKARS2

The purification of recombinant preKARS2 was performed as described in Gowher et al., 2013. *E. coli* strain BL21 were transformed with the pDEST17 plasmid and cultivated in LB medium to $OD_{600}$ = 0.6. The protein expression was induced by 0.5 mM IPTG for 2 h at 37°C. Harvested by centrifugation (6 000 *g*,10 min) cells were lysed by incubation with lysozyme (1 mg/ml) on ice for 30 min following sonication thrice for 20 s (Amplitude 37%, with 20 s rest on ice) in 50 mM $NaH_2PO_4$, pH 8, 300 mM NaCl and 20 mM imidazole. The cell lysate was centrifuged at 10 000 *g* for 15 min and the pellet was solubilized in the denaturing buffer consisting of 100 mM Tris-HCl, pH 8, 100 mM $NaH_2PO_4$, 10 mM imidazole and 8 M urea. After 15 min centrifugation at 12 000 *g* the supernatant was applied to a Ni-NTA column (Qiagen) for 2 h at 4°C. Weakly bound bacterial proteins were eliminated by washing three times with the denaturing buffer containing 20 mM imidazole, and the recombinant protein was eluted from the column with 200 mM imidazole, refolded by stepwise elimination of urea and dialyzed against 50 mM Tris-HCl, pH 8.0, 300 mM NaCl and 40% glycerol. The purity of the protein was checked by SDS-PAGE followed by Coomassie blue staining.

## 6. Analysis of interaction between tRK1 and recombinant Eno2p

### 6.1. Radioactive 5' end labeling of tRNA

Aqueous solution of T7 transcripts of tRNAs was heated at 92°C for 1 min. The standard 20 µl reaction mixture contained T7 transcripts (≈ 500 ng), 1x buffer for PolyNucleotideKinase (Promega), 1-3 µl (10 mCi/ml) γ-32P-ATP, 40 U RNAseOUT (Termo Fisher Scientific), 10 U of PolyNucleotideKinase. The reaction was carried out at 37°C for 1 hour.

Unincorporated nucleotides were removed by Micro Bio-Spin 6 columns (Bio Rad) following the provider's protocol or by PAGE. For PAGE purification, 20 µl 2x urea blue loading buffer was added to the reaction mixture. The sample was loaded onto a denaturing 8% polyacrylamide gel (1 mm thick).

The gel was run until the bromophenol blue reached the bottom . The band corresponding to tRNA was cut out under UV light. For the elution, the gel slice was placed into the 2-ml tube with 200 µl of elution buffer (0.5 M ammonium acetate, 10 mM magnesium

acetate, 0.1 mM EDTA, 0.1% SDS) and 50 µl of phenol saturated with 100 mM sodium acetate pH 5.0 and shaked at 4°C overnight.

RNA was precipitated from the aqueous phase with 10% of 3M sodium acetate pH 5.0 and 3 volumes of 100% ethanol and dissolved in milliQ water. The amount of labeled material was estimated using a scintillation counter in Cerenkov radiation measuring mode (LS 6500, Beckman Coulter)

## 6.2. Electrophoretic Mobility Shift Assay (EMSA)

γ-$^{32}$P 5' –labeled T7 tRNA was denaturated for 2 min at 90°C in milliQ water and slowly cooled down to room temperature in re-folding buffer (50 mM HEPES, 10 mM KCl, 10 mM $MgCl_2$, pH 6.7) or in 4 mM EDTA.

A typical 15 µl reaction mixture contained 3 000-5 000 cpm labeled tRNA, appropriate amounts of proteins and 1x EMSA buffer (25 mM HEPES-KOH, pH 7.5, 100 mM KCl, 1 mM $MgCl_2$, 0.1 mM EDTA) and incubated for 20 min at 30°C.

RNA-protein complexes were resolved on native 8% PAGE containing 5% glycerol in 0.5x TBE buffer. The gel was run in 0,5x TBE buffer at 10-15 mA at 4°C until the bromophenol blue reached the bottom of the gel, then dried, exposed against an phosphorimage plate (Fuji) overnight. The image plate was read by a Typhoon-Trio scanner and further analysed with the QuantTL software (GE Healthcare).

## 6.3. Isothermal titration microcalorimetry

ITC experiments were performed on a MicroCal ITC200 (GE Healthcare). Protein and RNA samples were dialyzed against the buffer composed of 25 mM HEPES-KOH, pH 7,5; 100 mM KCl; 1 mM $MgCl_2$; 0,1 mM EDTA. Experiments were carried out according to the manufacturer guidelines using 300 µl of the 30 µM protein solution in the main adiabatic cell, while the syringe was loaded with a solution containing 300 µM RNA refolded under the same conditions as for EMSA experiments. Injections of 1.5 µl of tRK1 solution were performed until complete titration was reached. Data treatment was performed with the software Origin 7.0.

## 7. *In vitro* import into isolated mitochondria (for more information Entelis et al, 2002)

### 7.1. Aminoacylation of labeled tRNA transcript

T7 transcripts of tRNA (≈ 500 ng) were prior labeled as in §6.1, diluted in 50 µl milliQ water and supplemented with 90°C pre-heated 20 mM $MgCl_2$. The mixture was incubated for 1 min at 90°C and cooled down to ambient temperature for 15-20 min.

Then tRNA solution was mixed with 100 µl 2x aminoacylation buffer (200 mM Tris-HCl, pH 7.5, 60 mM KCl, 20 mM $MgCl_2$, 4 mM ATP, 2 mM DTT, 0.1 mM Lysine) and 6,5 µl recombinant lysul-tRNA synthetase (KRS, 0.35 µg/ml; kindly provided by Dr. P. Kamenski) and incubated at 37°C for 15 min. RNA was extracted by acid phenol by adding 200 µl of phenol pH 5,0 to the reaction mixture, followed by vortexing and centrifugation. RNA was ethanol precipitated and dissolved in 10 mM Na-acetate pH 5.0.

### 7.2. *In vitro* import into isolated yeast mitochondria

Mitochondria should be freshly extracted or thawed. Mitochondria were mixed with breakage buffer (without EDTA, but supplemented with 1 mM succinate and 1 mM α-ketoglutarate), incubated at 37°C for 5 min and pelleted by centrifugation for 5 min at 13 000 *g* 4°C. In order to prevent unspecific binding of tRNA, mitochondria were incubated with *E. coli* ribosomal RNAs (Roche) (12 µg/mg of mitochondrial protein) for 5 min on ice. Then mitochondria were harvested and resuspended in import buffer (0.6 M sorbitol, 20 mM HEPES-KOH, pH 6.8, 20 mM KCl, 2.5 mM $MgCl_2$, 5mM ATP, 1 mM DTT, 0.1 mM Lysine, 0.5 mM phosphoenol pyruvate, 4 units of pyruvate kinase).

A standard *in vitro* import assay was carried out in a final volume of 100 µl using 100 µg of mitochondria, 50 000 cpm of 5'-$^{32}$P-labeled and aminoacylated tRNA, 60 nM of recombinant preMSK1p (kindly provided by Dr. M. Vysokikh) and other import factors at 30°C for 15-20 min. Non-imported RNAs were removed by addition of 50 µg/ml of RNase A (Sigma) followed by 10 min incubation on ice. The RNAse A was eliminated by washing mitochondria with a buffer containing 0.6 M sorbitol, 10 mM HEPES-KOH (pH 6.7) and 4 mM EDTA. Mitochondrial RNAs were extracted by TRIzol reagent (Termo Fisher Scientific) according to the provider's

protocol. RNAs were analyzed by 8% denaturing PAGE followed by phosphorimager detection using a Typhoon-Trio scanner.

## 8. Analysis of tRNA structure by In-line probing and enzymatic digestion

(for more information Biondi and Burke, 2014; Regulski and Breaker, 2008)

Transcripts of tRNA were labeled as discribed in §6.1. and PAGE-purified. 25 000 cpm of labeled tRNA were used per each reaction.

### 8.1. Preparation of Ladders

***Alkaline Digestion*.** This reaction cleaves the RNA molecule after each nucleotide. The reaction mixture contained 2 µl γ-$^{32}$P –labeled T7 tRNA, 1 µl of $Na_2CO_3$ buffer and 8 µl milliQ water, yielding a total volume of 10 µl. $Na_2CO_3$ buffer – 0.5 M $Na_2CO_3$, pH≥9, 10 mM EDTA, pH 8.0.

The reaction mixture was incubated for 5 min at 92°C and stopped with 10 µl of gel-loading buffer (8 M urea, 15 mM EDTA). The sample was stored at -20°C until use.

***Denaturing RNase T1 digestion.*** In denaturing conditions, RNase T1 cuts the RNA molecule 3' of each G residue. The reaction mixture contained 2 µl γ-$^{32}$P –labeled T7 tRNA, 1 µl 0.25 M Na-citrate buffer, pH 5, 1 µl (1 U/µl) RNase T1 and 6 µl gel-loading buffer (8 M urea, 15 mM EDTA), yielding a total volume of 10 µl.

The reaction mixture was incubated for 5 min at 55°C and stopped with 10 µl of gel-loading buffer. The sample was stored at -20°C until use.

### 8.2. In-line probing

Prior to experiments tRNAs should be refolded properly. Then tRNAs were placed under the following conditions:

1$^{st}$ buffer – 50 mM Tris-HCl, pH 8.3, 80 mM KCl, 10 mM MgCl2

2$^{nd}$ buffer – 50 mM Tris-HCl, pH 8.3, 80 mM KCl, 4 mM MgCl2

The reactions mixtures were incubated ≥40 h. The reactions were stopped by adding the gel-loading buffer and loaded onto a denaturing PAGE.

### 8.3. RNase digestion

***RNase T1 digestion***. RNase T1 cleaves after single stranded G residue. 2 µl γ-$^{32}$P –labeled T7 tRNA, 5 µl BS buffer (100 mM MES-KOH, pH 6.5, 200 mM KCl, 4 mM $MgCl_2$) and milliQ water up to a total volume of 9 µl were mixed. The reaction was started by adding 1 µl (0.1 U/µl) RNase T1. The mixture was incubated for 5 min at 37°C.

***RNase V1 digestion***. RNase V1 cleaves after double-stranded nucleotides and some other structures. 2 µl γ-$^{32}$P –labeled T7 tRNA, 5 µl BS buffer (100 mM MES-KOH, pH 6.5, 200 mM KCl, 4 mM $MgCl_2$) and milliQ water up to a total volume of 9 µl were mixed. The reaction was started by adding 1 µl ($1\times10^{-5}$ U/µl) RNase V1. The mixture was incubated for 5 min at 37°C.

The reactions were stopped with 10 µl of gel-loading buffer and stored at -20°C.

### 8.4. PAGE and gel analysis

10% acrylamide/bisacrilamide (19:1) gel solution containing 8 M urea and 1x TBE was mixed with 1/100 (v/v) 10% (w/v) APS and 1/1000 (v/v) TEMED. The gel was polymerized 1-2 h.

The gel was pre-run for 1 h at 60 W. Then samples and control not-treated tRNA in loading buffer with 0.025% bromophenol blue were loaded onto the gel and run at 45-60 W for several hours or until bromophenol blue was 10 cm from the bottom of the gel.

The gel was dried for 1 h at 80 °C and exposed to a PhosphorImager screen (Fuji) overnight. Autoradiograph was revealed by a Typhoon-Trio scanner and analysed with the QuantTL software (GE Healthcare).

## 9. Affinity chromatography with in vitro transcribed ARiBo-tagged tRNA

### 9.1. Preparation of λN$^+$-GST fusion protein (di Tomasso et al, 2012)

*E. coli* BL21 cells transfected with pET42a-λN⁺-L⁺-GST plasmid were cultivated in LB/ Kanamycin 25 µg/ml at 37 °C. The protein expression was induced by 0.5 mM IPTG for 4 h at 25°C. The cells were harvested by centrifugation and washed with pre-chilled milliQ water. The cells were re-suspended in homogenization buffer (20 mM Tris-HCl, pH 7.4, 1 M NaCl, 1 mM DTT, 0.2 mM EDTA, complete protease inhibitors cocktail (Roche) and lysed by 5 cycles of sonication per 10 s (Amplitude = 37%). Cell debris were removed by centrifugation for 1 h at 118 000 *g* at 4°C. The supernatant was mixed with GSH-Sepharose 4B resin (Healthcare GE) pre-equilibrated with homogenization buffer and incubated 1 h at 4°C. The resin was washed twice with homogenization buffer supplemented with 2 M urea and then twice with buffer containing 10 mM $Na_2HPO_4$, 2 mM $KH_2PO_4$, 2.7 mM KCl, 140 mM NaCl (pH 7.4). The resin was collected by 3 min centrifugation at 1 150 g.

The λN⁺-L⁺-GST protein was eluted by 20 mM reduced L-glutation in 50 mM Tris-HCl, pH 8.0 at room temperature. The purity of the protein was evaluated on a 10% SDS-PAGE. Selected fractions were pooled and dialyzed against 50 mM HEPES pH 8.0, 100 mM NaCl, 2 mM DTT, and 20% glycerol overnight at 4°C with slow stirring

### 9.2. Cloning of the plasmid DNA template for the ARiBo1-fused RNA.

***PCR of tRK1 gene***. The 20 µl PCR mixture contained 20 ng of DNA template per 1 µl, 10 µM primers solutions, 2 µl 2,5 mM dNTP, Phusion high-fidelity DNA polymerase, 1x HF buffer and milliQ water.

Conditions of PCR: 98°C – 5 min
denaturation/ 94°C – 10 s
hybridization of primers/ 50°C – 30 s } 28 cycles
elongation/ 72°C – 15 s
72°C – 3 min.

The PCR product was purified by 1% agarose gel following extraction by QIAquick gel extraction kit (Qiagen).

***Restriction digest of PCR product and plasmid:*** PCR product and ARiBo1-containing plasmid were digested by FastDigest restriction enzymes (Thermo Scientific) HindIII and ApaI according to the provider's protocol.

***Ligation*** of digested PCR product with plasmid was carried out for 10 min at 22°C. The 20 µl reaction mixture contained 30 ng digested plasmid DNA, 5.5 ng digested PCR product, 5 U T4 DNA ligase (Termo Scientific), 0.5 mM ATP in 1x FastDigest buffer. The reaction mixter was transformed into 200 µl aliquot of XL1Blue competent cells. For screening, cells were seeded on LB–ampicillin agar plates. The resulting colonies were used screened by PCR (PCR conditiones are dicribed above) and used by isolation of plasmid DNA. The plasmids were sequenced.

***Mutant strand synthesis reaction:*** for construction of plasmid DNA template for the ARiBo1-fused tRK40 (non-efficiently imported version of tRK1 bearing mutations in the aminoacceptor stem, which prevent interaction with preMSK1p), the QuickChange II XL Site-Directed Mutagenesis Kit (Agilent) was used according to the provider's manual.

Conditions of PCR: 95°C – 1 min
denaturation/ 95°C – 50 s
hybridization of primers/ 60°C – 50 s } 18 cycles
elongation/ 68°C – 3 min
68°C – 7 min
4°C – 3 min

The transformed XL1Blue cells were screened on LB–ampicillin agar plates. The resulting colonies were used by isolation of plasmid DNA. The plasmids were sequenced.

### 9.3. Affinity chromatography using in vitro transcribed ARiBo-tagged tRNAs as baits

***Cell lysate:*** yeast W303 cells grown in YPGly medium and disrupted as in §5.2. The lysate was centrifuged for 10 min at 16 000 *g* 4°C. The quantity of proteins in the supernatant was estimated by Bradford assay. The supernatant was kept on ice until use. The supernatant underwent heparin chromatography (as described in 5.4.) to obtain HP-0 fraction.

***Re-folding of ARiBo1-tagged RNA:*** 350 pmol of T7 ARiBo1 tagged-tRNA in milliQ water was incubated for 1 min at 92°C, then mixed with equal volume of 2x folding buffer (100 mM HEPES-KOH, pH 7.5, 20 mM KCl, 20 mM $MgCl_2$). The incubation was continued for 25 min at 37°C. The mixture was kept on ice until use.

350 pmol of $\lambda N^+$-$L^+$-GST fusion protein was mixed with 350 pmol re-folded T7 ARiBo1

tagged-tRNA in 1x Equilibration buffer (20 mM HEPES-KOH, pH 7.4, 100 mM KCl, 1 mM $MgCl_2$). The total volume was 350 µl. The binding reaction was carried out for 30 min on ice. Then 1 mg of cell lysate or HP-0 fraction proteins were added to RNA-fusion protein mixture following incubation for 15 min at 30°C.

1% of the reaction mixture was mixed with 1x Lammlie buffer in 100 µl and its protein content was analysed. 5% of the reaction mixture was mixed with Equilibration buffer in 500 µl and kept on ice until all elutions had been ready.

In the meantime, GSH-Sepharose matrix was prepared into the appropriate column. Beads should form thin layer on the bottom of the column (Poly-prep chromatography columns, Bio Rad). 70 µl of GSH-Sepharose resin was washed twice by 1 ml PBS buffer and Equilibration buffer. The RNA-protein mix was added to the washed resin and incubated for 15 min at 4°C on the column with end cap. The flow through was collected and re-loaded again onto the column with a sealed tap to increase protein binding efficiency.

Then the flow through was collected and the resin was washed with 2 ml of equilibration buffer three times (The last sample was collected). The complexes were eluted twice by 250 µl of buffer containing 50 mM Tris-HCl, pH 7.5, 10 mM $MgCl_2$, 10 mM GlcN6P after 15 min incubation at 37°C (E1). The remaining binding proteins were eluted twice by 250 µl of buffer containing 50 mM Tris-HCl, pH 8,0; 40 mM Glutatione after 15 min incubation at room temperature (E2).

Equal volumes of Aqua-P/C/I (ROTH) were mixed to the total protein solutions and elution samples in 2 ml tubes. RNA-protein complexes were dissociated by vigorous shaking for 20 seconds and incubated at room temperature for 5 minutes. The aqueous phases were collected in 2 ml tubes after 30 min centrifugation at 15 200 *g* at 15°C. RNAs were precipitated with 3 volumes of 100% ethanol and 1/10 volumes of 3M Na-acetate pH 5.0 with addition of 10-20 µg of glycogen. Organic phases were mixed with 3 volumes of ice-cold acetone and centrifugated for 1 h at 16 000 *g* at 4°C. The supernatants were carefully removed with a pipette The pellets were washed twice with 500 µl of cold acetone, air-dried overnight and dissolved in 50 µl of 1x Lammlie buffer.

### 9.4. Silver staining of proteins on SDS-PAGE

The protein material on SDS-PAGE was fixed by smooth stirring in buffer A (50% methanol, 12% acetic acid, 500 µl/L 37% formaldehyde) for 1 h. The gel was washed twice for 20 min with 50% ethanol and once with 30% ethanol for 20 min. The sensitization of gel was performed by soaking it in 0.02% $Na_2S_2O_3$ x $5H_2O$ (0.2 mg/ml) solution for 1 min with vigorous shaking following washing by milliQ water for 20 s three times. After addition of buffer B (2 g/L $AgNO_3$, 750µl/L 37% formaldehyde), the gel was incubated for 20 min with vigorous shaking and rinsed rapidly twice for 20 s. The developing was performed in buffer C (60 g/L $Na_2CO_3$, 500µl/L 37% formaldehyde, 4 mg/L $Na_2S_2O_3$ x $5H_2O$) by gentle stirring on shaker. The developing was stopped by 1% glycine solution.

## 10. Mass Spectromery Analysis

Mass spectrometry analysis was performed using MALDI-TOF/TOFIII Smartbeam (Bruker), TripleTOF® 5600 (AB SCIEX) and nanoLC-MS/MS (nanoU3000 (Dionex)-ESI-MicroTOFQII) (Bruker). Mass spectrometry data were analysed using the Mascot software (Matrix science). Mass spectrometry identification of proteins was done in collaboration with Philippe HAMMANN at the proteomic platform of the University of Strasbourg (Strasbourg Esplanade).

## 11. Transfection of human cell lines

### 11.1. Transfection with T7 tRNA and/or plasmid DNA

For transient DNA and RNA transfection, cells were grown in MEM or DMEM in 75 $cm^2$ to reach ≈ 60% of confluence. The serum-containing medium was substituted by OptiMEM (Invitrogen) prior for 2 h before transfection. The transfection was performed using Lipofectamin 2 000 (Invitrogen) according to the manufacturer's protocol. 10-15 µl of Lipofectamin and 3-3.5 µg RNA were diluted into 100 µl of OptiMEM and incubated for 5 min at room temperature. 45 µl of Lipofectamin and 37.5 µg of plasmid DNA were diluted into 100 µl of OptiMEM and incubated for 5 min at room temperature. The Lipofectamin-RNA and/or Lipofectamin-DNA complexes were added to cells in OptiMEM and incubated for 6 h. After 48

h, cells were collected and mitochondrial RNA import was analyzed by Northern blot hybridization.

### 11.2. Transient protein downregulation

Knock-down regulation was performed using small interfering RNA (siRNA):

**siRNA against enolase:**
sieno13: 5'-AACAAGCUGGCCAUGCAGGAGUUUU-3'
sieno31: 5'-AACUCCUGCAUGGCCAGCUUGUUUU-3'
sieno1: 5'-CUCAAAGGCUGUUGAGCACAUCAAUUU-3'
sieno2: 5'-AUUGAUGUGCUCAACAGCCUUUGAGUU-3'

**Control siRNA against aldolase:**
siald12**:** 5'-AGCGCUGUGCUCAGUACAAGAUU-3'
siald21**:** 5'-UCUUGUACUGAGCACAGCGCUUU-3'

Our optimised protocol consisted of two subsequent transfections: HepG2 cells were transfected in suspension with 40 nM of each siRNA using Lipofectamin RNAiMax transfection reagent (Invitrogen) according to the manufacturer's protocol. Briefly, 30μl of Lipofectamin and siRNA was diluted in 100μl of OptiMEM and incubated for 5min at room temperature. The cells were detached, washed with 1x PBS and seeded in 75cm$^2$ plate. The complex was added to the cells in suspension and incubated for 6 h in OptiMEM. After 24 h the monolayers of cells were transfected again with 40 nM of each siRNA using Lipofectamine 2000 (Invitrogen). After 48 h the down-regulated proteins were analysed by Western blot (5.5).

### 11.3. Purification of mitochondria RNA from human cells

Cells from 75 cm$^2$ were detached in 1x PBS (Sigma) supplemented with 1mM EDTA and centrifuged at 600 *g* for 10 min. Cells were re-suspended in 1.5 ml of cold breakage buffer (0.6 M sorbitol, 10mM HEPES-KOH, pH 6.7, 1mM EDTA) containing 0.3% BSA and disrupted though a needle (No16, 23GX1,0.6 25mm) using a syringe with ≈ 30 strokes. Cell debris were eliminated by centrifugation at 1 500 *g* for 5min at 4°C. The supernatant was centrifuged at 13 000 rpm for 30 min at 4°C, 30min. The mitochondrial pellet was re-suspended in 300 μl breakage buffer.

Mitochondria were treated with 300 µl 2x RNase A solution (12.5-25 µg/ml RNaseA (Sigma), 0.6M sorbitol, 10mM $MgCl_2$, 10mM HEPES-KOH pH 6.7) for 10 min at room temperature. RNase activity was then inhibited by addition of 800 µl of breakage buffer containing 5mM EDTA and several washes with the same buffer. Mitochondria were collected by centrifugation at 13 000g for 15 min at 4°C.

Digitonin treatment (20 µg/mg of mitochondrial protein) for 10 min at room temperature were used to generate the mitoplasts. The mtRNAs were extracted by TRIzol reagent (Invitrogen) according to the provider's recommendations.

**11.4. Northern Blot analysis** (Sambrook and Russel)

***Radioactive 5' end labeling of oligonucleotide probes:*** The 20 µl reaction mixture contained 50 pmol oligonucleotide probes, 1-5 µl γ-32P-ATP (10 mCi/ml, 5000 Ci/mmole), 1 U Polynucleotide Kinase (Promega) in 1x PolyNucleotideKinase buffer (Promega). The mixtures were incubated for 45 min at 37°C.

Unincorporated nucleotides were removed by Micro Bio-Spin 6 columns (Bio Rad) following the provider's protocol or by PAGE. Labeled oligonucleotides were diluted by equal volumes of 1M STE buffer (10 mM Tris-HCl, pH 7.5, 1 M NaCl, 1 mM EDTA) and pre-hybridization buffer (6x SSC, 10x Denhart solution, 0.2% SDS).

100x Denhart solution – 2% ficoll, 2% polyvinilpyrrolidone, 2% BSA

1x SSC – 0.15 M NaCl, 0.015 Na-citrate, pH 7.0

1M STE - 10 mM Tris-HCl, pH 7.5, 1 mM EDTA, 1M NaCl

***Northern Blot hybridization:*** The extracted mtRNA were separated on denaturing 10% PAGE. The gel and the Hybond-N membrane (Amersham) were sandwiched between sponge and Watman paper. The transfer was carried out in the Mini Trans-Blot cell (Bio Rad) in 0,5x TBE overnight at 4°C , 10V, 200 mA, under gentle stirring. After transfer, the membrane was dried at room temperature for 15min and RNAs were covalently fixed to the membrane by UV irradiation (0.8 J/$cm^2$) for 3min in an Ultraviolet crosslinker (GE healthcare).

Membrane was then pre-hybridized for 2h at 65°C in pre-hybridization buffer and hybridized with 5'-$^{32}$P-labeled oligonucleotide probe at appropriate temperature.

After hybridization, membranes were washed thee times for 10 min at 25°C in 2X SSC, 0.1% SDS and exposed to PhosphoImager plate. The signal were analyzed using Typhoon-Trio scanner and ImageQuantTL software. For re-hybridization, membrane was stripped by washing thee times for 15 min 0,2x SSC, 0,1% SDS at 80°C.

The absolute efficiency of tRNA import into mitochondria was calculated for total cells extracte as a ratio between the signal obtained with anti-tRK1 probe and the signal obtained with the probe against the human mitochondrial $tRNA^{Val}$ or $tRNA^{Lys}$, or

*[absolute import efficiency] = [tRK1]/[mt-* $tRNA^{Val}$ or $tRNA^{Lys}$*]*

The relative efficiency of tRNA import into mitochondria was calculated as a ratio between the absolute efficiency of tRNA import calculated for the studied cells and the absolute efficiency of tRNA import calculated for the control cells

$[\text{relative import efficiency}] = [\text{absolute import efficiency}]_{experiment} / [\text{absolute import efficiency}]_{control}$

## 12. SAXS data collection and analysis

The SAXS measurements were carried out at Synchrotron SOLEIL beamline SWING (Gif-sur-Yvette, France), using the beam wavelength of 1.033 Å and a sample-to-detector distance of 1800 mm. Samples were measured using a 17 x 17 $cm^2$ low-noise Aviex CCD detector. The resulting exploitable Q-range was 0.014-0.4 $A^{-1}$, where $Q=4\pi \sin\theta / \lambda$, and the scattering angle is $2\theta$.

To remove molecular aggregates, concentrated solutions of Eno2p, tRK1 or their mixture (25 µl, ≤ 9 mg/ml ) were injected into a Size Exclusion Column (Agilent Bio-sec3) using an Agilent High Performance Liquid Chromatography (HPLC) system and eluted directly into the SAXS flow-through capillary cell at a flow rate of 200 µl/min (David and Perez, 2009). SAXS data were collected online throughout the elution time, with frame duration of 0.5 s and a dead time between frames of 0.5 s. The frames corresponding to the main elution peak were

inspected and averaged using FOXTROT, a homemade program dedicated to data processing (Girardot et al, 2015). Twenty consecutive frames were averaged to produce a curve with the same Q-range with no attractive interactions at low angles. The scattering patterns of the corresponding buffer solutions were also recorded and the average buffer pattern was subtracted from the experimental pattern.

Data reduction and Guinier analysis were carried out using PRIMUS, and other programs of the ATSAS suite. The gyration radius *Rg* was avaluated using the Guinier approximation assuming that at very small angles ($Q < 1/3\ Rg$), intensity may be represented as $I(Q) = I(0) \exp(-(Q.Rg)^2/3)$. GNOME was used to obtain the maximum size $D_{max}$ and distance distribution function *P(r)*.

Low-resolution *ab initio* models of tRK1, Eno2p and their complex were generated using the program DAMMIF. A set of low-resolution models was averaged to select the common features. Scattering from the crystal structures (PDB for Eno1p - 1EBH, 1ONE) were calculated by CRYSOL. Low-resolution molecular shapes and crystallographic structures were aligned using SUPCOMB.

## 13. Crystallization of Eno2p

Initial screening for crystallization conditions of Eno2p alone or in complex with tRK1 were performed using commercial high-throughput screening kits – PEGRx, Index, and Natrix - from Hampton research. Crystallization trays were prepared with a Mosquito robot (TTP Labtech) in 96 wells Corning plates. A fixed volume of the recombinant Eno2p or complex samples was mixed with an equal volume of reservoir solution. Crystallization trays were kept at 20 °C.

Crystals of Eno2p wild type grew in 0.1 M Sodium citrate tribasic dihydrate pH 5.0, 30% v/v Jeffamine ED-2001 pH 7.0 and in 0.2 M Ammonium chloride, 0.01 M calcium chloride dihydrate, 0.05 M TRIS hydrochloride pH 8.5, 30% w/v polyethylene glycol 4 000 . Two mutants (H373F, and KK377-378AA) grew in 0.1 M Sodium citrate tribasic dihydrate pH 5.0, 30% v/v Jeffamine ED-2001 pH 7.0. No crystal of the complex could be obtained.

Diffraction data were collected at 100K at the macromolecular crystallography beamline X06DA at the Swiss light Source (SLS) and processed using XDS. Phase information was

obtained by the molecular replacement method using the crystal structure of *Trypanosoma cruzi* Eno1p (PDB: 4G7F) as a starting model. The first refinement steps were performed with Refmac. The reconstruction and refinement of the structure of the wild type, mutants H373F and KKA are under process.

# REFERENCES

1 Abe Y, Shodai T, Muto T, Mihara K, Torii H, Nishikawa S, Endo T, Kohda D (2000) Structural basis of presequence recognition by the mitochondrial protein import receptor Tom20. *Cell* **100:** 551-560

2 Adams KL, Palmer JD (2003) Evolution of mitochondrial gene content: gene loss and transfer to the nucleus. *Molecular Phylogenetics and Evolution* **29:** 380-395

3 Adhya S, Ghosh T, Das A, Bera SK, Mahapatra S (1997) Role of an RNA-binding protein in import of tRNA into Leishmania mitochondria. *Journal of Biological Chemistry* **272:** 21396-21402

4 Al-Giery AG, Brewer JM (1992) Characterization of the interaction of yeast enolase with polynucleotides. *Biochimica et Biophysica Acta (BBA) - Protein Structure and Molecular Enzymology* **1159:** 134-140

5 Alder NN, Sutherland J, Buhring AI, Jensen RE, Johnson AE (2008) Quaternary structure of the mitochondrial TIM23 complex reveals dynamic association between Tim23p and other subunits. *Molecular Biology of the Cell* **19:** 159-170

6 Allen JF (2003) Why Chloroplasts and Mitochondria Contain Genomes. *Comparative and functional genomics* **4:** 31-36

7 Allen JF (2015) Why chloroplasts and mitochondria retain their own genomes and genetic systems: Colocation for redox regulation of gene expression. *Proceedings of the National Academy of Sciences* **112:** 10231-10238

8 Araiso Y, Huot JL, Sekiguchi T, Frechin M, Fischer F, Enkler L, Senger B, Ishitani R, Becker HD, Nureki O (2014) Crystal structure of Saccharomyces cerevisiae mitochondrial GatFAB reveals a novel subunit assembly in tRNA-dependent amidotransferases. *Nucleic Acids Research* **42:** 6052-6063

9 Baleva M, Gowher A, Kamenski P, Tarassov I, Entelis N, Masquida B (2015) A Moonlighting Human Protein Is Involved in Mitochondrial Import of tRNA. *Int J Mol Sci* **16:** 9354-9367

10 Barbieri G, De Angelis L, Feo S, Cossu G, and Giallongo A (1990) Differential expression of muscle-specific enolase in embryonic and fetal myogenic cells during mouse development. *Differentiation*, **45**: 179–184

11 Becker T, Pfannschmidt S, Guiard B, Stojanovski D, Milenkovic D, Kutik S, Pfanner N, Meisinger C, Wiedemann N (2008) Biogenesis of the mitochondrial TOM complex - Mim1 promotes insertion and assembly of signal-anchored receptors. *Journal of Biological Chemistry* **283:** 120-127

12 Becker T, Wenz LS, Kruger V, Lehmann W, Muller JM, Goroncy L, Zufall N, Lithgow T, Guiard B, Chacinska A, Wagner R, Meisinger C, Pfanner N (2011a) The mitochondrial import protein Mim1 promotes biogenesis of multispanning outer membrane proteins. *Journal of Cell Biology* **194:** 387-395

13 Benjamin D, Colombi M, Hindupur SK, Betz C, Lane HA, El-Shemerly MYM, Lu M, Quagliata L, Terracciano L, Moes S, Sharpe T, Wodnar-Filipowicz A, Moroni C, and Hall MN (2016) Syrosingopine sensitizes cancer cells to killing by metformin. *Science Advances*, **2**(12).

14 Berge U (1993) Sjobring A novel plasminogen-binding protein from Streptococcus pyogenes**.** *J Biol Chem*, **268** (34): 25417–25424

15 Bhattacharyya SN, Chatterjee S, Adhya S (2002) Mitochondrial RNA import in Leishmania tropica: Aptamers homologous to multiple tRNA domains that interact cooperatively or antagonistically at the inner membrane. *Molecular and Cellular Biology* **22:** 4372-4382

16 Bhattacharyya SN, Chatterjee S, Adhya S (2002) Mitochondrial RNA import in Leishmania tropica: Aptamers homologous to multiple tRNA domains that interact cooperatively or antagonistically at the inner membrane. *Molecular and Cellular Biology* **22:** 4372-4382

17 Bhattacharyya SN, Chatterjee S, Goswami S, Tripathi G, Dey SN, Adhya S (2003) "Ping-Pong" interactions between mitochondrial tRNA import receptors within a multiprotein complex. *Molecular and Cellular Biology* **23:** 5217-5224

18 Bhattacharyya SN, Mukherjee S, Adhya S (2000) Mutations in a tRNA import signal define distinct receptors at the two membranes of Leishmania mitochondria. *Molecular and Cellular Biology* **20:** 7410-7417

19 Bolender N, Sickmann A, Wagner R, Meisinger C, Pfanner N (2008) Multiple pathways for sorting mitochondrial precursor proteins. *EMBO reports* **9:** 42-49

20 Böttinger L, Ellenrieder L, Becker T (2015) How lipids modulate mitochondrial protein import. *Journal of Bioenergetics and Biomembranes* **48:** 125-135

21 Bouzaidi-Tiali N, Aeby E, Charrière F, Pusnik M, Schneider A (2007) Elongation factor 1a mediates the specificity of mitochondrial tRNA import in T. brucei. *Embo J* **26:** 4302-4312

22 Brandina I, Graham J, Lemaitre-Guillier C, Entelis N, Krasheninnikov I, Sweetlove L, Tarassov I, Martin RP (2006) Enolase takes part in a macromolecular complex associated to mitochondria in yeast. *Biochimica et Biophysica Acta - Bioenergetics* **1757:** 1217-1228

23 Brandina I, Smirnov A, Kolesnikova O, Entelis N, Krasheninnikov IA, Martin RP, Tarassov I (2007) tRNA import into yeast mitochondria is regulated by the ubiquitin-proteasome system. *FEBS Letters* **581:** 4248-4254

24 Brix J, Dietmeier K, Pfanner N (1997) Differential recognition of preproteins by the purified cytosolic domains of the mitochondrial import receptors Tom20, Tom22, and Tom70. *Journal of Biological Chemistry* **272:** 20730-20735

25 Brokx RD, Bisland SK, Gariépy J. (2002) Designing peptide-based scaffolds as drug delivery vehicles. *Journal of Controlled Release*, Vol. 78, pp. 115-123.

26 Bruske EI, Sendfeld F, Schneider A (2009) Thiolated tRNAs of Trypanosoma brucei Are Imported into Mitochondria and Dethiolated after Import. *Journal of Biological Chemistry* **284:** 36491-36499

27 Campo ML, Peixoto PM, Martínez-Caballero S (2016) Revisiting trends on mitochondrial mega-channels for the import of proteins and nucleic acids. *Journal of Bioenergetics and Biomembranes*

28 Castello A, Fischer B, Eichelbaum K, Horos R, Beckmann BM, Strein C, Davey NE, Humphreys DT, Preiss T, Steinmetz LM, Krijgsveld J, Hentze MW (2012) Insights into RNA Biology from an Atlas of Mammalian mRNA-Binding Proteins. *Cell* **149:** 1393-1406

29 Capello M, Ferri-Borgogno S, Riganti C, Chattaragada MS, Principe M, Roux C, Zhou W, Petricoin EF, Capello P, and Novelli F. (2016) Targeting the Warburg effect in cancer cells through ENO1 knockdown rescues oxidative phosphorylation and induces growth arrest. *Oncotarget*, **7**(5): 5598–5612.

30 Chacinska A, Koehler CM, Milenkovic D, Lithgow T, Pfanner N. (2009) Importing Mitochondrial Proteins: Machineries and Mechanisms. *Cell*, Vol. 138, pp. 628-644.

31 Chacinska A, Pfannschmidt S, Wiedemann N, Kozjak V, Szklarz LKS, Schulze-Specking A, Truscott KN, Guiard B, Meisinger C, Pfanner N (2004) Essential role of Mia40 in import and assembly of mitochondrial intermembrane space proteins. *Embo Journal* **23:** 3735-3746

32 Chatterjee S, Home P, Mukherjee S, Mahata B, Goswami S, Dhar G, Adhya S (2006) An RNA-binding respiratory component mediates import of type II tRNAs into Leishmania mitochondria. *Journal of Biological Chemistry* **281:** 25270-25277

33 Crausaz Esseiva A, Marechal-Drouard L, Cosset A, Schneider A (2004) The T-stem determines the cytosolic or mitochondrial localization of trypanosomal tRNAsMet. *Molecular biology of the cell* **15:** 2750-2757

34 David G, Perez J (2009) Combined sampler robot and high-performance liquid chromatography: a fully automated system for biological small-angle X-ray scattering

experiments at the Synchrotron SOLEIL SWING beamline. *Journal of Applied Crystallography* **42:** 892-900

35 Delage L, Dietrich A, Cosset A, Marechal-Drouard L (2003a) In vitro import of a nuclearly encoded tRNA into mitochondria of Solanum tuberosum. *Molecular and Cellular Biology* **23:** 4000-4012

36 Delage L, Duchêne A-M, Zaepfel M, Maréchal-Drouard L (2003b) The anticodon and the D-domain sequences are essential determinants for plant cytosolic tRNAValimport into mitochondria. *The Plant Journal* **34:** 623-633

37 Di Tomasso G, Lampron P, Dagenais P, Omichinski JG, Legault P (2010) The ARiBo tag: a reliable tool for affinity purification of RNAs under native conditions. *Nucleic Acids Research* **39:** e18-e18

38 Díaz-Ramos À, Roig-Borrellas A, García-Melero A, López-Alemany R. (2012) $\alpha$-enolase, a multifunctional protein: Its role on pathophysiological situations. *Journal of Biomedicine and Biotechnology*, Vol. 2012.

39 Dietrich A, MarechalDrouard L, Carneiro V, Cosset A, Small I (1996) A single base change prevents import of cytosolic tRNA(Ala) into mitochondria in transgenic plants. *Plant Journal* **10:** 913-918

40 Dimmer KS, Papic D, Schumann B, Sperl D, Krumpe K, Walther DM, Rapaport D (2012) A crucial role for Mim2 in the biogenesis of mitochondrial outer membrane proteins. *Journal of Cell Science* **125:** 3464-3473

41 Doersen CJ, Guerriertakada C, Altman S, Attardi G (1985) Characterization of an Rnase P-Activity from Hela-Cell Mitochondria - Comparison with the Cytosol Rnase P-Activity. *Journal of Biological Chemistry* **260:** 5942-5949

42 Dörner M, Altmann M, Pääbo S, Mörl M (2001) Evidence for Import of a Lysyl-tRNA into Marsupial Mitochondria. *Molecular Biology of the Cell* **12:** 2688-2698

43 Duchêne A-M, El Farouk-Ameqrane S, Sieber F, Maréchal-Drouard L. (2011) Import of RNAs into Plant Mitochondria. In Kempken F (ed.), *Plant Mitochondria*. Springer New York, New York, NY, pp. 241-260.

44 Duchene AM, Giritch A, Hoffmann B, Cognat V, Lancelin D, Peeters NM, Zaepfel M, Marechal-Drouard L, Small ID (2005) Dual targeting is the rule for organellar aminoacyl-tRNA synthetases in Arabidopsis thaliana. *Proceedings of the National Academy of Sciences* **102:** 16484-16489

45 Dyall SD, Brown MT, Johnson PJ (2004) Ancient invasions: From endosymbionts to organelles. *Science* **304:** 253-257

46 Endo T, Kohda D (2002) Functions of outer membrane receptors in mitochondrial protein import. *Biochimica et Biophysica Acta (BBA) - Molecular Cell Research* **1592:** 3-14

47 Entelis N, Brandina I, Kamenski P, Krasheninnikov IA, Martin RP, Tarassov I (2006) A glycolytic enzyme, enolase, is recruited as a cofactor of tRNA targeting toward mitochondria in Saccharomyces cerevisiae. *Genes & Development* **20:** 1609-1620

48 Entelis NS, Kieffer S, Kolesnikova OA, Martin RP, Tarassov IA (1998) Structural requirements of tRNALys for its import into yeast mitochondria. *Proceedings of the National Academy of Sciences* **95:** 2838-2843

49 Entelis NS, Kolesnikova OA, Dogan S, Martin RP, Tarassov IA (2001) 5 S rRNA and tRNA import into human mitochondria - Comparison of in vitro requirements. *Journal of Biological Chemistry* **276:** 45642-45653

50 Entelis NS, Krasheninnikov IA, Martin RP, Tarassov IA (1996) Mitochondrial import of a yeast cytoplasmic tRNALys: possible roles of aminoacylation and modified nucleosides in subcellular partitioning. *FEBS Lett* **384:** 38-42

51 Entian KD, Meurer B, Kohler H, Mann KH, Mecke D (1987) Studies on the regulation of enolases and compartmentation of cytosolic enzymes in Saccharomyces cerevisiae. *Biochim Biophys Acta* **923:** 214-221

52 Feo S, Arcuri D, Piddini E, Passantino R, Giallongo A (2000) ENO1 gene product binds to the c-myc promoter and acts as a transcriptional repressor: Relationship with Myc promoter-binding protein 1 (MBP-1). *FEBS Letters* **473:** 47-52

53 Florentz C, Sohm B, Tryoen-Toth P, Putz J, Sissler M (2003) Human mitochondrial tRNAs in health and disease. *Cellular and Molecular Life Sciences* **60:** 1356-1375

54 Folta-Stogniew E, Williams KR (1999) Determination of molecular masses of proteins in solution: Implementation of an HPLC size exclusion chromatography and laser light scattering service in a core laboratory. *J Biomol Tech* **10:** 51-63

55 Frechin M, Senger B, Braye M, Kern D, Martin RP, Becker HD (2009) Yeast mitochondrial Gln-tRNAGln is generated by a GatFAB-mediated transamidation pathway involving Arc1p-controlled subcellular sorting of cytosolic GluRS. *Genes & Development* **23:** 1119-1130

56 Fukasawa Y, Tsuji J, Fu SC, Tomii K, Horton P, Imai K (2015) MitoFates: Improved Prediction of Mitochondrial Targeting Sequences and Their Cleavage Sites. *Molecular & Cellular Proteomics* **14:** 1113-1126

57 Gessmann D, Flinner N, Pfannstiel J, Schlösinger A, Schleiff E, Nussberger S, Mirus O (2011) Structural elements of the mitochondrial preprotein-conducting channel

Tom40 dissolved by bioinformatics and mass spectrometry. *Biochimica et Biophysica Acta - Bioenergetics* **1807:** 1647-1657

58 Girardot R, Viguier G, Pérez J, Ounsy M (2015). Foxtrot:a java-based application to reduce and analyze SAXS and WAXS piles of 2D data at synchrotron SOLEIL. *The 8th meeting on collective action for nomadic small angle scatterrers*; Tokai, Japan.

59 Glick BS, Brandt A, Cunningham K, Muller S, Hallberg RL, Schatz G (1992) Cytochromes-C1 and Cytochromes-B2 Are Sorted to the Intermembrane Space of Yeast Mitochondria by a Stop-Transfer Mechanism. *Cell* **69:** 809-822

60 Gobert A, Gutmann B, Taschner A, Gössringer M, Holzmann J, Hartmann RK, Rossmanith W, Giegé P (2010) A single Arabidopsis organellar protein has RNase P activity. *Nature structural & molecular biology* **17:** 740-744

61 Gomes RA, Oliveira LMA, Silva M, Ascenso C, Quintas A, Costa G, Coelho AV, Silva MS, Ferreira AEN, Freire AP, Cordeiro C (2008) Protein glycation in vivo: functional and structural effects on yeast enolase. *Biochemical Journal* **416:** 317-326

62 Gornicka A, Bragoszewski P, Chroscicki P, Wenz LS, Schulz C, Rehling P, Chacinska A (2014) A discrete pathway for the transfer of intermembrane space proteins across the outer membrane of mitochondria. *Molecular Biology of the Cell* **25:** 3999-4009

63 Gowher A, Smirnov A, Tarassov I, Entelis N (2013) Induced tRNA Import into Human Mitochondria: Implication of a Host Aminoacyl-tRNA-Synthetase. *Plos One* **8**

64 Gray MW (2012) Mitochondrial evolution. *Cold Spring Harbor Perspectives in Biology* **4**

65 Hafner A, Obermajer N, Kos J (2012) Gamma-Enolase C-terminal peptide promotes cell survival and neurite outgrowth by activation of the PI3K/Akt and MAPK/ERK signalling pathways. *Biochem J* **443**, 439–50

66 Holleman WH (1973) The use of absorption optics to measure dissociation of yeast enolase into enzymatically active monomers. *Biochim Biophys Acta* **327:** 176-185

67 Holzmann J, Frank P, Loffler E, Bennett KL, Gerner C, Rossmanith W (2008) RNase P without RNA: Identification and Functional Reconstitution of the Human Mitochondrial tRNA Processing Enzyme. *Cell* **135:** 462-474

68 Ieva R, Schrempp SG, Opalinski L, Wollweber F, Hoss P, Heisswolf AK, Gebert M, Zhang Y, Guiard B, Rospert S, Becker T, Chacinska A, Pfanner N, van der Laan M (2014) Mgr2 Functions as Lateral Gatekeeper for Preprotein Sorting in the Mitochondrial Inner Membrane. *Molecular Cell* **56:** 641-652

69 Iida H and Yahara I (1985) Yeast heat-shock protein of $M_r$ 48,000 is an isoprotein of enolase. *Nature* **315**: 688 – 690

70 Isgrò MA, Bottoni P, Scatena R (2015) Neuron-Specific Enolase as a Biomarker: Biochemical and Clinical Aspects. *Adv Exp Med Biol* **867**:125-43

71 Jeffery CJ. (2016) Protein species and moonlighting proteins: Very small changes in a protein's covalent structure can change its biochemical function. *Journal of Proteomics* **134**: 19-24

72 Jung DW, Kim WH, Park SH, Lee J, Kim J, Su D, Ha HH, Chang YT, and Williams DR (2013) A unique small molecule inhibitor of enolase clarifies its role in fundamental biological processes *ACS Chemical Biology* **8** (6): 1271-1282

73 Kamenski P, Kolesnikova O, Jubenot V, Entelis N, Krasheninnikov IA, Martin RP, Tarassov I (2007) Evidence for an adaptation mechanism of mitochondrial translation via tRNA import from the cytosol. *Molecular Cell* **26:** 625-637

74 Kanaji S, Iwahashi J, Kida Y, Sakaguchi M, Mihara K (2000) Characterization of the Signal That Directs Tom20 to the Mitochondrial Outer Membrane. *The Journal of Cell Biology* **151:** 277-288

75 Kaneko T, Suzuki T, Kapushoc ST, Rubio MA, Ghazvini J, Watanabe K, Simpson L, Suzuki T (2003) Wobble modification differences and subcellular localization of tRNAs in Leishmania tarentolae: Implication for tRNA sorting mechanism. *EMBO Journal* **22:** 657-667

76 Keller A, Peltzer J, Carpentier G, Horváth I, Oláh J, Duchesnay A, Orosz F, and Ovádi J (2007) Interactions of enolase isoforms with tubulin and microtubules during myogenesis. *BBA - General Subjects* **1770** (6): 919-926

77 Keresztes-Nagy S, Orman R (1971) Dissociation of yeast enolase into active monomers. *Biochemistry* **10:** 2506-2508

78 Klein A, Israel L, Lackey SWK, Nargang FE, Imhof A, Baumeister W, Neupert W, Thomas DR (2012) Characterization of the insertase for $\beta$ -barrel proteins of the outer mitochondrial membrane. *J Cell Biol* **199:** 599-611

79 Klemm BP, Wu N, Chen Y, Liu X, Kaitany KJ, Howard MJ, Fierke CA (2016) The Diversity of Ribonuclease P: Protein and RNA Catalysts with Analogous Biological Functions. *Biomolecules* **6:** 27

80 Kolesnikova O, Kazakova H, Comte C, Steinberg S, Kamenski P, Martin RP, Tarassov I, Entelis N (2010) Selection of RNA aptamers imported into yeast and human mitochondria. *RNA (New York, NY)* **16:** 926-941

81 Kolesnikova OA, Entelis NS, Jacquin-Becker C, Goltzene F, Chrzanowska-Lightowlers ZM, Lightowlers RN, Martin RP, Tarassov I (2004) Nuclear DNA-encoded tRNAs targeted into mitochondria can rescue a mitochondrial DNA mutation associated with the MERRF syndrome in cultured human cells. *Human Molecular Genetics* **13:** 2519-2534

82 Koley S, Adhya S (2013) A voltage-gated pore for translocation of tRNA. *Biochemical and Biophysical Research Communications* **439:** 23-29

83 Kozjak V, Wiedemann N, Milenkovic D, Lohaus C, Meyer HE, Guiard B, Meisinger C, Pfanner N (2003) An essential role of Sam50 in the protein sorting and assembly machinery of the mitochondrial outer membrane. *Journal of Biological Chemistry* **278:** 48520-48523

84 Krissinel E (2010) Crystal Contacts as Nature's Docking Solutions. *J Comput Chem* **31:** 133-143

85 Kühlbrandt W (2015) Structure and function of mitochondrial membrane protein complexes. *BMC Biology* **13:** 89

86 Kutik S, Stojanovski D, Becker L, Becker T, Meinecke M, Krüger V, Prinz C, Meisinger C, Guiard B, Wagner R, Pfanner N, Wiedemann N (2008) Dissecting Membrane Insertion of Mitochondrial $\beta$ -Barrel Proteins. *Cell* **132:** 1011-1024

87 Laforest M-J, Delage L, Maréchal-Drouard L (2005) The T-domain of cytosolic tRNAVal, an essential determinant for mitochondrial import. *FEBS Lett* **579:** 1072-1078

88 Lebioda L, Stec B, Brewer JM (1989) The Structure of Yeast Enolase at 2.25-A resolution. An 8-fold beta-alpha-barrel with a novel beta-beta-alpha-alpha(beta-alpha)6-topology. *Journal of Biological Chemistry* **264:** 3685-3693

89 Lima BD, Simpson L (1996) Sequence-dependent in vivo importation of tRNAs into the mitochondrion of Leishmania tarentolae. *RNA (New York, NY)* **2:** 429-440

90 Lithgow T, Schneider A (2010) Evolution of macromolecular import pathways in mitochondria, hydrogenosomes and mitosomes. *Philosophical Transactions of the Royal Society B-Biological Sciences* **365:** 799-817

91 Mcalister L, Holland MJ (1982) Targeted Deletion of a Yeast Enolase Structural Gene - Identification and Isolation of Yeast Enolase Isozymes. *Journal of Biological Chemistry* **257:** 7181-7188

92 Meinecke M (2006) Tim50 Maintains the Permeability Barrier of the Mitochondrial Inner Membrane. *Science* **312:** 1523-1526

93 Mercer TR, Neph S, Dinger ME, Crawford J, Smith MA, Shearwood AMJ, Haugen E, Bracken CP, Rackham O, Stamatoyannopoulos JA, Filipovska A, Mattick JS (2011) The Human Mitochondrial Transcriptome. *Cell* **146:** 645-658

94 Milenkovic D, Gabriel K, Guiard B, Schulze-Specking A, Pfanner N, Chacinska A (2007) Biogenesis of the essential Tim9-Tim10 chaperone complex of mitochondria - Site-specific recognition of cysteine residues by the intermembrane space receptor Mia40. *Journal of Biological Chemistry* **282:** 22472-22480

95 Milenkovic D, Ramming T, Muller JM, Wenz LS, Gebert N, Schulze-Specking A, Stojanovski D, Rospert S, Chacinska A (2009) Identification of the Signal Directing Tim9 and Tim10 into the Intermembrane Space of Mitochondria. *Molecular Biology of the Cell* **20:** 2530-2539

96 Milojevic T, Sonnleitner E, Romeo A, Djinovic-Carugo K, Blasi U (2013) False positive RNA binding activities after Ni-affinity purification from Escherichia coli. *Rna Biology* **10:** 1066-1069

97 Mokranjac D, Popov-Celeketic D, Hell K, Neupert W (2005) Role of Tim21 in mitochondrial translocation contact sites. *Journal of Biological Chemistry* **280:** 23437-23440

98 Mordas A, Tokatlidis K (2015) The MIA Pathway: A Key Regulator of Mitochondrial Oxidative Protein Folding and Biogenesis. *Accounts of Chemical Research* **48:** 2191-2199

99 Mukherjee S, Basu S, Home P, Dhar G, Adhya S (2007) Necessary and sufficient factors for the import of transfer RNA into the kinetoplast mitochondrion. *EMBO reports* **8:** 589-595

100 Nurmohamed S, McKay AR, Robinson CV, Luisi BF (2010) Molecular recognition between Escherichia coli enolase and ribonuclease E. *Acta Crystallographica Section D: Biological Crystallography* **66:** 1036-1040

101 Pancholi V (2001) Multifunctional alpha-enolase: its role in diseases. *Cellular and molecular life sciences : CMLS* **58:** 902-920

102 Papić D, Krumpe K, Dukanovic J, Dimmer KS, Rapaport D (2011) Multispan mitochondrial outer membrane protein Ugo1 follows a unique Mim1-dependent import pathway. *Journal of Cell Biology* **194:** 397-405

103 Paris Z, Rubio MAT, Lukes J, Alfonzo JD (2009) Mitochondrial tRNA import in Trypanosoma brucei is independent of thiolation and the Rieske protein. *RNA (New York, NY)* **15:** 1398-1406

104 Peixoto PMV, Grana F, Roy TJ, Dunn CD, Flores M, Jensen RE, Campo ML (2007) Awaking TIM22, a dynamic ligand-gated channel for protein insertion in the mitochondrial inner membrane. *Journal of Biological Chemistry* **282:** 18694-18701

105 Pino P, Aeby E, Foth BJ, Sheiner L, Soldati T, Schneider A, Soldati-Favre D (2010) Mitochondrial translation in absence of local tRNA aminoacylation and methionyl tRNAMet formylation in Apicomplexa. *Molecular Microbiology* **76:** 706-718

106 Poyner RR, Cleland WW, and Reed GH (2001) Role of metal ions in catalysis by enolase: an ordered kinetic mechanism for a single substrate, enzyme. *Biochemistry*, **40** (27): 8009-8017

107 Puranam RS, Attardi G (2001) The RNase P associated with HeLa cell mitochondria contains an essential RNA component identical in sequence to that of the nuclear RNase P. *Molecular and Cellular Biology* **21:** 548-561

108 Pusnik M, Charriere F, Maser P, Waller RF, Dagley MJ, Lithgow T, Schneider A (2009) The Single Mitochondrial Porin of Trypanosoma brucei is the Main Metabolite Transporter in the Outer Mitochondrial Membrane. *Molecular Biology and Evolution* **26:** 671-680

109 Quiros PM, Langer T, Lopez-Otin C (2015) New roles for mitochondrial proteases in health, ageing and disease. *Nature Reviews Molecular Cell Biology* **16:** 345-359

110 Rao S, Schmidt O, Harbauer AB, Schoenfisch B, Guiard B, Pfanner N, Meisinger C (2012) Biogenesis of the preprotein translocase of the outer mitochondrial membrane: protein kinase A phosphorylates the precursor of Tom40 and impairs its import. *Molecular Biology of the Cell* **23:** 1618-1627

111 Rehling P (2003) Protein Insertion into the Mitochondrial Inner Membrane by a Twin-Pore Translocase. *Science* **299:** 1747-1751

112 Reichmann D, Coute Y, de Choudens SO (2015) Dual Activity of Quinolinate Synthase: Triose Phosphate Isomerase and Dehydration Activities Play Together To Form Quinolinate. *Biochemistry* **54:** 6443-6446

113 Reverter-Branchat G, Cabiscol E, Tamarit J, Ros J (2004) Oxidative damage to specific proteins in replicative and chronological-aged Saccharomyces cerevisiae - Common targets and prevention by calorie restriction. *Journal of Biological Chemistry* **279:** 31983-31989

114 Rinehart J, Krett B, Rubio MAT, Alfonzo JD, Soll D (2005) Saccharomyces cerevisiae imports the cytosolic pathway for Gln-tRNA synthesis into the mitochondrion. *Genes & Development* **19:** 583-592

115 Royds JA, Parsons MA, Taylor CB, and Timperley WR (1982) Enolase isoenzyme distribution in the human brain and its tumours. *J. Pathol.* **137**: 37–49.

116 Rubio MAT, Rinehart JJ, Krett B, Duvezin-Caubet S, Reichert AS, Soll D, Alfonzo JD (2008) Mammalian mitochondria have the innate ability to import tRNAs by a mechanism distinct from protein import. *Proceedings of the National Academy of Sciences of the United States of America* **105:** 9186-9191

117 Rusconi CP, Cech TR (1996) The anticodon is the signal sequence for mitochondrial import of glutamine tRNA in Tetrahymena. *Genes & Development* **10:** 2870-2880

118 Ryan MT, Hoogenraad NJ, Høj PB (1994) Isolation of a cDNA clone specifying rat chaperonin 10, a stress-inducible mitochondrial matrix protein synthesised without a cleavable presequence. *FEBS Letters* **337:** 152-156

119 Salinas T, Duchene AM, Delage L, Nilsson S, Glaser E, Zaepfel M, Marechal-Drouard L (2006) The voltage-dependent anion channel, a major component of the tRNA import machinery in plant mitochondria. *Proceedings of the National Academy of Sciences of the United States of America* **103:** 18362-18367

120 Salinas T, Duchêne AM, Maréchal-Drouard L. (2008) Recent advances in tRNA mitochondrial import. *Trends in Biochemical Sciences*, Vol. 33, pp. 320-329.

121 Salinas T, El Farouk-Ameqrane S, Ubrig E, Sauter C, Duchene AM, Marechal-Drouard L (2014) Molecular basis for the differential interaction of plant mitochondrial VDAC proteins with tRNAs. *Nucleic Acids Research* **42:** 9937-9948

122 Schneider A (2011) Mitochondrial tRNA import and its consequences for mitochondrial translation. *Annual review of biochemistry* **80:** 1033-1053

123 Schneider A, Maréchal-Drouard L. (2000) Mitochondrial tRNA import: Are there distinct mechanisms? *Trends in Cell Biology*, Vol. 10, pp. 509-513.

124 Schneider D, Kaiser W, Stutz C, Holinski A, Mayans O, Babinger P (2015) YbiB from Escherichia coli, the Defining Member of the Novel TrpD2 Family of Prokaryotic DNA-binding Proteins. *Journal of Biological Chemistry* **290:** 19527-19539

125 Schulz C, Lytovchenko O, Melin J, Chacinska A, Guiard B, Neumann P, Ficner R, Jahn O, Schmidt B, Rehling P (2011) Tim50's presequence receptor domain is essential for signal driven transport across the TIM23 complex. *Journal of Cell Biology* **195:** 643-656

126 Schulz C, Schendzielorz A, Rehling P. (2015) Unlocking the presequence import pathway. *Trends in Cell Biology*, Vol. 25, pp. 265-275.

127 Seidman D, Johnson D, Gerbasi V, Golden D, Orlando R, Hajduk S (2012) Mitochondrial Membrane Complex That Contains Proteins Necessary for tRNA Import in Trypanosoma brucei. *Journal of Biological Chemistry* **287:** 8892-8903

128 Shadel GS. (2004) Coupling the mitochondrial transcription machinery to human disease. *Trends in Genetics*, Vol. 20, pp. 513-519.

129 Sherman EL, Go NE, Nargang FE (2005) Functions of the small proteins in the TOM complex of Neurospora crasssa. *Molecular Biology of the Cell* **16:** 4172-4182

130 Shiota T, Imai K, Qiu J, Hewitt VL, Tan K, Shen HH, Sakiyama N, Fukasawa Y, Hayat S, Kamiya M, Elofsson A, Tomii K, Horton P, Wiedemann N, Pfanner N, Lithgow T, Endo T (2015) Molecular architecture of the active mitochondrial protein gate. *Science* **349:** 1544-1548

131 Shiota T, Mabuchi H, Tanaka-Yamano S, Yamano K, Endo T (2011) In vivo protein-interaction mapping of a mitochondrial translocator protein Tom22 at work. *Proceedings of the National Academy of Sciences of the United States of America* **108:** 15179-15183

132 Smirnov A, Comte C, Mager-Heckel AM, Addis V, Krasheninnikov IA, Martin RP, Entelis N, Tarassov I (2010) Mitochondrial Enzyme Rhodanese Is Essential for 5 S Ribosomal RNA Import into Human Mitochondria. *Journal of Biological Chemistry* **285:** 30792-30803

133 Smirnov A, Tarassov I, Mager-Heckel AM, Letzelter M, Martin RP, Krasheninnikov IA, Entelis N (2008a) Two distinct structural elements of 5S rRNA are needed for its import into human mitochondria. *Rna-a Publication of the Rna Society* **14:** 749-759

134 Smirnov AV, Entelis NS, Krasheninnikov IA, Martin R, Tarassov IA (2008b) Specific Features of 5S rRNA Structure - Its Interactions with Macromolecules and Possible Functions. *Biochemistry-Moscow+* **73:** 1418-+

135 Stohl LL, Clayton DA (1992) Saccharomyces-Cerevisiae Contains an Rnase Mrp That Cleaves at a Conserved Mitochondrial Rna Sequence Implicated in Replication Priming. *Molecular and Cellular Biology* **12:** 2561-2569

136 Stroud DA, Becker T, Qiu J, Stojanovski D, Pfannschmidt S, Wirth C, Hunte C, Guiard B, Meisinger C, Pfanner N, Wiedemann N (2011) Biogenesis of mitochondrial beta-barrel proteins: the POTRA domain is involved in precursor release from the SAM complex. *Molecular Biology of the Cell* **22:** 2823-2833

137 Subramanian A and Miller DM (2000) Structural analysis of alpha-enolase. Mapping the functional domains involved in down-regulation of the c-myc protooncogene. *J. Biol. Chem.* **275**: 5958 – 5965

138 Tan THP, Pach R, Crausaz A, Ivens A, Schneider A (2002) tRNAs in Trypanosoma brucei: Genomic organization, expression, and mitochondrial import. *Molecular and Cellular Biology* **22:** 3707-3716

139 Tanaka M, Sugisaki K, and Nakashima K (1985) Switching in levels of translatable mRNAs for enolase isozymes during development of chicken skeletal muscle, *Biochemical and Biophysical Research Communications*, **133**(3): 868–872.

140 Tarassov I, Entelis N, Martin RP (1995a) An intact protein translocating machinery is required for mitochondrial import of a yeast cytoplasmic tRNA. *J Mol Biol* **245:** 315-323

141 Tarassov I, Entelis N, Martin RP (1995b) Mitochondrial import of a cytoplasmic lysine-tRNA in yeast is mediated by cooperation of cytoplasmic and mitochondrial lysyl-tRNA synthetases. *Embo J* **14:** 3461-3471

142 Tarassov IA, Entelis NS (1992) Mitochondrially-imported cytoplasmic tRNALys(CUU) ofSaccharomyces cerevisiae:in vivo andin vitrotargetting systems. *Nucleic Acids Research* **20:** 1277-1281

143 Taylor AB, Smith BS, Kitada S, Kojima K, Miyaura H, Otwinowski Z, Ito A, Deisenhofer J (2001) Crystal structures of mitochondrial processing peptidase reveal the mode for specific cleavage of import signal sequences. *Structure* **9:** 615-625

144 Trojanowicz B, Winkler A, Hammje K, Chen Z, Sekulla C, Glanz D, Schmutzler C, Mentrup B, Hombach-Klonisch S, Klonisch T, Finke R, Kohrle J, Dralle H, and Hoang-Vu C (2009) Retinoic acid-mediated down-regulation of ENO1/MBP-1 gene products caused decreased invasiveness of the follicular thyroid carcinoma cell lines. *J Mol Endocrinol*. **42**: 249–60.

145 Tschopp F, Charrière F, Schneider A (2011) In vivo study in Trypanosoma brucei links mitochondrial transfer RNA import to mitochondrial protein import. *EMBO reports* **12:** 825-832

146 Waegemann K, Popov-Čeleketić D, Neupert W, Azem A, Mokranjac D (2015) Cooperation of TOM and TIM23 Complexes during Translocation of Proteins into Mitochondria. *J Mol Biol* **427:** 1075-1084

147 Waizenegger T, Habib SJ, Lech M, Mokranjac D, Paschen SA, Hell K, Neupert W, Rapaport D (2004) Tob38, a novel essential component in the biogenesis of beta-barrel proteins of mitochondria. *EMBO reports* **5:** 704-709

148 Wang G, Chen HW, Oktay Y, Zhang J, Allen EL, Smith GM, Fan KC, Hong JS, French SW, McCaffery JM, Lightowlers RN, Morse HC, Koehler CM, Teitell MA (2010) PNPASE Regulates RNA Import into Mitochondria. *Cell* **142:** 456-467

149 Wang G, Shimada E, Zhang J, Hong JS, Smith GM, Teitell MA, Koehler CM (2012) Correcting human mitochondrial mutations with targeted RNA import. *Proceedings of the National Academy of Sciences of the United States of America* **109:** 4840-4845

150 Wang W (2005) Identification of -enolase as a nuclear DNA-binding protein in the zona fasciculata but not the zona reticularis of the human adrenal cortex. *Journal of Endocrinology* **184:** 85-94

151 Weber C, Hartig A, Hartmann RK, Rossmanith W (2014) Playing RNase P Evolution: Swapping the RNA Catalyst for a Protein Reveals Functional Uniformity of Highly Divergent Enzyme Forms. *Plos Genetics* **10**

152 Wenz LS, Opaliński Ł, Wiedemann N, Becker T. (2015) Cooperation of protein machineries in mitochondrial protein sorting. *Biochimica et Biophysica Acta - Molecular Cell Research*, Vol. 1853, pp. 1119-1129.

153 Wiedemann N, Kozjak V, Chacinska A, Schonfisch B, Rospert S, Ryan MT, Pfanner N, Meisinger C (2003) Machinery for protein sorting and assembly in the mitochondrial outer membrane. *Nature* **424:** 565-571

154 Wiedemann N, Pfanner N, Ryan MT (2001) The three modules of ADP/ATP carrier cooperate in receptor recruitment and translocation into mitochondria. *Embo Journal* **20:** 951-960

155 Wistow GJ, Lietman T, Williams LA, Stapel SO, Jong WW, Horwitz J. et al. (1988) Taucrystallin/alpha-enolase: one gene encodes both an enzyme and a lens structural protein. J. Cell Biol. 107: 2729 – 2736

156 Yamano K, Yatsukawa YI, Esaki M, Hobbs AEA, Jensen RE, Endo T (2008) Tom20 and Tom22 share the common signal recognition pathway in mitochondrial protein import. *Journal of Biological Chemistry* **283:** 3799-3807

157 Yan T, Skaftnesmo KO, Leiss L, Sleire L, Wang J, Li X, and Enger PØ (2011) Neuronal markers are expressed in human gliomas and NSE knockdown sensitizes glioblastoma cells to radiotherapy and temozolomide. *BMC Cancer*, **11**: 524.

# RÉSUMÉ DE THÈSE

## Introduction et objectifs

Les mitochondries possèdent leur propre génome. Toutefois la capacité de codage de leur ADN est restreinte à un jeu mineur de protéines et d'ARN. Chez le plus grand nombre des eucaryotes, la biogénèse et les fonctions mitochondriales requièrent donc l'import d'un grand nombre de protéines mais aussi de certains ARN. Alors que l'import mitochondrial des ARNt est observé chez de nombreux organismes, différents mécanismes ont apparemment été adaptés. Chez *Saccharomyces cerevisiae*, une petite fraction de l'ARNt$^{Lys}_{CUU}$ (tRK1) est retrouvée dans la mitochondrie, bien que leur ADN code un jeu complet d'ARNt qui inclut l'ARNt$^{Lys}_{UUU}$ (tRK3) (Tarassov and Entelis, 1992). Ce processus semble sélectif. En effet, le second isoaccepteur cytosolique l'ARNt$^{Lys}_{UUU}$ (tRK2) n'est pas localisé dans la mitochondrie.

Le mécanisme d'import mitochondrial de tRK1 semble reposer sur la colaboration entre plusieurs protéines cytosoliques. Tout d'abord tRK1 est amino-acylé par la lysyl-ARNt synthétase cytosolique (KRS) (Tarassov et al, 1995b), puis reconnue spécifiquement par un complexe protéique contenant une des deux isoformes de l'enzyme glycolytique énolase, Eno2p (Entelis et al, 2006). Il a été suggéré qu'Eno2p discrimine entre les molecules à importer en induisant la formation d'une structure alternative dénommée forme F (Kolesnikova et al, 2010). Eno2p transporte tRK1 vers la surface mitochondriale où il est pris en charge par le précurseur de la lysyl-ARNt synthétase mitochondriale (preMSK1p) (Tarassov et al, 1995b), qui est produite principalement à proximité des mitochondries (Entelis et al, 2006). En complexe avec preMSK1p, tRK1 adopte une conformation intermédiaire qui facilite son repliement dans la classique forme en L (Kolesnikova et al, 2010). Eno2p est intégrée dans un complexe multiprotéique glycolytique associé à la membrane mitochondriale externe, alors que preMSK1p promeut la translocation de tRK1 dans la mitochondrie (Entelis et al, 2006). Bien que le mécanisme de translocation de tRK1

n'ait pas été élucidé, il requiert de l'ATP, un potentiel de membrane et une machinerie protéique d'import mitochondrial intacte.

Il a pu être montré que les transcrits synthétiques de tRK1 de levure peuvent être spécifiquement importés dans des mitochondries humaines isolées en presence de facteurs solubles de levure ou humains, indiquant que les cellules humaines maintiennent une machinerie d'import active. Comme preMSK1p dans la levure, le précurseur de la lysyl-ARNt synthétase mitochondriale humaine, preKARS2, semble impliqué in vitro et in vivo dans l'import d'ARNt dans la mitochondrie humaine (Gowher et al, 2013). De plus, les énolases de levure et de lapin facilitent l'interaction entre tRK1 et preKARS2 et l'import de tRK1 dans les mitochondries humaines isolées. Si l'énolase est un composant essentiel du système d'import mitochondrial, au moins l'une des trois isoformes humaines de cet enzyme doit être engagée dans ce mécanisme.

La présente thèse a consisté à étudier le mécanismes d'import des ARNt dans les mitochondries de levure et humaines. Le travail s'est focalisé sur l'étape initiale de l'import mitochondrial de tRK1 et plus spécifiquement sur le rôle de l'énolase dans ce processus. Pour remplir nos objectifs, nous avons caractérisé l'action des énolases humaines pour importer tRK1 dans les mitochondries humaines in vitro et in vivo. Nous avons aussi étudié les conformations en solution de tRK1 et tRK2 libres et dans les complexes impliqués dans l'import dans les mitochondries de levure.

## Résultats

Les cellules humaines, comme celles de tous les vertébrés, possèdent trois isoformes d'énolase, l'α-énolase (énolase 1), la β-énolase (énolase 3) spécifique du muscle et la γ-énolase (énolase 2) qui est spécifique des neurones (Díaz-Ramos et al., 2012). Nous avons étudié la capacité des énolases recombinantes humaines à participer au processus d'import mitochondrial de tRK1 par des experiences de retard sur gel (EMSA) et par des tests d'import mitochondrial in vitro. Les trois isoformes montrent des capacités comparables in vitro pour l'import de tRK1 dans des mitochondries isolées à partir de cellules humaines en présence de

preKARS2. D'après les données d'EMSA, les énolases humaines recombinantes sont affines pour les transcrits synthétiques de tRK1. Les Kd apparents de cette interaction se trouvent dans la zone micromolaire comme les Kd apparents pour l'interaction entre tRK1 et Eno2p (Entelis et al., 2006). Les énolases humaines comme Eno2p présentent une affinité pour tRK1 plus basse que preKARS2 (ou preMSK1p chez la levure). En présence de preKARS2, la totalité de tRK1 présente dans l'échantillon est retardée en formant un complexe tRK1-preKARS2. De plus, les énolase humaines facilitent la formation du complexe entre tRK1 et preKARS2 en diminuant le Kd apparent d'un facteur 10, de 300 à moins de 20 nM. La même tendance est observée pour Eno2p recombinante. En résumé, nos résultats suggèrent que les trois isoformes d'énolase présentent une fonction "clair de lune" en permettant l'import mitochondrial d'ARN dans les cellules humaines, de façon similaire à la situation dans la levure (Publication I Baleva et al., 2015).

Afin de vérifier le rôle des énolases humaines in vivo, nous avons testé l'effet d'une diminution ou d'une augmentation de l'expression de leurs isoformes sur l'efficacité de l'import mitochondrial de tRK1 dans des cellules humaines. L'expression des énolases est réprimée par transfection d'un mélange d'ARNsi conçus pour cibler spécifiquement les trois isoformes d'énolase humaines. Une seconde transfection permet d'introduire tRK1 dans les cellules. Les ARN totaux et mitochondriaux des cellules contrôles et des cellules dans lesquelles l'expression des énolases est réprimée furent comparés par hybridation northern. En parallèle, l'import de tRK1 dans des cellules de lignée HepG2 ou Hek293T surexprimant les énolases $\alpha$ ou $\beta$ est testé. Les cellules sont transfectées transitoirement avec le plasmide codant chaque isoforme, suivi par la transfection de tRK1. A nouveau les ARN totaux et mitochondriaux sont analysés par hybridation northern. Nos résultats indiquent une légère diminution de l'import de tRK1 dans les cellules dans lesquelles l'énolase est sous-exprimée, alors que la sur-expression ne semble pas produire d'effet, suggérant ainsi l'existence d'un mécanisme de régulation de ce phénomène.

Dans ce travail, nous avons également exploré des aspects structuraux du complexe formé entre tRK1 et Eno2p. Nous avons tout d'abord optimisé le protocole de purification de l'Eno2p recombinante étiquettée en C-terminus en ajoutant des étapes de chromatographie

en aval de la purification sur billes de Ni-NTA. Alors que la pureté d'Eno2p augmente, nous constatons la diminution significative de sa capacité à retarder tRK1 en EMSA. L'absence d'interaction entre ENo2p et tRK1 est confirmée par ITC. Pour tester la contribution des protéines d'E.coli contaminant les échantillons d'Eno2p, les protéines d'E.coli présentant de l'affinité pour la résine Ni-NTA ont été extraites et testés en EMSA. Nous observons que les protéines extraites d'E.coli par Ni-NTA permettent de retarder tRK1 en générant un complexe de taille sensiblement comparable à celui observé avec l'Eno2p recombinante. Afin de nous affranchir de la contamination par les protéines d'E.coli, nous avons décidé de travailler avec des fractions enrichies en Eno2p obtenues directement à partir d'extraits de levure. La capacité de ces nouveaux échantillons à promouvoir l'import mitochondrial de tRK1 in vitro a été évaluée. Les résultats confirment qu'Eno2p augmente significativement l'efficacité d'import au contraire des fractions des protéines d'E.coli présentant de l'affinité pour tRK1. Nous avons ensuite testé si des facteurs additionnels étaient requis pour médier l'interaction entre tRK1 et Eno2p. Pour cela, nous avons déterminé comment la composition relative en protéines des fractions enrichies en Eno2p pouvait affecter l'import mitochondrial in vitro. Deux stratégies ont été suivies, la première basée sur le fractionnement sériel d'extraits de levure par des concentrations croissantes de sulphate d'ammonium et la seconde consistant à fractionner les extraits par chromatographie d'affinité sur matrice substituée à l'héparine. Seules les fractions contenant Eno2p sont à la fois capables de retarder tRK1 en EMSA et de promouvoir son import mitochondrial in vitro. De plus, les fractions de protéines de levure enrichies en Eno2p présentent des sélectivités différentes pour tRK1 et tRK2 (Publication II Baleva et al. Soumis). Notre étude révèle qu'Eno2p n'interagit pas directement avec les transcrits de tRK1 in vitro. D'autre part, l'interaction entre certaines fractions protéiques sans Eno2p est observée en EMSA. Néanmoins, la présence d'Eno2p est nécessaire pour l'import de tRK1 dans les mitochondries. Puisqu'Eno2p seule n'est pas suffisante pour promouvoir l'import, d'autres facteurs cellulaires semblent nécessaires.

Dans ce contexte, l'étape suivante consistait à identifier les facteurs cellulaires interagissant avec tRK1 chez la levure. Nous avons utilisé une approche de chromatographie d'affinité basée sur l'utilisation d'une étiquette ARiBo1. Celle-ci contient un ribozyme GlmS activable décoré par des motifs λ*BoxB* provenant du phage λ. Nos ARN d'intérêt sont greffés en 3' de l'étiquette. Nous avons utilisé tRK1 et une version comprenant des mutations dans le bras

accepteur diminuant l'efficacité d'import sous le seuil de 5% afin de déterminer des candidats protéiques spécifiques de l'interaction avec tRK1. Des expériences contrôles adéquates avec l'ARN ARiBo1 seul ou sans ARN permettent de vérifier la spécificité des candidats obtenus. Après rétention de l'ARN sur les billes de glutathion-sépharose par les motifs λ*BoxB*, les extraits protéiques de levure sont ajoutés et incubés. L'élution est induite par l'activation du ribozyme GlmS et les fractions obtenues sont analysées par spectrométrie de masse. Nos données ne montrent la présence d'aucun facteur d'import mitochondrial d'ARN connu comme KRS ou preMSK1p, ce qui semble indiquer que les expériences doivent être optimisées. Néanmoins, certaines protéines sont enrichies spécifiquement dans les fractions contenant tRK1, et pourraient donc être liées au processus d'import. Ces possibilités devront être validées.

## Conclusions et perspectives.

Les résultats obtenus au cours de cette thèse permettent de conclure que les Eno2p recombinante ou purifiée à partir de levure dirigent l'import de tRK1 in vitro en présence de preMSK1p. Les protéines d'E.coli extraites dans les mêmes conditions que l'Eno2p recombinante sont affines pour les transcrits de tRK1 en EMSA mais ne sont pas capables de diriger l'import mitochondrial de tRK1 in vitro en présence de preMSK1p. Finalement, des facteurs additionnels devraient contribuer à la formation d'un complexe moléculaire englobant tRK1 et Eno2p ainsi qu'à la sélectivité de l'import mitochondrial de tRK1. Ce travail révèle le besoin d'affiner notre compréhension du mécanisme d'import de ARNt chez la levure. Une direction que prendront nos études futures sera d'identifier les facteurs protéiques qui, avec l'énolase, interagissent avec tRK1 pour diriger l'import mitochondrial. La stratégie expérimentale que nous avons développée a donnée des résultats encourageants bien que des améliorations doivent être mises en œuvre. En particulier, la complexité moléculaire initiale des protéines "proies" doit être diminuée pour améliorer la détection de protéines nécessairement peu abondantes. Une fois identifiés les facteurs manquants, nous nous efforcerons de résoudre une structure cristallographique du complexe d'import de tRK1. Une telle structure nous aidera à mieux comprendre l'organisation et le fonctionnement de la première étape d'import et notamment éclairera les mécanismes de sélectivité et de régulation du processus d'import des ARNt.

## Liste de publications et communications.

1. Baleva, M., Gowher, A., Kamenski, P., Tarassov, I., Entelis, N., and Masquida, B. (2015). A Moonlighting Human Protein Is Involved in Mitochondrial Import of tRNA. Int J Mol Sci 16, 9354-9367.

2. Baleva, M., Meyer, M., Entelis, N., Tarassov, I., Kamenski, P., and Masquida, B. Factors beyond enolas 2 and mitochondrial lysyl-tRNA synthetase precursor are required fir tRNA import in yeast mitochondria (submitted)

1. Baleva, M., Meyer, M., Gowher, A., Entelis, N., Masquida, B. «A non-canonical tRNA complex involved in tRNA mitochondrial import» 6th world congress on targeting mitochondria, Berlin, Germany, october, 2015

2. Baleva, M., Smirnov, A., Entelis, N., Tarassov, I., Masquida, B. «Factors beyond enolas and mitochondrial lysyl-tRNA synthetase precursor are required fir tRNA import tRNA in yeast mitochondria » RNA 2016, Kyoto, Japan, june-july, 2016

# SUMMERY

## Introduction and objectives

Mitochondria possess their own genome, although the coding capacities of their mtDNA is limited to a minor set of proteins and RNAs. In most eukaryotes, mitochondrial biogenesis and functions not only require the import of a large number of proteins but also of some cytosolic tRNAs. While tRNA mitochondrial import takes place in many organisms, different molecular mechanisms have apparently been adapted. In *Saccharomyces cerevisiae* a small subset of cytosolic $tRNA^{Lys}_{CUU}$ (tRK1) is found within mitochondria, even though their mitochondrial DNA encodes a complete set of the tRNAs required for translation including the mitochondrial $tRNA^{Lys}_{UUU}$ (tRK3) (Tarassov and Entelis, 1992). This process is highly selective as the second cytosolic isoacceptor $tRNA^{Lys}_{UUU}$ (tRK2) does not localize in mitochondria.

The mechanism of tRK1 mitochondrial import appears to rely on the work in concert of several cytosolic protein factors. Thus, the imported tRK1 is firstly amino-acylated by the cytosolic lysyl-tRNA synthetase (KRS) (Tarassov et al., 1995), and then specifically recognized by a protein complex including Eno2p - one of two isoforms of glycolytic enzyme enolase (Entelis et al., 2006). It was suggested that Eno2p discriminates imported molecules by inducing the formation of an alternative structure (named the F-form) (Kolesnikova et al., 2010). Eno2p carries tRK1 toward the mitochondrial surface, where it is handed to the precursor of mitochondrial lysyl-tRNA synthetase (preMSK1p) (Tarassov et al., 1995), which is synthesized mainly in the vicinity of mitochondria (Entelis et al., 2006). In complex with preMSK1p, tRK1 adopts an “intermediate” conformation, which thereafter facilitates its re-folding into a classic L-shape structure (Kolesnikova et al., 2010). Eno2p integrates into a glycolytic multiprotein complex associated with the mitochondrial outer membrane, whereas preMSK1p promotes the translocation of tRK1 into mitochondria (Entelis et al., 2006). While a mechanism of tRK1 translocation across the mitochondrial membrane has not

yet been elucidated, it requires ATP and membrane potential as well as an intact protein mitochondrial import machinery.

It was previously found that the synthetic transcripts of yeast tRK1 could be specifically imported into isolated human mitochondria in the presence of yeast or human soluble factors, indicating that the human cells maintain an active import machinery. Like preMSK1p in yeast cells, the precursor of human mitochondrial lysyl-tRNA synthetase, preKARS2, appeared to be involved both *in vitro* and *in vivo* in tRNA import into human mitochondria (Gowher et al., 2013). Moreover, yeast or rabbit enolase facilitated tRK1-preKARS2 interaction and subsequent import of tRK1 into isolated human mitochondria. If enolase is an essential component of the mitochondrial import system, at least one of the three human isoforms of this enzyme may be engaged into tRK1 mitochondrial import *in vivo*.

The present work proceeds with studying the mechanisms of tRNA targeting into yeast and human mitochondria. The work focused mainly on the initial step of tRK1 import into mitochondria, and more specifically in better understanding the role of the enzyme Eno2p in this process. In order to reach the stated objective, we studied the role of human enolases in tRK1 import into human mitochondria *in vitro* and *in vivo*. We also focused on conformational features of tRK1 and tRK2 in solution and on structures of tRK1-protein complexes involved in tRK1 import into yeast mitochondria.

## Results

Human cells, as all vertabrates, have three isoforms of enolase, the α-enolase (enolase 1), the muscle-specific β-enolase (enolase 3) and the neuron-specific γ-enolase (enolase 2) (Díaz-Ramos et al., 2012). We studied the capacity of recombinant human enolases to participate in tRK1 import process by means of electrophoretic mobility shift assay (EMSA) and *in vitro* import approach. All isoforms exhibited comparable capabilities to direct import of synthetic tRK1 into isolated human mitochondria in the presence of recombinant preKARS2. According to results of EMSA, recombinant human enolases possess affinities to labeled synthetic tRK1 transcript. The apparent $K_d$ for this interaction resides in the micromolar range like the apparent $K_d$ for the interaction of tRK1 and Eno2p (Entelis et al., 2006). Human enolases as well as yeast Eno2p showed

lower affinity to tRK1 transcript than preKARS2 (or preMSK1p in yeast). In the presence of preKARS2, all tRK1 was shifted to form a tRK1-preKARS2 complex. In addition, human enolases facilitated tRK1-preKARS2 complex formation resulting in decreasing the apparent $K_d$ by 10 fold from 300 nM to less than 20 nM. The same trend was observed for the yeast recombinant Eno2p. To summarize, the present results suggest that the three enolase isoforms may perform a moonlighting function in RNA mitochondrial import in human cells, similarly to yeast Eno2p (Publication I Baleva et al., 2015).

To verify the role of human enolases in *in vivo* import, we have tested the effect of enolase down-regulation or overexpression on the efficiency of tRK1 mitochondrial import in human cells. The expression of enolases was repressed by transfection of a mixture of siRNAs specifically designed against all human enolases. Thereafter, cells were transfected with the T7 transcript of tRK1. Total RNAs and mitochondrial RNAs isolated from control and down-regulated cells were analysed by northern blot. In parallel, we tested tRK1 import in human HepG2 or Hek293T cell lines overexpressing α or β enolases. Cells were transiently transfected with the plasmid expressing these isoforms followed by transfection with the T7 transcripts of tRK1. Total RNAs and mitochondrial RNAs isolated from cells over-expressing enolases and from the control cells transfected without enolase-expression plasmids were analysed by northern blot. The results showed a slight decrease of tRK1 import in cells where enolase was down-regulated, while the overexpression of human enolases did not show any effect on import efficiency of tRK1, suggesting a potential regulation of the import mechanisms.

As a part of this work, the structural aspects of the complex formed between yeast Eno2p and tRK1 was investigated. We optimized the purification protocol of the $His_6$-tagged recombinant Eno2p by undertaking chromatographic steps downstream from the Ni-NTA purification step. While the purity of the recombinant Eno2p sample increased, its ability to retardate tRK1 in EMSA decreased significantly. The absence of interaction between tRK1 and Eno2p was also confirmed by ITC. To check the contribution of *E. coli* proteins contamination to EMSA results, we extracted *E. coli* proteins presenting affinity to Ni-NTA resin and so might copurify with recombinant

Eno2p. We could observe that *E. coli* proteins could also bind tRK1 in EMSA yielding a complex of same size as with Eno2p samples. To avoid false-positive results due to *E.coli* contamination as well as to confirm the role of Eno2p in promoting tRK1 mitochondrial import, Eno2p-enriched protein samples were obtained directly from yeast extracts. The ability of these samples to direct mitochondrial import of tRK1 was evaluated by *in vitro* import assay in the presence of preMSK1p. The results confirmed that Eno2p significantly increases import efficiency unlike the fractions of *E. coli* proteins showing affinity for tRK1. To check the hypothesis that additional factors may be required to mediate Eno2p interaction with tRK1, we studied how the relative protein composition of Eno2p-enriched fractions could affect RNA mitochondrial import in vitro. Two strategies were exploited. The first one was based on serial fractionation of yeast extracts using increasing ammonium sulfate concentrations and the second one consisted in performing affinity chromatography on heparin matrix. Only fractions containing Eno2p retardated tRK1 in EMSA as well as presented import directing activity. In addition, the yeast Eno2p-enriched fractions did not show the same selectivity towards tRK1 and tRK2 transcripts (Publication II Baleva et al., Submitted). The study revealed that Eno2p does not interact with tRK1 transcripts *in vitro*. Moreover interactions between some Eno2p-deprived protein fractions and tRK1 could be observed in EMSA. Nevertheless, the presence of Eno2p is required for import of tRK1 into mitochondria. Since Eno2p alone is not able to direct *in vitro* mitochondrial import of tRK1, cellular unknown factors adding to Eno2p are thus necessary to direct import.

In this context, the next step was to search for factors interacting with tRK1 in yeast. We used an affinity chromatography approach based on the ARiBo1 tag. It consists in an activatable *glmS* ribozyme fused to a λ*BoxB* RNA. The ARiBo1 tag was fused to the 3′-end of the transcripts of interest. We used tRK1 and a version bearing mutations in the aminoacceptor stem, which showed in previous experiments less than 5% of import efficiency as compared to tRK1 to figure out candidates for interacting with tRK1. Adequate control experiments were performed using just the ARiBo1 tag RNA or without RNA at all. ARiBo-fusion RNAs were captured on Glutathione-Sepharose resin via a GST/λN-fusion protein and

incubated with yeast lysates. Fractions eluted upon induction of ***glmS*** ribozyme activity were analyzed by mass-spectrometry. Our data did not contain any mitochondrial import factors identified previously such as KRS or preMSK1 indicating that additional optimization is required. Nevertheless, certain proteins were enriched in the tRK1-containing samples. These candidates representing cellular processes involving tRK1 may potentially be linked to the import process. These possibilities will need to be validated.

## Conclusions and perspectives

The results obtained during this work permitted to conclude that both recombinant and yeast purified Eno2p direct the import of tRK1 in vitro in the presence of preMSK1p. *E.coli* proteins extracted under the same conditions as recombinant Eno2p possess affinity to yeast tRK1 transcript in EMSA but are not able to direct tRK1 in vitro import in the presence of preMSK1p. Finaly, additional factor(s) may contribute to the structure of tRK1-Eno2p complex as well as to the selectivity of tRK1 mitochondrial import in yeast. Our work exposed the need to refine the tRNA targeting process in yeast. An important direction of future studies would be to identify missing factor(s) that together with enolase interact with tRK1 to direct it into mitochondria. The experimental strategy developed in the present work yielded promising results but some improvements are required. In particular, the complexity of the pool of potential «prey» proteins need to be decreased (e.g. by introduction of additional fractionation steps) to improve the detection of low-abundant import factors. Once the missed targeting factors would be identified, we will strive to solve the crystal structure of the tRK1-targeting complex. This would help to better understand the organization and functioning of the first import step and shed light on concerns about the selectivity and regulation of the tRNA import process.